Neuronal IL-17 controls *C. elegans* developmental diapause through CEP-1/p53

Abhishiktha Godthi[1,2,3], Sehee Min[1,2,3], Srijit Das[1,3], Johnny Cruz-Corchado[1,2,3], Andrew Deonarine[1,3], Kara Misel-Wuchter[4], Priya D. Issuree[4] and Veena Prahlad[1,2,3] *

Affiliations: [1]Department of Biology,
338 Biology Building East,
143 Biology Building, Iowa City, IA 52242-1324.

[2]Department of Cell Stress Biology
Roswell Park - Comprehensive Cancer Center
Elm and Carlton Streets
CGP-BLSC L3-307
Buffalo, New York 14263

[3]Iowa Neuroscience Institute
169 Newton Road, 2312 Pappajohn Biomedical Discovery Building
Iowa City, IA 52242

[4]Department of Internal Medicine,
503 Eckstein Medical Research Building,
431 Newton Road, Iowa City, IA 52242

* Corresponding author email: : veena.prahlad@roswellpark.org

Abstract. How metazoan development is coordinated with nutrient availability remains unclear. Here, we show that the activity of CEP-1, the *C. elegans* ortholog of the tumor suppressor p53, switches organismal development between reproductive growth and dormancy by responding to nutrient availability signaled by neuronal cytokine, ILC-17.1. Specifically, ILC-17.1 released from amphid neurons upon food availability promotes glucose utilization and represses CEP-1/p53: CEP-1/p53 repression promotes growth. ILC-17.1 deficiency activates CEP-1/p53 in post-embryonically dividing progenitor blast cells, increases the expression of cell-cycle inhibitors, decreases cytochrome C levels, and causes larvae to arrest as stress-resistant, quiescent dauers. Increasing CEP-1/p53 levels alone also has the same effect. IL-17 also represses p53 in human epithelial cells. We propose a model whereby ILC-17.1 signaling links nutrient availability and energy metabolism to cell cycle progression and cell fate decisions during development through CEP-1/p53. These findings provide insights relevant to our understanding of neuroimmune mechanisms in cancer.

15 **Main**

16 During metazoan development, nutrient availability is coordinated with the division, growth and
17 metabolic activity of individual cells through cell-cell communication. This is also the case in the
18 invertebrate *C. elegans*, a free-living bacterivore, which displays a dramatic developmental
19 plasticity to ensure that its growth and reproduction match available resources[1-10]. When *C.*
20 *elegans* larvae hatch under optimal conditions (e.g., in the laboratory at 20°C, at low population
21 densities, on abundant food provided by lawns of the *E. coli* strain, OP50) they continue
22 development into reproducing adults. However, if they hatch under suboptimal conditions, such
23 as in the paucity of food, at high population densities, or high ambient temperatures, larvae
24 implement an alternative developmental program and arrest as quiescent, stress-resistant larvae
25 called 'dauer' larvae. Dauer larvae display metabolic and organismal phenotypes specialized for
26 dispersal and survival, and can remain for months in an arrested state to resume development
27 into reproductive adults when conditions become favorable again[1-10]. Studies from several labs
28 have identified molecular pathways that mediate the dauer decision, showing that growth
29 promoting molecules, the best-characterized of which are the insulins, the transforming β growth
30 factor (TGFβ/DAF-7) and lipid based dafachronic acid hormones, are released by sensory
31 neurons and other cells to license continued growth and development; adverse environments
32 inhibit these growth promoting signals and trigger dauer arrest[1-11]. In addition, a number of
33 quantitative trait loci (QTL) also modulate dauer arrest[12]. Yet, how the dauer entry decision results
34 in a coordinated change in cell fates across different tissues and is linked with the systemic shut-
35 down of anabolic pathways still remains poorly understood.

36

37 An important group of proteins that mediate cell-cell communication and metabolism in metazoa
38 are secreted proteins called cytokines[13,14]. The IL-17 cytokines are one such evolutionarily
39 conserved family of proinflammatory cytokines that are released by specialized immune cells at
40 the interface between an organism and the outside world[15,16] to activate immune surveillance,

41 barrier function and wound healing, but in humans, also promote autoimmune disease such as
42 psoriasis and cancers[15,16]. Here, we show that the *C. elegans* IL-17 ortholog, ILC-17.1, is released
43 from amphid neurons in response to food, and coordinates cell division and cell fate decisions
44 with metabolism through the *C. elegans* tumor suppressor p53 ortholog, CEP-1. Remarkably,
45 CEP-1/p53 activated upon the loss of ILC-17.1, switches whole organism development between
46 continuous growth and dormancy in response to nutrient availability. The p53-like tumor
47 suppressor genes are found in all multicellular animals where they prevent the transmission of
48 damaged DNA by activating a multifaceted program that controls cell cycle checkpoints, mediates
49 reversible growth arrest or apoptosis, and controls metabolic flux in cells [17-20]. Our studies show
50 that these functions of CEP-1/p53 also act to control developmental quiescence of a whole
51 organism, *C. elegans*, suggesting that the developmental function of the p53- gene family could
52 have shaped their evolution[21-23].
53
54 **Results**
55 **ILC-17.1 is released by *C. elegans* amphid neurons in response to food and prevents dauer**
56 **arrest.**
57 *C. elegans* express three IL-17 orthologs[24,25]. Of these, ILC-17.1, which has been shown to act
58 as a neuromodulator, is expressed by a subset of specialized neurons called amphid neurons
59 that are exposed to the outside and sense information from the environment[24-26]. We discovered
60 that a deletion of *ilc-17.1,* syb5296*,* that removes almost all the coding sequence (2173bp out of
61 2980 bp; Supplementary Fig. S1a) and abolishes mRNA expression (Supplementary Fig. S1b)
62 caused larvae to constitutively enter the dauer state even under optimal growth conditions
63 (Supplementary Fig. S1c-d). Dauer larvae can be identified by their growth arrest, distinct
64 morphology that includes specialized cuticular structures called alae, a constricted pharynx, and
65 arrested germline, as well as decreased pharyngeal pumping rates and detergent (1% SDS)
66 resistance[3-9]. *ilc-17.1*(syb5296)X dauer larvae displayed all these characteristic morphological

67 and physiological features (Supplementary Fig. S1c-j). Under optimal growth conditions at 20°C,
68 *ilc-17.1* deleted larvae entered the dauer state transiently: approximately 30% (31.2 ±5%) were
69 SDS-resistant 48 hours post-hatching on OP50 bacteria, and most larvae exited dauer and
70 become reproductive adults by 72 hrs (Supplementary Fig. S1c, d). Under the same conditions,
71 none of the wildtype larvae were detergent resistant, nor did any larvae arrest as dauers
72 (Supplementary Fig. S1c, d). However, as with other mutations that promote dauer entry[3,4,27], the
73 dauer arrest of *ilc-17.1* deletion mutants was dramatically accentuated at the slightly more
74 stressful ambient temperature of 25°C, which still supported the growth of all wildtype larvae into
75 reproductive adults, but caused practically 100% of larvae lacking *ilc-17.1* to enter and persist in
76 the arrested dauer state (Fig.1a-d).
77
78 Because the molecular basis for dauer regulation has been the target of extensive genetic
79 screens[3,5,28-30], and ILC-17s had not been previously implicated in the regulation of dauer, we
80 confirmed the role of *ilc-17.1* in dauer entry by examining the developmental phenotype of another
81 independently generated CRISPR deletion in *ilc-17.1,* syb5297 (loss of 2188bp of 2980 bp;
82 Supplementary Fig. S1a), and by downregulating *ilc-17.1* and its signaling pathways[24,25] in
83 wildtype (N2) larvae using RNA interference (RNAi; Supplementary Fig. S1k; Figure 1 a, b, e).
84 Like *ilc-17.1* (syb5296), *ilc-17.1* (syb5297) created using a different guide RNA (see Materials and
85 Methods) also displayed completely penetrant dauer arrest at 25°C (Fig. 1a,b). RNAi-mediated
86 downregulation of *ilc-17.1* in wildtype (N2) animals, but not control RNAi treatment, also caused
87 a small but significant number of larvae to arrest as SDS-resistant dauer larvae at 25°C,
88 (Supplementary Fig. S1k). Like all cytokines, ILC-17.1 signals though cytokine receptors which
89 in *C. elegans* consists of ILCR-1/ILCR-2[24,25]. The ILCR-2 subunit is widely expressed, as
90 determined using a bicistronic SL2 cassette to tag the *ilcr-2* receptor at its endogenous locus with
91 GFP (Supplementary Fig. S2a). Downregulation of *ilcr-2* in wildtype (N2) animals through RNAi
92 also caused over one-third, 39.6% ± 4%, of the wildtype larvae to arrest as dauers and did not

93 alter the dauer entry of *ilc-17.1* deleted larvae (Fig. 1e). Thus, together, these observations
94 confirmed the role of *ilc-17.1* in the *C. elegans* dauer pathway and indicated that during normal
95 development, ILC-17.1 signaling, likely through the ubiquitously expressed ILCR-2 receptors, was
96 required for growth of larvae to reproducing adults; in the absence of ILC-17.1, larvae arrested
97 growth and entered the dauer state, transiently, or for prolonged durations.
98
99 The dauer phenotype of *ilc-17.1* deletion mutants could be rescued by re-expressing *ilc-17.1*
100 under the control of its own promoter and 3' UTR regions (Fig.1b; see Supplementary Fig. S2b
101 for expression levels of rescue construct in comparison to the endogenous gene). The extent of
102 rescue varied based on the animal's diet (Average percent dauer on OP50 bacteria, Fig 1b, is
103 37.4 ± 9.6%, vs. 68.2 ± 6% rescue on HT115 bacteria, Supplementary Fig. S2c; Chi-squaredd =
104 121, df = 1, p-value <2e-16), suggesting that the role of ILC-17.1 signaling in dauer might be
105 related to food, a prominent modulator of the *C.elegans* dauer decision[3-9]. The systemic effects
106 of the *ilc-17.1* deletion and rescue were surprising, because previous studies using transgenic *ilc-*
107 *17.1* reporter constructs had shown that *ilc-17.1* mRNA expression is restricted to a small subset
108 of neurons, a pair of amphid sensory neurons (ASE) and two pairs of interneurons (AUA and
109 RMG)[24]. The expression of the endogenous *ilc-17.1* gene was also restricted to a few neurons:
110 mCherry expressed as a bicistronic SL2 cassette along with *ilc-17.1* mRNA from the endogenous
111 *ilc-17.1* locus was also only visible in a few dye-filling amphid neurons (Supplementary Fig. S2d).
112 Therefore, to understand how ILC-17.1 acts systemically, we re-expressed *ilc-17.1* ectopically in
113 *ilc-17.1* deleted larvae, remote from its normal site of expression, using the muscle-specific *unc-*
114 *54* promoter (Supplementary Fig. S2e), and asked whether ILC-17.1 could act in a cell non-
115 autonomous manner to promote development, or whether its only functioned cell autonomously
116 in amphid neurons. Our expectation was that if ILC-17.1 controlled developmental pathways by
117 acting in a cell-autonomous manner in the amphid neurons, ectopic expression would not rescue
118 the dauer arrest, whereas a cell non-autonomous or endocrine mode of activity could result in a

119 rescue. Consistent with a cell non-autonomous mode of action, and as was the case for the
120 previously reported effects of ILC-17.1 on behavior[24], ILC-17.1 expressed ectopically from the
121 *unc-54* promoter rescued dauer arrest of *ilc-17.1* deleted larvae (Fig.1b and Supplementary Fig.
122 S2c). The rescue was larger under some conditions (Fig 1b), likely because of its higher
123 expression levels when compared to that from the endogenous promoter (Supplementary Fig.
124 S2b, f). RNAi mediated downregulation of *ilcr-2* reduced the percentage of *ilc-17.1* larvae that
125 were rescued from dauer arrest by re-expressing ILC-17.1 either under its own promoter, or from
126 the muscle promoter (Fig. 1e). This effect was significant, but only ~10%, reflecting our limited
127 understanding of the stoichiometry of ILC-17.1 ligand-receptor interactions as they relate to the
128 timing of dauer arrest that occurs in the absence of ILC-17.1. Nevertheless, these studies
129 indicated that ILC-17.1 signaling was required for continuous growth and suggested that ILC-17.1
130 might normally be secreted to act cell non-autonomously to promote development, likely through
131 the ILCR-2 receptors.
132
133 Therefore, to more directly examine whether ILC-17.1 was normally secreted from amphid
134 neurons, we immunolocalized ILC-17.1 protein in *C. elegans* larvae using strains expressing ILC-
135 17.1 tagged at its endogenous locus using a HA-tag. Suspecting that food played a role in ILC-
136 17.1 signaling, we conducted these studies on larvae that were hatched in the absence or
137 presence of food (OP50; Fig. 1f). While *ilc-17.1* mRNA localization was not altered by food
138 availability, and remained restricted to the amphid neurons both in the presence and absence of
139 food as detected by mCherry expressed from the endogenous *ilc-17.1* locus (Fig. 1f; left), ILC-
140 17.1 protein was present outside the amphid neurons, concentrated in the pharynx when larvae
141 were exposed to food (OP50), but not when larvae hatched in the absence of food (Fig.1f; right,
142 quantification in Supplementary Fig. S2g). This suggested that ILC-17.1 protein was secreted
143 and either retained, stabilized, or taken up by the pharynx in response to food signals [we could
144 not reliably detect ILC-17.1 protein in distal tissues such as the intestine or coelomocytes]. The

145 secretion of ILC-17.1 protein was also supported by immunolocalization studies on the muscle-
146 expressed ILC-17.1 protein which, although expressed under a well-characterized muscle-
147 specific promoter (i.e. *unc-54* ; Supplementary Fig. S2e), could be constitutively detected outside
148 muscle cells, throughout the animal (Supplementary Fig.S2h). Thus, the presence of ILC-17.1
149 protein in regions outside its cellular sites of mRNA synthesis provided strong support that ILC-
150 17.1 is secreted, and in the case of the endogenous ILC-17.1 protein, secretion occurs in
151 response to food availability.
152
153 Sequencing total RNA (RNA-seq) extracted from bleach synchronized larvae grown for 32-36
154 hours at 25°C when *ilc-17.1* mutant larvae were *en route* to dauer arrest showed that *ilc-17.1*
155 mutant larvae had expressed the molecular signatures of dauer larvae[6,31-33] that was distinct from
156 wildtype larvae and from *ilc-17.1* deletion mutants that re-expressed ILC-17.1 (Supplementary
157 Figure S3a; Supplementary Table 1-3). Thus, anabolic processes such as DNA replication and
158 ribosome biogenesis were downregulated (Fig. 1g), and catabolic processes and stress
159 responses such as autophagy, fatty acid metabolism, glutathione metabolism, and xenobiotic
160 defense pathways were upregulated (Fig. 1h). In addition, *ilc-17.1* deleted larvae expressed
161 dauer-specific collagen genes that differ from the collagens of larvae undergoing continuous
162 development[34] (Fig. 1i; Supplementary Table 4). To evaluate the extent to which the *ilc-17.1*
163 deleted dauers were similar to previously described *C. elegans* dauers that accumulate in the
164 population upon starvation or crowding, we compared the global gene expression changes of *ilc-*
165 *17.1* mutant larvae with previously published gene expression changes in larvae entering dauer
166 in response to starvation[33], or pheromone treatment[33] (Supplementary Fig. S3 b,c; Supplementary
167 Tables 5, 6). Consistent with a role for ILC-17.1 in signaling nutrient availability, the expression
168 profile of *ilc-17.1* deleted larvae was more closely correlated to dauer larvae generated by
169 starvation[33] (Supplementary Fig. S3b), compared to ascaroside induced dauers[32] (Supplementary

170 Fig. S3c). These differences were surprising and suggest that perhaps the trigger and route of
171 dauer entry determines the gene expression profile of *C. elegans* dauer larvae[35,36].
172
173 **ILC-17.1 loss activates CEP-1/p53 to trigger dauer entry through the activation of DAF-**
174 **16/FOXO and DAF-3/SMAD-DAF-5/Ski complex.**
175 To understand how the loss of ILC-17.1 was triggering dauer entry we first considered the
176 possibility that, through its role as a neuromodulator[24], the secretion of ILC-17.1 modulated the
177 animals' sensory perception of food or feeding behavior, and the lack of *ilc-17.1* prevented larvae
178 from finding or ingesting food. However, this did not seem to be the case (Supplementary Fig.
179 S4a): *ilc-17.1* deleted animals did not exhibit decreased chemotaxis towards lawns of OP50, or
180 towards organic molecules like lysine or diacetyl thought to mimic the presence of bacteria[37].
181 Animals lacking ILC-17.1 were also able to feed like wildtype animals, and the rate of pharyngeal
182 pumping, a measure that is typically correlated with food uptake, was the same in wildtype animals
183 and animals lacking ILC-17.1, both in the presence and absence of food (Supplementary Fig.
184 S4b). Also, prior to their dauer entry, *ilc-17.1* deletion mutants accumulated slightly, but not
185 significantly fewer numbers of red latex beads in their intestinal lumen that served as a proxy for
186 rates of bacterial ingestion (Supplementary Fig. S4c). These data suggested that *ilc-17.1* deficient
187 larvae arrested development and entered a dauer diapause state despite being able to find and
188 ingest nutrients.
189
190 Therefore, to answer how the loss of ILC-17.1 triggered dauer entry we next adopted a genetic
191 approach, leveraging the wealth of studies on *C. elegans* dauer formation[2-11,27]. In *C. elegans*,
192 insulins released in the presence of optimal food act through the sole insulin receptor ortholog,
193 DAF-2, to inhibit the Forkhead transcription factor DAF-16, and support continuous growth
194 programs: loss of DAF-2 signaling leads to the activation of DAF-16 and promotes dauer entry[2-
195 11,27]. Likewise, TGFβ/DAF-7 ligands released under optimal growth conditions antagonize the

196 activity of the transcription factor complex, DAF-3/SMAD-DAF-5/Ski, to permit continuous growth:
197 inhibition of DAF-7 activates DAF-3/SMAD-DAF-5/Ski and leads to dauer formation[2-11,27]. Both
198 insulins and TGF-β result in the production of the lipid based dafachronic acid hormones that act
199 through DAF-12, a nuclear hormone receptor, to support the development of adult reproductive
200 physiology[2-11,27]. The absence of dafachronic acid pathway components also triggers dauer arrest,
201 and providing exogenous dafachronic acids to mutant animals deficient in insulin or TGFβ
202 signaling can bypass their dauer arrest[3,38]. Finally, a mutation in a transmembrane guanylyl
203 cyclase *daf-11,* that causes chemosensory defects also triggers dauer arrest[3,39]. *ilc-17.1* deletion
204 mutants lacked obvious chemosensory defects (Supplementary Fig. 4a-c), and continued to
205 arrest as dauers on 5mM 8-Bromo-cGMP, which is known to rescue *daf-11*-associated dauer
206 formation[3,39] (Supplementary Fig. 4d). Therefore, to identify signal transduction pathways through
207 which the loss of ILC-17.1 might act to control the dauer decision, we examined whether the other
208 dauer effectors, *daf-16, daf-5*, or dafachronic acid signaling, modulated dauer formation of *ilc-*
209 *17.1* mutant larvae.
210
211 A *daf-16* loss of function mutation, mu86[40], completely suppressed dauer formation in animals
212 lacking ILC-17.1, indicating that activation of DAF-16 was one mechanism responsible for their
213 dauer arrest (Fig. 2a). The activation of DAF-16 in animals lacking ILC-17.1 could be quantified
214 by an increase in larvae with DAF-16::GFP[41] positive intestinal nuclei even at 20°C (Fig. 2b), and
215 the upregulation of DAF-16 target genes[42,43] both at 20°C (Supplementary Fig. S4e) and 25°C
216 (Fig.2c). DAF-16 activation could be suppressed by re-expressing ILC-17.1 in *ilc-17.1* deletion
217 mutants under its exogenous promoter, or ectopically, under the muscle-specific promoter
218 (Fig.2c). Similarly, a loss of function mutation in *daf-5*, e1386[44] also completely suppressed the
219 dauer arrest of *ilc-17.1* mutant larvae (Fig. 2d). Finally, and consistent with the role of the DAF-
220 12 pathway downstream of DAF-16 and DAF-5/DAF-3, exposing *ilc-17.1* deficient larvae to
221 exogenous Δ7-dafachronic acid at concentrations of 50 nM[38], partially but significantly

222 suppressed their dauer arrest and only ~65% instead of ~100% of the larvae were dauers (Fig
223 2e). The activation of DAF-16/FOXO and DAF-3/SMAD-DAF-5/Ski by the loss of ILC-17.1 was
224 not simply because *ilc-17.1* deleted larvae were deficient in the expression of insulin signaling
225 and TGFβ/ DAF-7 signaling pathway components. The expression levels of *daf-2* mRNA and the
226 28 insulin ligands[45,46] were not decreased in *ilc-17.1* deletion mutants, (Supplementary Fig. S5a
227 *daf-2* boxed; Supplementary Table 7), and the expression of *ins-4* was even slightly higher
228 (Supplementary Fig. S5b). The expression of insulin peptides INS-4 and DAF-28[46] were also not
229 altered in larvae deficient in *ilc-17.1*, as seen using GFP translational reporters of these insulin
230 ligands (Supplementary Fig. S5c, d). In addition, the dauer arrest of a mutation in the insulin
231 receptor, *daf-2* (e1370)[47], could not be rescued by ILC-17.1 overexpression, suggesting that ILC-
232 17.1 did not act genetically downstream of *daf-2* (Supplementary Fig. S5e). Similarly, the mRNA
233 expression levels of the main TGFβ components were mostly unaltered in *ilc-17.1*, and *daf-5*
234 levels were even downregulated (Supplementary Fig. S5f; Supplementary Table 8). Thus, these
235 data together indicated that ILC-17.1 acted upstream of DAF-16/FOXO, DAF-3/SMAD-DAF-5/Ski,
236 and the likely the DAF-9/DAF-12 endocrine pathways to modulate dauer entry.
237
238 In wildtype animals, DAF-16/FOXO and DAF-3/SMAD-DAF-5/Ski complex are thought to act
239 independently, and in parallel to modulate the dauer decision[3,5]. Therefore, to identify
240 mechanism(s) that led to the activation of both these pathways in *ilc-17.1* deleted larvae, we used
241 RNAi to downregulate genes known to interact with these dauer effectors[48-55] (Supplementary Fig.
242 S5g). Intriguingly, amongst the possible candidates, we found that the downregulation of *cep-1*,
243 the *C. elegans* ortholog of p53[56,57] (Supplementary Fig. S5g), or a deletion in *cep-1*, gk138,
244 completely rescued the dauer arrest of *ilc-17.1* deletion mutants and nearly all (98%) of *cep-1;ilc-*
245 *17.1* double mutant larvae grew into reproductive adults (Fig 2f-h).
246

247 Although p53 is best studied as a tumor suppressor, p53-like proteins modulate vertebrate
248 development through as yet poorly understood mechanisms[17-23]. The *C. elegans* p53 ortholog,
249 *cep-1* has not been previously implicated in *C. elegans* development. Nevertheless, as could be
250 predicted by the dauer rescue of *ilc-17.1* larvae upon *cep-1* deletion, the overexpression of CEP-
251 1 alone was sufficient to arrest growth and promote an almost completely penetrant dauer
252 phenotype in larvae that developed at 25°C (Fig. 3a, b; see Supplementary Fig. S6a for mRNA
253 levels). CEP-1 overexpression was achieved by expressing a functional, fluorescently tagged
254 CEP-1 under its own promoter, CEP-1::GFP, that was able to complement a *cep-1* deletion, *cep-*
255 *1*(*lg12501*),[58-60] as a genomically integrated multicopy array in a wildtype background. CEP-
256 1::GFP did not induce dauer arrest in the background of the *cep-1* deletion, *cep-1*(*lg12501*),
257 (Figure 3c), indicating that it was the higher expression levels of *cep-1* (Supplementary Fig. S6a),
258 and not the GFP tag on CEP-1/p53, that was responsible for the dauer arrest of CEP-1::GFP
259 overexpressing larvae. CEP-1/p53 overexpression not only caused dauer arrest at 25°C, but also
260 prompted larvae to transiently enter dauer at 20°C, as seen by their SDS-resistance
261 (Supplementary Fig. S6b), phenocopying the *ilc-17.1* deletion. RNA-seq analysis showed that
262 genes differentially expressed in CEP-1/p53 overexpressing larvae *en route* to their dauer arrest
263 significantly overlapped with those expressed in larvae lacking ILC-17.1 (65% of the 15,443
264 differentially expressed genes overlapped, padj.< 0.05; Supplementary Fig. S6c; Supplementary
265 Tables 9, 10). CEP-1/p53 overexpressing larvae also upregulated dauer-specific collagens
266 (Supplementary Fig. S6d; Supplementary Table 4), downregulated genes involved in anabolism
267 (Supplementary Fig. S6e), and upregulated genes involved in catabolism (Supplementary Fig.
268 S6f). In addition, between 15 hours to 32 hours post-hatching at 25°C, CEP-1/p53 overexpressing
269 larvae and *ilc-17.1* deletion mutants showed a remarkably constant level of gene expression, and
270 only 340 and 34 genes respectively changed expression ($p<0.05$), compared to the > 10,000
271 genes that were either upregulated or downregulated in wildtype larvae and *cep-1;ilc-17.1* double

272 mutant larvae that were in the process of developing into reproductive adults (PCA analysis;
273 Supplementary Fig. S6g; Supplementary Table 11).
274
275 Like in the ILC-17.1 deficient animals, the completely penetrant 25°C-dauer arrest of larvae
276 overexpressing CEP-1 was dependent on DAF-16, DAF-5 and the steroid hormone pathway.
277 Downregulating *daf-16* expression by RNAi (Fig. 3d; we could not generate CEP-1/p53
278 overexpressing and *daf-16* double mutant larvae, perhaps because of the site of integration of
279 CEP-1::GFP transgene into the genome) or crossing CEP-1/p53 overexpressing larvae into *daf-*
280 *5*, e1386, suppressed their dauer arrest (Fig. 3e). Treatment with 50nM exogenous Δ7-
281 dafachronic acid also allowed a significant proportion of CEP-1/p53 overexpressing larvae to
282 bypass dauer arrest (Fig. 3e). In accordance, DAF-16 target genes were also upregulated in
283 larvae overexpressing CEP-1/p53 at both 25°C (Fig 3f) and 20°C (Supplementary Fig. S7a). In
284 addition, and most convincing, the upregulation of *daf-16* target genes in *ilc-71.1* deletion mutant
285 larvae was *cep-1* dependent at both 25°C and 20°C (Fig 3f; Supplementary Fig. S7a). As we
286 showed for ILC-17.1, CEP-1/p53 induced dauer entry appeared to be somewhat specific to
287 reduced ILC-17.1 signaling, as the 25°C-dauer arrest of *daf-2*(e1370) III larvae that occurred due
288 to reduced insulin signaling did not depend on *cep-1* (Supplementary Fig. S7b). Moreover, in
289 agreement with previous reports[61,62], *cep-1* was not required for dauer induction at high
290 temperatures as *cep-1* (gk138) I larvae could enter dauer at 27°C just like wildtype animals
291 (Supplementary Fig. S7c).
292
293 To confirm that CEP-1/p53 was indeed activated in the absence of ILC-17.1, we tested whether
294 known targets of CEP-1/p53, the BH3-only proteins *egl-1* and *ced*-13[63-66], were upregulated in *ilc-*
295 *17.1* deleted larvae in a CEP-1/p53 dependent manner. As could be expected, *egl-1* and *ced-13*
296 mRNA levels were upregulated upon CEP-1/p53 overexpression in larvae both at 25°C (Fig 3g)
297 and 20°C (Supplementary Fig. S7d). *egl-1* and *ced-13* were also upregulated in a CEP-1/p53-

298 dependent manner in *ilc-17.1* deletion mutants at both 25°C and 20°C, and could be suppressed
299 by rescuing *ilc-17.1* deletion mutants with ILC-17.1 re-expressed under its endogenous-, or
300 muscle-specific promoters (Fig 3g; Supplementary Fig. S7d). In addition, Chromatin
301 Immunoprecipitation followed by quantitative PCR (ChIP-qPCR) using animals carrying an
302 endogenous CRISPR/Cas9 FLAG tagged *cep-1* showed that more CEP-1/p53 was bound to the
303 promoter regions of *elg-1* and *ced-13* in larvae lacking *ilc-17.1* when compared to wildtype larvae,
304 and the increased occupancy was abrogated when *ilc-17.1* deletion mutants were rescued from
305 dauer arrest by re-expressing ILC-17.1 (Fig. 3h).
306
307 In mammalian cells, activation of p53 in response to stress increases p53 protein levels due to its
308 escape from constitutive degradation mediated by the E3 ubiquitin ligase MDM2[17,19]. *C. elegans*
309 genome lacks MDM2 orthologs, but CEP-1/p53 is controlled through translational and
310 posttranslational modifications[58,67], although the mechanisms of activation remain incompletely
311 understood. Western analysis of FLAG-tagged endogenous CEP-1/p53 in *C. elegans* showed
312 that CEP-1::FLAG expression was increased in larvae lacking *ilc-17.1* (Fig 3i). As a positive
313 control we used gamma irradiation at doses known to activate CEP-1/p53 in the germline, and
314 this also increased CEP-1::FLAG levels (Fig 3i)[63,65]. These results together showed that CEP-
315 1/p53 was activated upon loss of ILC-17.1 signaling, and triggered the dauer arrest of *ilc-17.1*
316 deletion mutants through the DAF-16/FOXO and DAF-3/SMAD-DAF-5/Ski (and likely DAF-12)
317 pathways. Thus, it appeared that ILC-17.1-CEP-1/p53 could act as a node to integrate and
318 coordinate the diverse cellular, physiological and metabolic effects of the DAF-2/Insulin signaling-
319 and TGFβ/DAF-7-growth hormone signaling pathways that normally act in parallel to control dauer
320 arrest. However, as we showed for DAF-2, these transcription complexes also likely receive
321 independent information through the insulin receptor, DAF-2, and the TGFβ/DAF-7 receptors.
322

323 **ILC-17.1 modulates CEP-1/p53 activity in ventral blast cells (P cells) of larvae and directly**
324 **or indirectly controls cell cycle progression and cell fate programs.**
325 During *C. elegans* development, most cell divisions are completed during embryogenesis, but a
326 subset of somatic and germline cells divide post-embryonically, during and beyond the L1 stage,
327 to generate adult tissues[68-73]. Previous studies have shown that upon dauer entry these cells
328 maintain or re-establish multipotency to be able to continue development when conditions
329 become favorable again[74,75], and this is mediated by the known dauer signaling pathways that act
330 to different extents, in different post-embryonically developing tissues, to modulate their cell cycle
331 G1/S transition, natural re-programming, and/or differentiation[76-83]. Because of its conserved
332 functions in promoting reversible cell cycle arrest and stem cell differentiation[18-20,84], we
333 speculated that CEP-1/p53 activated by the loss of ILC-17.1, was also restraining cell cycle
334 progression and suppressing adult fates in post-embryonically developing cells when nutrients
335 were scarce. To test this possibility, we (i) examined the localization of CEP-1/p53 in developing
336 *ilc-17.1* deleted larvae and *cep-1* overexpressing larvae during their dauer entry, (ii) examined
337 whether CEP-1/p53 activity in *ilc-17.1* deletion mutants (and CEP-1/p53 overexpressing larvae)
338 altered cell fate or increased the expression of cell cycle inhibitors [85,86], and (iii) examined whether
339 decreasing the expression of the cell cycle inhibitors that may be upregulated could systemically
340 rescue dauer arrest.
341
342 Previous studies have shown that CEP-1/p53 is expressed in the adult germline, and in a subset
343 of larval pharyngeal muscle and neuronal cells[56,58]. This has been visualized by other groups
344 using the same functional, fluorescently tagged CEP-1, CEP-1::GFP which complements the *cep-*
345 *1* deletion, *cep-1*(*lg12501*), where endogenous CEP-1 protein is not expressed[58]. We found that
346 in addition to these cells, CEP-1/p53 was also expressed in the ventral somatic progenitor blast
347 cells (P cells) early during larval development (15-20 hours post-hatching; Fig. 4a). The ventral P
348 blast cells are multipotent progenitor cells that divide post-embryonically during larval stage 1 (L1)

349 to generate neuroblasts, hypodermal blast cells and vulval precursor cells which later form adult
350 tissue [68,69,73,87] and express the Paired-box gene *pax*-3, the sole *C. elegans* PAX-3 transcription
351 factor homolog, during these early stages of development[88]. CEP-1::GFP colocalized with
352 approximately 50% of *pax*-3-driven mCherry that can be used to mark P cells, 15 hours post-
353 hatching at 20°C, and accumulated in more *pax-3* expressing cells under dauer inducing
354 conditions of 25°C (Fig. 4a, b). In addition, CEP-1::GFP expression levels in P blast cells
355 increased at 25°C in larvae overexpressing CEP-1/p53 or lacking ILC-17.1, when compared to
356 larvae at 20°C, or when compared to CEP-1::GFP expression in *cep-1* (lg12501) larvae that do
357 not arrest as dauers (Fig. 4c; also see Fig 3c). Notably, CEP-1::GFP expression in blast cells of
358 *cep-1* (lg12501) larvae did not vary between 20°C and 25°C (Fig. 4c), indicating that increased
359 CEP-1/p53 levels in blast cells of larvae overexpressing CEP-1/p53, or lacking ILC-17.1, was
360 likely related to their dauer entry and not due to changes in temperature *per se*. Thus, during
361 dauer arrest of *ilc-17* deletion mutants, or CEP-1/p53 overexpressing larvae, CEP-1/p53
362 appeared to be activated in the ventral P blast cells that would arrest lineage progression as
363 dauers.
364
365 Larvae overexpressing CEP-1/p53 and *ilc-17.1* deleted larvae also upregulated cell cycle
366 inhibitors that are known to be direct or indirect targets of CEP-1/p53[86]. One of the two p21
367 homologs, *cki-1,* and *phg-1,* the *C. elegans* homologue of Growth arrest-specific 1 or Gas1 were
368 upregulated (Fig. 4d). *phg-1,* but not *cki-1,* was a direct target of CEP-1/p53, as *ilc-17.1*
369 deletion mutants displayed increased occupancy of CEP-1/p53 at the promoter of the *phg-1*
370 gene (Fig. 4e), but not the *cki-1* gene (Supplementary Fig. S7e). The increased expression of
371 these genes and occupancy at *phg-1* promoter was restored to wildtype levels upon re-
372 expressing ILC-17.1 (Fig. 4d, e). For technical reasons we could not localize *phg-1* or *cki-1*
373 mRNA in larvae during these early stages of development and therefore do not know whether
374 the increased expression occurred in the P blast cells. Nevetheless, the increased expression

375 of *phg-1* and *cki-1* played a causal role in dauer arrest: downregulation by RNAi was sufficient
376 to significantly, but modestly rescue dauer arrest in *ilc-17.1* deletion mutants and CEP-1/p53
377 overexpressing larvae, and promote their development into adults (Supplementary Fig. S7f).
378 Crossing *ilc-17.1* deletion mutants into *phg-1* deletion mutants, ok2741, resulted in a greater
379 rescue and ~40% escaped dauer arrest and grew into reproductive adults, but surprisingly, over
380 60% of the *ilc-17.1;phg-1* double mutants still remained arrested as dauers (Fig. 4f;
381 Supplementary Fig. S7g), suggesting that CEP-1/p53 activity might be acting in cooperation
382 with the other cell cycle or dauer pathways. In addition, a proportion of *ilc-17.1* deletion mutant
383 and CEP-1/p53 overexpressing larvae that appeared morphologically dauer, displayed modest
384 but significant non-dauer physiological traits on *phg-1* and *cki-1* RNAi such as increased rates of
385 sporadic pumping (Supplementary Fig. S7h; wildtype larvae at larval stage 2, L2, were used as
386 controls), suggesting there there may also occur a wider, albeit incomplete, dauer rescue in
387 some tissues. The dauer arrest of *daf-2* mutant larvae that did not depend on *cep-1* was not
388 rescued upon downregulating *phg-1* or *cki-1*, nor were the pumping rates of *daf-2* dauers
389 altered, and these remained even lower than in *ilc-17.1* deleted or CEP-1/p53 overexpressing
390 dauers (Supplementary Fig. S7f, h). These data together showed that cell cycle inhibitors that
391 were CEP-1/p53-targets were upregulated upon loss of ILC-17.1 signaling or overexpressing
392 CEP-1/p53 and downregulating these inhibitors was sufficient, at least in part, to cause a
393 systemic rescue from dauer arrest.
394
395 Given these observations, we asked whether overexpressing CEP-1/p53 in P blast cells alone,
396 under the *pax-3* promoter, might drive larvae to arrest as dauers. This hypothesis turned out to
397 be too simplistic, and was not supported, as the majority (85.7 ± 5%; n=6 experiments, 122 larvae
398 total) of *pax-3p::CEP-1* expressing larvae grew into adults at 25°C, although 14.3 ± 4.5% did not
399 complete development and arrested at various early larval (<L4) stages. However, CEP-1/p53
400 expression in the P blast cells caused anteroposterior patterning defects in larvae and 11.8 ±2.9%

401 of larvae displayed dorsalization, vulvaless and dumpy phenotypes (representative example; Fig.
402 4g) suggesting that CEP-1/p53 expression could alter the cell fates of the P blast cell lineages[72,89-
403 91]. Consistent with these observations, in larvae lacking ILC-17.1 or overexpressing CEP-1/p53,
404 HOM-C homeobox genes required for anterio-posterior body patterning[72,89-91] were differentially
405 expressed compared to wildtype or *ilc-17.1; cep-1* double mutant larvae (Fig 4h; $p < 0.05$). This
406 included *lin*-39 (Scr/Dfd/Hox3–5) which maintains P cells competent to respond to later inductive
407 signals and prevents aberrant cell fusions, and *mab-5* (Antp/Hox6–8) and *egl*-5 (Abd-A/Abd-
408 B/Hox9–13), involved in mid- and posterior body patterning, which were maintained at modestly,
409 but significantly higher levels when compared to larvae continuously developing into adults
410 (compare expression levels between 15 hr and 32 hr larvae in Supplementary Table 12). Thus,
411 while further studies are required to better understand how CEP-1/p53 activity in *ilc-17.1* deleted
412 larvae triggers dauer arrest, these data together indicate that CEP-1/p53-induced increase in cell
413 cycle inhibitors such as *phg-1* (in P cells or other cells), and its ability to directly or indirectly
414 modulate cell fate in the ventral P cell lineage during development, where CEP-1/p53
415 accumulates during dauer arrest, may collaborate to pause growth programs of the animal.
416

417 **ILC-17.1 links glucose metabolism to CEP-1/p53 activity in progenitor blast cells (P cells)**
418 **of larvae.**

419 The release of ILC-17.1 from amphid neurons in response to food suggested the intriguing
420 possibility that ILC-17.1 signaling linked CEP-1/p53-mediated cell fate decisions to energy
421 metabolism, since limited nutrient availability, glucose starvation or energy deprivation are all
422 known to activate p53 in mammalian cells[84,92]. Indeed, the dauer arrest of *ilc-17.1* mutant larvae
423 appeared related to an impairment in their ability to utilize glucose normally available through their
424 diets: decreasing glucose availability by downregulating *fgt-1,* the main Glucose transporter
425 (GLUT) responsible for glucose absorption in *C. elegans*[93], decreased the numbers of *ilc-17.1*
426 mutant larvae that could be prevented from arresting as dauers by ILC-17.1 re-expression (Fig.

427 5a). Similarly, *fgt-1* RNAi increased the numbers of *ilc-17.1* deletion mutant larvae that arrested
428 as dauers under optimal conditions at 20°C (Fig. 5b). Promoting glucose utilization and/or
429 metabolism by providing extra glucose[94] rescued the dauer arrest of *ilc-17.1* deficient larvae (Fig.
430 5c; Supplementary Fig. S8a). This effect of glucose supplementation also depended on glucose
431 utilization and metabolism. Impairing glucose import through *fgt-1* RNAi decreased the
432 percentage of larvae that were rescued by the extra glucose (Supplementary Fig. S8b), and no
433 rescue was observed on the non-hydrolyzable glucose analog 2-Deoxy-d-glucose (2-DOG;
434 Supplementary Fig. S8c) which cannot undergo glycolysis and does not enter the metabolic
435 pathway. We ruled out the involvement of mitochondrial reactive oxygen species, ROS, known to
436 be increased under glucose-rich diets[94] by using mitochondria-targeted antioxidant, Mito-Tempo,
437 that scavenges ROS (Supplementary Fig. S8c). The rescue also did not appear to be due to the
438 non-specific effect of nutritional supplementation (e.g. L-glutamine, another important carbon
439 source for metabolism, or skim milk powder that can be ingested by *C.* elegans[95]; Supplementary
440 Fig. S8d). Downregulating *fgt-1* in wildtype larvae, while not sufficient to trigger dauer arrest,
441 modestly increased the expression of CEP-1/p53 target *egl-1* (but not *ced-13*; Supplementary
442 Fig. S8e). Thus, these data supported the possibility that the activation of CEP-1/p53 upon the
443 loss of ILC-17.1 could, at least in part, occur due an impairment in the larvae's ability to utilize
444 glucose.
445
446 If glucose impairment was responsible for CEP-1/p53 activation, glucose supplementation should
447 also rescue the dauer arrest of larvae overexpressing CEP-1/p53. This was the case (Fig 5c;
448 Supplementary Fig. S8a), also arguing that decreased glucose intake in the absence of ILC-17.1
449 was not a consequence of CEP-1/p53 activation, but instead acted logically upstream of CEP-
450 1/p53 activation. In agreement, providing extra glucose decreased the levels of CEP-1::GFP that
451 accumulated in the ventral P blast cells (Fig. 5d), suppressed the increased expression of *phg-1*
452 the direct target of CEP-1/p53, which was in part responsible for dauer arrest of *ilc-17.1* deleted

453 animals (Fig. 5e), and decreased DAF-16/FOXO activation (Fig.5e). However, not only did CEP-
454 1/p53 appear to be activated by the inability of *ilc-17.1* to utilize glucose normally, but CEP-1/p53
455 activity, in turn decreased the expression levels of key metabolic enzymes involved in glucose
456 metabolism[96]: phosphofructokinase-1.2 (*pfk-1.2*), the rate limiting enzyme in glycolysis, and
457 cytochrome *c* (*cyc-2.2*), the subunit of complex IV of the electron transport chain responsible for
458 the final transfer of reducing equivalents to O_2. This was visible in the RNA-seq data
459 (Supplementary Figure S9 a-f; Supplementary Table 13) and confirmed by qRT-PCR
460 (Supplementary Figure S9g, Fig. 5f). In mammalian cells, p53 activity is known to decrease the
461 expression of enzymes required for glycolysis[84] and indeed, the decrease in mRNA expression
462 of *pfk-1.2* was a consequence of CEP-1/p53 activation in the *ilc-17.1* deleted larvae: the deletion
463 of *cep-1* rescued the low mRNA levels (Supplementary Figure S9g). Surprisingly, the decrease
464 in *cyc-2.*2 expression was also dependent on CEP-1/p53*,* but also on DAF-16/FOXO, as the
465 deletion of *cep-1* or *daf-16* rescued the low *cyc-2.2* mRNA levels in *ilc-17.1* deleted larvae (Fig.
466 5f). Moreover, although the downregulation of *pfk-1.2* or *cyc-2.2* alone was not sufficient to induce
467 dauer in wildtype animals, RNAi induced downregulation of *cyc-2.2* in *ilc-17.1* deleted larvae
468 increased the percentage of larvae that arrested as dauers under optimal conditions at
469 temperatures of 20°C, suggesting that CEP-1/p53-dependent decrease of *cyc-2.2* could feedback
470 onto *ilc-17.1* loss to increase dauer propensity (Supplementary Figure S9h). These data,
471 together, strongly suggested that the loss of ILC-17.1 resulted in an impairment in glucose
472 utilization and thus activated CEP-1/p53, which, upon activation, could further limit glucose
473 utilization by downregulating genes important for glycolysis and OXPHOS. Thus, ILC-17 secretion
474 from amphid neurons that occurred in response to food availability appeared to link cell fate
475 decisions with energy metabolism through CEP-1/p53.
476
477 **ILC-17.1 suppresses CEP-1/p53 in *C. elegans* and human epithelial cells.**

478 Since our data pointed towards a model whereby ILC-17.1 signaling that occurred constitutively,
479 under favorable conditions in the presence of food, suppressed CEP-1/p53 to promote continuous
480 development, we directly examined whether IL-17 suppressed CEP-1/p53 activity. As was shown
481 in B lymphoma cells[97], stimulation of untransformed human epithelial cells with human
482 recombinant IL-17A also induced a modest but significant downregulation of p53 expression
483 levels (Fig. 6a). This was similar to the decrease in CEP-1/p53 levels seen in *C. elegans* upon
484 overexpression of ILC-17.1 (Fig. 3i). For the experiments in mammalian cells, IL-17A stimulation
485 of epithelial cells was confirmed by measurement of secreted CXCL5, a key cytokine downstream
486 of IL-17A signaling[98] (Supplementary Fig. S10a).
487
488 In *C. elegans* too, increased ILC-17.1 levels suppressed CEP-1/p53 activation: overexpressing
489 ILC-17.1 in animals also overexpressing CEP-1/p53 inhibited their dauer arrest (Fig. 6b),
490 inhibited the increase in mRNA levels of CEP-1/p53 target genes, *egl-1*, *ced-13* (Fig 3g;
491 Supplementary Fig S7d), *cki-1* and *phg-1* (Fig. 4d), and partially restored the decreased *cyc-2.2*
492 mRNA levels (Fig 5f) that resulted from CEP-1/p53 overexpression. In *C. elegans* the activity of
493 CEP-1/p53 has been best studied in the adult germline where CEP-1/p53 controls germline
494 apoptosis in response to genotoxic insults[56,58,63,64]. Therefore, we used gamma irradiation to
495 cause DNA damage in day-one adult animals, and measured the number of germline apoptotic
496 corpses that result 24 hr. later, to determine whether increased ILC-17.1 levels could also inhibit
497 this canonical activity of CEP-1/p53 (Fig 6c). As has been previously shown[64], and consistent
498 with the role of p53 in controlling DNA-damage induced-, but not physiological apoptosis, *cep-1*
499 *(gk138)* adults lacking functional CEP-1/p53 displayed only a mild decrease in the rates of
500 physiological apoptosis when compared to wildtype animals (Fig. 6c). However, as also shown
501 previously[64], in these animals gamma irradiation did not induce a significant increase in
502 apoptosis (Fig. 6c). CEP-1/p53 overexpression, surprisingly, caused a significant increase in
503 physiological apoptosis, and a marked increase in irradiation-induced apoptosis, both of which

504 were decreased upon also overexpressing ILC-17.1 in these animals (Fig 6c). Overexpressing
505 *ilc-17.1* alone also decreased both physiological or irradiation-induced apoptosis compared to
506 that in wildtype animals, but this effect was mild and did not reach significance (average nos. of
507 cells undergoing physiological apoptosis in N2 v ILC-17.1 overexpressing animals were 3.56 ±
508 1.3 and 2.53 ± 1.1 cells, and upon irradiation, these increased to 7.1 ± 1.8 in N2, and 5.72 ± 2.2
509 in IL-17 overexpressing animals). Also, for reasons we do not understand, *ilc-17.1* deletion
510 mutants did not display changes in apoptosis when compared to wildtype animals, suggesting
511 perhaps that the functions of ILC-17.1 in adult tissue, and/or germline cells may be more
512 nuanced when compared to its developmental function. Nevertheless, these data confirmed
513 that, consistent with our working model (Fig. 6d), ILC-17.1 could inhibit CEP-1/p53. In addition,
514 they suggested the possibility that the roles of *ilc-17.1* signaling and CEP-1/p53 activity might
515 diverge post-development.
516
517 **Discussion**
518 Here we show, for the first time, a role for p53 in the development of an invertebrate species, *C.*
519 *elegans*. Specifically, we show that CEP-1/p53 repression during early larval development
520 ensures the continuous growth of the animal into reproductive adults, and this repression is
521 mediated by ILC-17.1 released by amphid neurons upon food availability. Reduced ILC-17.1
522 signaling, expected to occur when food is scarce, activates CEP-1/p53, which then triggers daurer
523 arrest through the well characterized dauer activating pathways, DAF-16/FOXO, DAF-3/SMAD-
524 DAF-5/Ski and decreased steroid hormone signaling. In its role in promoting dauer arrest CEP-
525 1/p53 accumulates in multipotent P blast cells that differentiate postembryonically into adult
526 tissues, restrains cell cycle progression, and alters cell fate decisions. In addition, CEP-1/p53
527 alters metabolic flux by directly, or indirectly, controlling the levels of phosphofructokinase (*pfk*-1)
528 and cytochrome C (*cyc-2.2*), causing larvae to persist in their dauer state. Notably, all these are
529 functions of p53 in its role as a tumor suppressor. We propose a working model whereby ILC-

530 17.1 secretion from amphid neurons that occurrs in response to food availability links cell fate
531 decisions with energy metabolism through the conserved, multifaceted program of CEP-1/p53
532 (Fig. 6d). Whether the dauer-promoting activities of ILC-17.1/CEP-1 occur in collaboration with
533 the known dauer pathways, or whether they involve different pathway components remains to be
534 explored. In addition, we are yet to dissect the temporal requirements, sites of action, and
535 mechanisms and consequences of ILC-17.1 signaling and CEP-1/p53 activation, as well as its
536 effects on adult traits such as longevity and stress resistance--traits linked to other dauer-
537 activating pathways. While the discovery of new *C. elegans* dauer pathway genes is surprising
538 given the extensive genetic screens that have been conducted[3,5,28-30], genes that require a
539 complete deletion to confer a dauer phenotype, QTLs, or genes that show functional redundancy
540 and tolerance to quantitative variation such as seen with CEP-1/p53 overexpression, could have
541 been missed. Intriguingly, our RNA-seq data show that gene expression changes between 15 hr.
542 post-hatching and 32 hr. post-hatching are negligible in *ilc-17.1* deletion mutants and CEP-1/p53
543 overexpressing larvae, suggesting that this pathway is one of the very early checkpoints in the
544 larval decision between continuous growth and dauer arrest[3,4]. Thus, it is plausible that ILC-17.1
545 and CEP-1/p53 could even act as early as in the maternal germline, or during embryogenesis, to
546 modulate developmental decisions.

547

548 The role of CEP-1/p53 during normal *C. elegans* development in modulating P blast cell fate
549 also remains to be explored. In mammals, normal p53 activity is essential for maintaining stem
550 cell quiescence in the hematopoietic system and other organs during steady state tissue
551 homeostasis[99,100], and unrestrained p53 activity is associated with a developmental syndrome
552 resembling CHARGE (coloboma, heart defects, atresia choanae, growth retardation, genital
553 abnormalities, and ear abnormalities), through its effects on cell cycle progression, apoptosis
554 and the migrartion of neural crest cells[23]. In mammalian cells too, cytokines such as IL-17

555 modulate glucose metabolism and glucose deprivation can, in turn, activate p53[84,92]. Thus, as
556 seen in *C. elegans*, the ability of p53-proteins to link metabolic control with cell cycle
557 progression and stem cell fate could be a conserved mechanism leveraged by several signaling
558 pathways similar to IL-17s to coordinate metazoan development with nutrient availability.
559
560 It is interesting that ILC-17.1 is secreted by *C. elegans* sensory neurons to control CEP-1/p53
561 activity. Neurons control dauer entry also though TGFβ, insulin and steroid hormone signaling. In
562 addition, other stress-responsive transcriptional programs such as the cellular response to protein
563 misfolding that are cell autonomous in individual cells are controlled through neuronal signaling
564 in a metazoan such as *C. elegans*, allowing the nervous system to coordinate tissue-specific
565 transcriptional and epigenetic responses with organismal physiology and behavior[101-104]. Nutrient
566 scarcity has shaped much of evolution, and the ability of cells and organisms to sense nutrient
567 availability and prepare in anticipation to pause cell cycle progression and growth and maintain a
568 quiescent state until resources are optimal, has unquestionable selective advantages. For *C.*
569 *elegans*, like for most organisms, the availability of food is not guaranteed. Neuronal ILC-17.1
570 signaling appears to be one mechanism which allows the animal to match the cell fate programs
571 in the developing larvae with metabolic requirements. In mammals, resident neurons and immune
572 molecules in peripheral tissue profoundly influence cell fate decisions to remodel tissue
573 architecture during development, organogenesis, inflammatory responses, and in diseases such
574 as cancer[105,106]. It is therefore not far-fetched to imagine that mammalian neurons control p53
575 activity, cell quiescence and stem cell fate in response to nutrient availability through IL-17s, as
576 seen in *C. elegans*, although, perhaps in mammals this occurs locally through peripheral
577 innervation and immune cells. Such a control mechanism could open new avenues for therapeutic
578 intervention in cancer and other IL-17-mediated diseases.
579

580 **Materials and Methods**

581 ***C. elegans* strains**

582 *C. elegans* strains used in this study are listed in Table 1. Strains were procured from
583 Caenorhabditis Genetics Center (CGC, Twin Cities, MN), generated in the laboratory or
584 generated by Suny Biotech (Suzhou, Jiangsu, China 215028). All strains will be available upon
585 request, after publication.

Strain Name	**Gene name**	**Source**	**Additional information**
N2, *C. elegans* var *Bristol*	N2, Wild-type	Caenorhabditis Genetics Center	
TJ1	*cep-1* (gk138) I	Caenorhabditis Genetics Center	
CF1038	*daf-16* (mu86) I	Caenorhabditis Genetics Center	
TG12	*cep-1*(lg12501) I*; unc-119* (ed4) III; gtIs1 [CEP-1::GFP + *unc-119* (+)]	Caenorhabditis Genetics Center	Pcep-1::CEP-1(let-585 3'UTR)::GFP; from construct pRH53
CB1370	*daf-2* (e1370) III	Caenorhabditis Genetics Center	
VEP024	praEx021 (*ilc-17.1*p::*ilc-17.1* cDNA::3XFLAG::*ilc-17.1* 3'UTR; p*myo-2*::mCherry::*unc-54* 3'UTR)	Prahlad Lab	ILC-17.1 overexpression under its own promoter and 3'UTR

VEP031	praEx022 (*unc-54*p::*ilc-17.1* cDNA::3XFLAG::*tbb-2* 3'UTR; p*dat-1*::GFP::*unc-54* 3'UTR)	Prahlad Lab	ILC-17.1 overexpression under the muscle promoter and 3'UTR
VEP032	*ilc-17.1* (syb5296) X	Prahlad Lab/ SunyBiotech	*ilc-17.1* deletion, 2173bp deletion, and the 15bp and 127bp sequences were left in the 5' and 3' deletion end, respectively of the 2315 bp *ilc-17.1* gene
VEP033	*ilc-17.1* (syb5296) X; praEx022 (*unc-54*p::*ilc-17.1* cDNA::3XFLAG ::*tbb-2* 3'UTR; p*dat-1*::GFP::*unc-54* 3'UTR)	Prahlad Lab	ILC-17.1 paracrine rescue of *ilc-17.1* deletion
VEP034	*ilc-17.1* (syb5296)X; *cep-1* (gk138) I	Prahlad Lab	
VEP035	*ilc-17.1* (syb5296); *daf-16* (mu86) I	Prahlad Lab	
VEP036	*unc-119* (ed4); gtIs1 [CEP-1::GFP + *unc-119* (+)]	Prahlad Lab	CEP-1 overexpression (ref: [56])
VEP037	*ilc-17.1* (syb5296); praEx022 (*unc-54*p::*ilc-17.1* cDNA:: 3XFLAG::*tbb-2* 3'UTR; p*dat-1*::GFP::*unc-54* 3'UTR);	Prahlad Lab	IL-17.1 overexpression;

	unc-119 (ed4); gtIs1 [CEP-1::GFP + *unc-119* (+)]		CEP-1/p53 overexpression
VEP038	*ilc-17.1* (syb5296); praEx022 (*unc-54*p::*ilc-17.1* cDNA:: 3XFLAG::*tbb-2* 3'UTR; p*dat-1*::GFP::*unc-54* 3'UTR); *daf-2* (e1370) III	Prahlad Lab	
VEP039	*daf-2* (e1370) III; *cep-1* (gk138) I	Prahlad Lab	
VEP040	*cep-1* ((syb6099) [*cep-1*::3XFLAG]) I	Prahlad Lab/ SunyBiotech	Endogenous *cep-1* 3X FLAG tagged at C-terminus
VEP041	*ilc-17.1* (syb5296)X ; *cep-1* (pra02 [*cep-1*::3XFLAG]) I	Prahlad Lab	
VEP042	praEx022 (*unc-54*p::*ilc-17.1* cDNA::3XFLAG::*tbb-2* 3'UTR; p*dat-1*::GFP::*unc-54* 3'UTR); *ilc-17.1* (syb5296) X ; *cep-1* (pra02 [cep-1::3XFLAG]) I	Prahlad Lab	
VEP043	*ilc-17.1* (pra03 [*ilc-17.1*::SL2::mCherry]) X	Prahlad Lab/ SunyBiotech	
VEP044	*ilc-17.1* (pra04 [*ilc-17.1*::3xHA]) X	Prahlad Lab/ SunyBiotech	
VEP045	*ilcr-2* (pra05 [*ilcr-2*::SL2::GFP]) II	Prahlad Lab/ SunyBiotech	
CB1386	daf-5(e1386) II	Caenorhabditis Genetics Center	

VEP061	*ilc-17.1* (syb5297)	Prahlad Lab/ SunyBiotech	*ilc-17.1* deletion, 2188bp deletion, and the 9bp and 118bp sequences were left in the 5' and 3' deletion end, respectively of the 2315 bp *ilc-17.1* gene
RW10645	stIs10645 [pax-3p::HIS-24::mCherry + *unc-119*(+); *unc-119* (ed3)	Caenorhabditis Genetics Center	
VEP062	stIs10645 [pax-3p::HIS-24::mCherry + *unc-119*(+); *unc-119* (ed3); *ilc-17.1*(syb5296)	Prahlad Lab	
VEP059	stIs10645 [pax-3p::HIS-24::mCherry + *unc-119*(+); *unc-119* (ed3); gtIs1[cep-1::GFP + *unc-119*(+)]	Prahlad Lab	
VEP063	praEx026(*pax-3*p::CEP-1A cDNA::3xFLAG::*unc-54* UTR; p*myo-2*::mCherry::*unc-54* UTR)	Prahlad Lab	

586

587 **Generation of CRISPR strains**

588 CRISPR/Cas9 was used to create following *C. elegans* strains:

Background Strain	Type of editing	Description/position of editing	Gene	Resulting strain
N2, *C. elegans* var Bristol	Deletion (syb5296)	2173bp deletion, and the 15bp and 127bp sequences were left in the 5' and 3' deletion end, respectively of the 2135 bp *ilc-17.1* gene. **sgRNA used - CCAAAATCACCACACAGGACAAA**	(*ilc-17.1*)X	VEP032
N2, *C. elegans* var Bristol	Deletion (syb5297)	2188bp deletion, and the 9bp and 118bp sequences were left in the 5' and 3' deletion end, respectively of the 2135 bp *ilc-17.1* gene. **sgRNA used- tagGCAAATGCGAATGCGGATGG**	(*ilc-17.1*)X	VEP032
N2, *C. elegans* var Bristol	Insertion; *SL2::mCherry*	C'-terminus	(*ilc-17.1*)X	VEP043
N2, *C. elegans* var Bristol	Insertion; 3X HA	C'-terminus	(*ilc-17.1*)X	VEP044
N2, *C. elegans* var Bristol	Insertion; SL2::GFP	C'-terminus	(*ilcr-2*)II	VEP045
N2, *C. elegans* var Bristol	Insertion; 3X FLAG	C'-terminus	(*cep-1*)I	VEP040

589 **Generation of transgenic strains**

590 **i) Generation of *cep-1* overexpression strain**

591 TG12 (*cep-1*(lg12501) I; *unc-119* (ed4) III; [CEP-1::GFP + *unc-119* (+)]) is a strain that expresses
592 functional CEP-1 tagged with GFP, as determined by the rescue of *cep-1*(lg1250) phenotype[58].
593 To overexpress CEP-1 we backcrossed the TG12 strain with wild-type (N2) worms and selected
594 F2 progeny that were homozygous for the wild-type *cep-1* gene, lacked the *cep-1*(lg12501) I
595 mutation (confirmed by PCR), and were homozygous for the CEP-1::GFP transgene (confirmed
596 by 100% GFP expression amongst the F3 and F4 progeny). Overexpression of cep-1 mRNA was
597 verified by qPCR (Supplementary Figure S6d). The CEP-1::GFP construct was PCR amplified
598 from the final transgenic VEP037 *C. elegans* strain, and sequence verified.

599 **ii) Generation of ILC-17.1 overexpression strain under its own promoter and 3'UTR**

600 To generate the strain VEP024 – praEx021 [(*ilc-17.1*p::*ilc-17.1* (cDNA)::3xFLAG::*ilc-17.1*
601 3'UTR); p*myo-2*::mCherry::*unc-54* 3'UTR], which overexpressed *ilc-17.1* under the endogenous
602 *ilc-17.1* promoter and *ilc-17.1* 3'UTR, we first amplified 3 kb of genomic sequence upstream of
603 the translational start site (*ilc-17.1* promotor) and 1 kb of genomic sequence downstream from
604 the translational stop codon (*ilc-17.1* 3' UTR). These regions were cloned using Gateway
605 technology into pDONR221. *ilc-17.1* cDNA fused to C-terminal 3xFLAG sequence was
606 synthesized as a gBlock (Integrated DNA technologies). These three fragments were then
607 submitted for gene synthesis service through GenScript to generate the expression vector
608 pUC57(*ilc-17.1*p:: *ilc-17.1* (cDNA)::3xFLAG:: *ilc-17.1* 3'UTR). All plasmids were sequence
609 verified. The *ilc-17.1* expression vector was then injected at 97.5 ng/ul along with the co-
610 injection marker pCFJ90 (p*myo-2*::mCherry::*unc-54* 3'UTR) at 2.5 ng/ul by InVivo Biosystems
611 injection express service. Animals expressing mCherry were singled, lines transmitting the
612 extrachromosomal array were established, and mCherry positive progeny were PCR verified to
613 ensure they were transmitting *ilc-17.1*p:: *ilc-17.1* (cDNA)::3xFLAG:: *ilc-17.1* 3'UTR. These lines
614 were then harvested for Western blot to verify expression of protein.

615 **iii) Generation of ILC-17.1 overexpression strain under the *unc-54* muscle promoter**
616 **and *tbb-2* 3'UTR**

617 To generate VEP031, we overexpressed ILC-17.1 under muscle promoter by fusing - [(*unc-*
618 *54*p:: *ilc-17.1* (cDNA)::3xFLAG] which was synthesized as a gBlock (Integrated DNA
619 technologies) and *tbb-2* 3' UTR which was amplified from genomic DNA. The two fragments
620 were cloned into pUC19 plasmid as the backbone using Gibson assembly[107] to create the
621 overexpression plasmid [(*unc-54*p:: *ilc-17.1* (cDNA)::3xFLAG::*tbb-2* 3'UTR); p*dat-1*::ssmito] and
622 sequence verified. The construct was injected at 100 ng/ul along with the co-injection marker
623 that expressed GFP in the dopaminergic neurons under a *dat-1* promoter [p*dat-1*], at 10 ng/ul
624 into wildtype (N2) worms. Animals expressing GFP in their dopaminergic neurons were singled,
625 lines were established, and GFP-positive progeny were PCR verified to ensure that they were
626 also transmitting harbored the *ilc-17.1* transgene. These lines were then harvested for Western
627 blot to verify expression of protein.

628 **iv) Generation of CEP-1 overexpression strain under the *pax-3* P-cell promoter and**
629 ***unc-54* 3'UTR**

630 To generate the strain VEP063 – praEx026(*pax-3*p::CEP-1A cDNA::3xFLAG::*unc-54* UTR;
631 p*myo-2*::mCherry::*unc-54* UTR)], which overexpressed CEP-1 under the P-cell promotor *pax-3*
632 and *unc-54* 3'UTR, we first amplified 2655 bp of genomic sequence upstream of the
633 translational start site (*pax-3* promotor), 1932 bp of CEP-1A full length cDNA sequence without
634 a stop codon from N2 cDNA, and 851 bp of sequence was amplified from vector pDONRP2r-
635 P3(3xFLAG::*unc-54* 3'UTR). These three sequences were then cloned using a BP reaction into
636 the appropriate DONR vectors for the Multisite Gateway Pro cloning kit (Invitrogen) according to
637 manufacturer's guidelines. An expression vector was created by performing the multisite LR
638 reaction using pDEST R1-R2 with the three entry clones generated above to generate pDEST
639 R1-R2 (*pax-3*p::CEP-1A::3xFLAG::*unc-54* 3' UTR) according to manufacturer's instructions. All
640 plasmids were sequence verified. The CEP-1 expression vector was then injected at 120 ng/ul
641 along with the co-injection marker pCFJ90 (p*myo-2*::mCherry::*unc-54* 3'UTR) at 5 ng/ul into N2
642 wildtype animals. Animals expressing mCherry were singled, lines transmitting the

643 extrachromosomal array were established, and mCherry positive progeny were then harvested
644 for Western blot to verify expression of protein.

645 **v) Generation of crosses.**

646 Crosses between strains were generated according to standard procedures. The primers used to
647 genotype strains are included in the table below.

	Forward primer	Reverse primer
VEP032	TGAATGAGCAAATCGACCAG	AGTTTTGAGATTGAGGGCAAA
	CAGGTCAAGGGGCTAAAACA	CCCACATTAATACTCGCACCT
CF1038	CGGATCAGGAAGAACCAGAA	CATTCCCCGAGTACGAGCTA
	AAGCTGCTGCCTTCACTCTC	ATGGGACTCGAGTTGAGTGG
TJ1	CGGTCTTTTTGGACGATGAA	GTAAACATTGCCGCGTTTTT
	GCGATTCGAAATCCAAGAAG	AGGAACGCATCCATGAAGAC
TJ12	GCCTTCCTCTATTCACTTGAAAC	ACCGAGAGCTCCATGAAGAA
	TCACTCTTTGAATTGGTTCTTTTG	GCTTACGTTCGATTGGCTTC
	AAAAACGCGGCAATGTTTAC	GAGCTTTGTGGGAAGCAATC
RB2075	GACAGTTACGCTGTGCTTGG	CTCCCGGGGTATTCTGAAAT
	GGTGATTCTCCCGTTGGTAA	AAACGGAAATGGCAGAGAGA
CB1370	TAA ATC TCG GAA TTC TGG TGA A	GGA TGA GAC TGT CAA GAT TGG A
	AAG ATG AAC GAG CTG GAG GA	AGA TTG GAG ATT TCG GAA TGG
VEP040	AGA ATT CGA GAA ACA TAA TGA CAT CTT	AAA AAT GCG ATT ATA AAA AGG AAC A
CB1386	CGG CTT GAT CGG ATA GTG AT	AAG AGC AAG GAG TGC GAA AA
	Wild-type PCR product was digested by BstNI	

648

649 **Antibodies used:Growth conditions for *C. elegans* strains**

650 All strains were grown and maintained at 20°C unless otherwise mentioned. Animals were grown
651 in 20°C incubators (humidity controlled) on 60mm nematode growth media (NGM) plates by
652 passaging 8-15 L4s (depending on the strain) onto a fresh plates. Extra care was taken to ensure
653 equal worm densities across all strains. Animals were fed *Escherichia coli* OP50 obtained from
654 Caenorhabditis Genetics Center (CGC) that were seeded (OD_{600}=1.5 and this was strictly
655 maintained throughout the experiments) onto culture plates 2 days before use. The NGM plate
656 thickness was controlled by pouring 8.9ml of autoclaved liquid NGM per 60mm plate. Laboratory
657 temperature was maintained at 20°C and monitored throughout. For all experiments, age-
658 matched day-one hermaphrodites, or larvae timed to reach specific developmental stages as
659 mentioned in the figure legend, were used.

660 For all experiments with larvae, the timings were adjusted to account for the differences in growth
661 rates at different temperatures. Thus, at 25°C, larvae were harvested 30-36 hrs. post bleach hatch
662 or egg lay, and at 20°C, larvae were harvested 40 hrs. post bleach hatch or egg lay.

663

664 **Obtaining synchronized embryos by 'bleach-hatching'**

665 Bleach-hatching' was performed as previously described[101]. Populations of 250-300 gravid adults
666 were generated by passaging L4s, as described above. These plates were used for obtaining
667 synchronized embryos by bleach-induced solubilization of the adults. Specifically, animals were
668 washed off the plates with 1X PBS and pelleted by centrifuging at 2665Xg for 30s. The PBS was
669 removed carefully, and worms were gently vortexed in the presence of bleaching solution [250µl
670 1N NaOH, 200µl standard (regular) bleach and 550µl sterile water] until all the worm bodies had
671 dissolved (approximately 5-6 minutes), and only eggs were viable. The eggs were pelleted by
672 centrifugation (2665Xg for 45s), bleaching solution was carefully removed and then embryos were
673 washed with sterile water 3-4 times and counted under the microscope. The desired number of
674 embryos were seeded on fresh OP50 plates and allowed to grow at 20°C or 25°C for specific time

675 periods depending on the experimental need. If >5% eggs remained unhatched, these plates
676 were discarded.
677
678 **Dauer Assay**
679 Embryos were allowed to hatch and grow on OP50 plates at 20°C or 25°C for this assay. Embryos
680 were generated according to one of the following two methods: (i) Day-one gravid adults that had
681 grown under normal culture conditions (on OP50 at 20°C) were bleach dissolved as described
682 above, and ~50-100 embryos obtained from these gravid adults were seeded on fresh OP50
683 plates or (ii) day-one gravid adults were allowed to lay eggs on fresh OP50 (or RNAi) plates for
684 2-4 hours at 20°C, the adults were removed, and then embryos were allowed to develop at 20°C
685 or 25°C under humified condition for 48-72 hrs. The number of larvae that arrested as dauers
686 (determined by phenotype and/or resistance to 1%SDS) and those that developed into L4s or
687 adults were counted and percentage of dauers was calculated. The total number of embryos in
688 each plate was ~50-100. Each experiment was performed in triplicate or more.
689
690 **SDS treatment**
691 Larvae were washed off the dauer assay plates, washed 1X with PBS to remove bacteria, treated
692 with 1% sodium dodecyl sulfate (SDS) for 30 minutes, washed again with M9, and then transferred
693 onto a fresh plate. Larvae could be scored easily as dead/dissolved or as live dauer larvae (based
694 on their phenotype, and movement).
695
696 **RNAi mediated downregulation of genes**
697 All RNAi clones used were verified by sequencing, and plates were seeded with RNAi bacteria
698 for a maximum of two days before being used. Day-one gravid adults grown on OP50 were
699 allowed to lay eggs on RNAi-bacteria seeded plates for 2-4 hours at 20°C. A second generation
700 of RNAi knockdown was performed where necessary by transferring L4's on existing RNAi

701 plates to fresh plates for knockdown in their progeny. The adults were allowed lay eggs and
702 then removed, and the embryos were transferred to 25°C (or kept at 20°C) under humified
703 condition for 48-72 hrs. The number of larvae that arrested as dauers (determined by phenotype
704 and/or resistance to 1%SDS) and those that developed into L4s or adults were counted and
705 percentage of dauers was calculated.
706

707 **Exposure to food [OP50] availability**

708 Gravid day-one *ilc-17.1*(pra03 [*ilc-17.1*::SL2::mCherry]) X adults or *ilc-17.1*(pra04 [*ilc-*
709 *17.1*::3xHA]) X adults were bleach dissolved and embryos were placed either on empty plates
710 with no food or NGM plates seeded with OP50 and allowed to grow for 24-36 hours at 25°C. To
711 observe mRNA expression of *ilc-17.1, ilc-17.1*(pra03 [*ilc-17. 1:*SL2::mCherry]) X larvae were
712 anesthetized with 1mM levamisole, mounted on 1% agarose pads, and imaged using a
713 Confocal SPE microscope using optimal settings. mCherry expression served to mark cells that
714 expressed *ilc-17.1* mRNA. To identify where ILC-17.1 protein was expressed prior to food
715 exposure, and after food exposure, 24-36 hour *ilc-17.1*(pra04 [*ilc-17.1*::3xHA]) X larvae were
716 fixed and immunostained using Bouin's Tube Fixation method (see below).
717

718 **Immunofluorescence**

719 Nematodes were fixed and immunostained using a modification of the Bouin's Tube Fixation
720 method [108]. Worms were fixed for 30 min. at room temperature (RT) in 400 µl Bouin's fix (Sigma
721 Aldrich) + 600 µl methanol and 10 µl β-mercaptoethanol by tumbling, freeze cracked three times
722 in liquid nitrogen and again tumbled for 30 mins at RT. For permeabilization, the fixative was
723 removed and exchanged for borate-Triton-βmercaptoethanol (BTB: 1xBorate Buffer, 0.5% Triton
724 and 2% β-mercaptoethanol) solution. Worms were tumbled 3 times for 1 hour each in fresh BTB
725 solution at RT. Worms were washed with PBS-0.05% Tween and incubated in block-solution
726 (5% BSA). Staining with primary antibody was performed overnight at 4 °C, incubation with

727 secondary antibody (Donkey anti-Mouse Alexa Fluor 488, 1:2000) for 2-4 hours at RT. All
728 antibody dilutions were performed using antibody buffer containing 5% BSA. Samples were
729 mounted onto glass slides using VECTASHIELD antifade mounting medium (Vector
730 Laboratories, Burlingame, CA, USA). Primary antibodies used: (i) Monoclonal ANTI-FLAG M2,
731 Sigma Aldrich, 1:500, (ii) Mouse anti-HA antibody, Thermofisher; 2-2.2.14, at 1:1000), (iii) anti β-
732 Actin, Cell Signaling Technology, #4967, 1:1000.
733

734 **Chemotaxis**

735 Chemotaxis assay was performed on 9 cm petri dishes containing NGM. Two marks were made
736 on the back of the plate at opposite sides of the plate about 0.5 cm from the edge of the agar.
737 About 5 µl of attractant diluted in water was placed on the agar over one mark, and 5 µl of water
738 was placed as the control over the opposite mark. Attractants and concentrations used are
739 listed in drugs and metabolites section. 5 ul sodium azide with the concentration of 1M was also
740 placed at both the attractant source and the control source. This drug could anesthetize animals
741 within about a 0.5-cm radius of the attractant. Age synchronized day-one adult worms were
742 transferred to the middle of the NGM plates at a point equidistant from the middle of each
743 odorant. After 1 hr., the assay was quantified by counting the number of worms that had left the
744 center origin a chemotaxis index was calculated [#Odor - #Control] / [#Odor + #Control]. Each
745 repeat consisted of 50 worms, and experiments were repeated a minimum of three times.
746

747 **Measuring Pharyngeal pumping**

748 Synchronized day-one adults were singled onto NGM plates seeded with OP50, and onto plates
749 without OP50. Pharyngeal pumping rates were determined by recording the pharyngeal region of
750 animals by video using a Leica S9i digital stereo microscope at 5X magnification and slowing
751 down the video to manually count the number of 'pumps' in 10 seconds, three times per animal.
752 The mean of these pumps was determined and the number of pumps/minute calculated. One

753 complete cycle of synchronous contraction and relaxation of the corpus and the terminal bulb was
754 counted as a pump.
755
756 **Feeding of fluorescent latex beads**
757 Overnight 5ml OP50 culture LB was pelleted and resuspended in fresh 0.5ml LB to concentrate
758 bacteria. 1 µl of fluorescent beads of 0.5µm mean particle size that mimic size of *E. coli*. (Sigma
759 L3280, red fluorescence) was added to 1 ml of concentrated OP50 [1:1000 ratio (v/v)], and 100ul
760 of the mixture was seeded onto NGM plates [109]. Synchronized day-one adults were allowed to lay
761 eggs on the bead containing plates for 2 hours at 20°C and then removed. After 40 hours, larvae
762 were picked onto 1% agarose pads on glass slides and anesthetized using 10mM levamisole. Z-
763 stack images of the larvae were taken on Leica TCS SPE confocal microscope and number of
764 beads within a set area near the tail region per larvae was quantified.
765
766 **Drug and metabolite treatment**
767 The following drugs or metabolites were used:

Drug/metabolite	Source	Final concentration
Glucose	Research products International	50/100mM
2-Deoxy-d-glucose	R&D systems	50mM
Mitotempo	Millipore sigma	0.1mM
L-Glutamine	Sigma-Aldrich	0.26mM
Skim Milk powder	HyVee - instant nonfat dry milk	20mM
Diacetyl	Sigma-Aldrich	0.01% v/v
Lysine	Sigma-Aldrich	1M
(25S)-Δ7-Dafachronic Acid	Cayman Chemical	50nM
8-Bromo-cGMP	Cayman Chemical	5mM

768 The drug solution (0.5 ml) was spread onto NGM agar plates containing an OP50 lawn and left
769 for 1 hr. to dry or used for chemotaxis assays as described. Age synchronized day-one adult
770 worms were transferred to the middle of the NGM plates for 4 hrs. and dauer assay were
771 performed as described. Sterile water was used as control.
772 8-Bromo-cGMP solution was first added to standard NGM plates and allowed to dry for 1 hour.
773 1.5 OD op50 was added on top and allowed to grow for 1 day before starting the dauer assay as
774 described.
775 Plates containing D-glucose were prepared as described in published methods [94], except
776 previously except that we seeded live OP50 onto Glocose plates. Stock solutions of 0.1 and 1M
777 Sterile D-glucose was prepared and added into NGM agar to obtain final concentration of 5mM
778 and 50mM, respectively. For control plate, equivalent amount of sterile water was added to
779 NGM agar. The plates were left to dry for 2 days at RT before seeding 1.5 OD OP50 onto them.
780 After drying at RT for another 1day, dauer assays were performed as described.

781

782 **Fluorescence Image analysis**

783 ImageJ (Fiji) v1.53i was used for measuring fluorescence intensity as follows: single planes [,
784 DAF-16::GFP, CEP-1::GFP, TG12] or projections of z-planes [DAF-28, INS-4, fluorescent latex
785 beads,pax-3p::mCherry] were used for measuring fluorescence intensity. The region of interest
786 was circled using the circle selection tool. The mean fluorescence intensity of each circled area
787 was recorded using the measurement tool. When appropriate, the background fluorescence
788 intensity was measured and subtracted. Quantification of measurements was done in Microsoft
789 excel/GraphPad.

790

791 **RNA-sequencing and Data analysis**

792 **a) RNA isolation, library preparation and sequencing**

793 For the Total RNA-seq samples: Day-one adult worms were bleach-hatched and ~3200
794 eggs/genotype (~800 eggs/plate and 4 plates/genotype) were seeded on fresh OP50
795 plates and allowed to grow for 30-34 hrs. at 25°C. Worms were washed with sterile water
796 and total RNA was extracted from biological triplicates using the Direct-zol RNA Miniprep
797 Kits (catalog no. R2050, Zymo Research). Libraries were prepared using the Illumina
798 Stranded Total RNA Prep
799 with Ribo-Zero Plus, for rRNA depletion (catalog no. 20040525, Illumina). Samples
800 were sequenced in one lane of the Illumina NovaSeq 6000, generating 2x150bp paired-
801 end reads.
802 For the mRNA-seq samples : Day-one adult worms were bleach-hatched and ~3200
803 eggs/genotype (~800 eggs/plate and 4 plates/genotype) were seeded on fresh OP50
804 plates and allowed to grow for either 15 hours or 32 hours at 25°C. Worms were washed
805 with sterile water and total RNA was extracted from biological triplicates using the Direct-
806 zol RNA Miniprep. Libraries were prepared using Illumina TruSeq Stranded mRNA kit.
807 Samples were sequenced in one lane of the Illumina NovaSeq 6000, generating 2x100bp
808 paired-end reads.
809
810 **b) RNA-seq analysis**
811 The quality of the RNA sequences was assessed with FastQC. Adapters and sequence
812 reads with a quality lower than Q25 were trimmed by using Trimgalore [110](v0.67).
813 Ribosomal RNA (rRNA) contamination was filtered with sortmeRNA[111] (version 4.3.4).
814 Sequencing reads were aligned to the *C. elegans* genome (WBcel235[112]) using the Star
815 aligner[113] (v2.7.9a) and then the aligned reads were quantified with FeatureCounts
816 v2.0.1 from the R package Rsubread[114] . Differential expression analysis was performed
817 using DESeq2[115] and genes with FDR corrected p-value of < 0.05 were considered

818 significant. Pairwise distance analysis (sample-to-sample) was performed by using
819 normalized counts coupled with the variance stabilization transformation (VST) on the
820 complete set of genes and calculating the Euclidean distance between the replicates.
821 Principal Component Analysis (PCA) was done using the plotPCA function in DESeq2[115]
822 with the VST transformed data. The mRNA-seq was analyzed following a similar
823 protocol as described above, excluding the SortmeRNA step.
824 The microarray data for the *C. elegans* dauer stage was obtained from the
825 Supplementary Table 1 of the study by Wang, J. & Kim (2003)[33]. The expression values
826 of the dauer stage were defined as the dauers expression (fold-change) at 0hr relative to
827 the mixed staged reference RNA. Sequences IDs from the array were converted to
828 standard gene nomenclature using Simplemine in Wormbase[116]. The correlation
829 between the expression at the dauer stage and the fold change in expression in the *ilc-*
830 *17.1* deletion mutant relative to the wild type, was determined by performing a Spearman
831 Rank Test.
832 The expression of C. elegans larvae (L1) treated with ascaroside cocktail was obtained
833 from Cohen, et al. [117]. The correlation between the Fold-Change in expression in the
834 larvae treated with ascaroside relative to N2 larvae and the fold change in expression in
835 the *ilc-17.1* deletion mutant relative to the wild type, was determined by performing a
836 Spearman Rank Test. The differentially expressed genes (DEGs) between N2 and daf-
837 1(m40) was obtained from. Hu, et al. [118] and were presented as Log_2(Fold-Change)
838 values. The overlap between differentially expressed genes (DEGs) in the cep-1
839 overexpression mutant and the *ilc-17.1* deletion mutant was tested using Fisher exact
840 test from the Gene Overlap package[119]. Venn diagram was done using the R package
841 VennDiagram[120].
842 **c) Functional analysis**

843 Gene ontology analysis (GO) and KEGG enrichment analysis was performed on the
844 differentially expressed genes by using ClusterProfiler 4.0[121]. Terms with an FDR
845 corrected p-value <0.05 were considered significant. The annotations were obtained
846 from R package org.Ce.eg.db[122] (version 3.14) and the KEGG database[123]. The
847 annotations of genes as part of the metabolic pathways were obtained from the
848 database Wormpaths[96] and heatmaps were done using the R packages
849 Complexheatmap and pheatmap[124,125].
850

851 **Progenitor blast cell (P cells) imaging and quantification.**

852 Synchronized day-one adults were allowed to lay eggs on OP50 plates for 2 hours at 20°C and
853 then removed. The plates were then placed at 20C or 25°C. After 15 hours, about 10 L1 larvae
854 were picked onto 1% agarose pads on glass slides and anesthetized using 10mM levamisole and
855 imaged on a Leica SP8. Cells expressing pax-3p::mCherry and CEP-1::GFP were scored, and
856 the percent pax-3p::mCherry cells that also expressed CEP-1::GFP was calculated for individual
857 worms.
858

859 **DiO dye filling assay to identify amphid neurons**

860 A stock dye solution containing 2mg/ml DiO (Molecular Probes, catalog # D-275) in dimethyl
861 formamide is made and maintained under dark conditions. Day-one adult worms were
862 transferred into an eppendorf tube with 1 ml of M9, spun down at 2000-3000 rpm and
863 supernatant removed. Worms were resuspended in 1 ml of M9 and 5 microliter DiO stock sol
864 (1:200 dilution) was added and incubated on a slow shaker for 2 hours at room temperature.
865 Worms were spun down and washed with M9 twice before transferring them onto agar pads
866 with 1mM levamisole to visualize by fluorescence using a Leica TCS SPE confocal microscope.
867

868 **Dauer pharyngeal pumping**

869 Synchronized day-one adults were allowed to lay eggs on OP50 plates for 2 hours at 20°C and
870 then removed. The plates were then placed at 25°C, and larvae were allowed to arrest as dauers
871 or grow into L4 larvae (RNAi treatment) . On day 3, larvae that remained arrested as dauers were
872 used to measure pharyngeal pumping rates using Zeiss Axio Observer.A1 at 40X magnification.
873 WT (N2) L2 stage larvae were used to measure pumping rates as controls. Pumping rates were
874 measured by counting the number of grinder movements in the terminal bulb per minute. The
875 average of three biological replicates consisting of 10 dauer larvae each was quantified.
876

877 **Scoring apoptotic nuclei with Acridine Orange**

878 Acridine orange (AO) staining was performed as previously described (Hefel et al. 2021). AO
879 staining to detect apoptotic germline cells was performed by picking 50 L4 animals to a fresh
880 plate and allowing them to grow into day-one adults for 24 hours at 20°C. Day 1 adults were
881 then either exposed to 75 Gy from a Cesium source or left unirradiated. 24 hours later, AO
882 staining was performed.. For each trial, 10 mg/ml AO stain was freshly prepared and then
883 diluted 1:400 with M9 buffer. Worms were then picked to a tube of the diluted AO stain, wrapped
884 tightly with foil, and rotated at room temperature for 1 hour. After mixing, worms were
885 transferred to a fresh OP50 plate and allowed to crawl away from residual AO stain for 1 hour
886 before being picked to a droplet of 10 mM levamisole on a 1% agarose pad. A cover slip was
887 added, and worms were imaged immediately using the Leica fluorescence microscope on 60x
888 magnification. It was important to visualize AO within 10 mins after mounting animals on the
889 pad. The number of AO stain positive cells found in 12 individual gonad arms per experiment
890 were recorded for each sample.
891

892 **Gamma irradiating *C. elegans* to activate CEP-1/p53**

893 100 L4 larvae were picked onto an OP50 seeded plate, allowed to mature into day-one adults
894 and exposed to 75 Gy gamma irradiation, and subsequently harvested for Western blot

895 analysis. To determine the number of AO positive apoptotic nuclei, at least 50 L4 larvae were
896 exposed to 75 Gy gamma irradiation. The number of AO positive cells were scored 24 hrs. later,
897 when animals had matured into day-one adults.
898
899 **Western blot analysis**
900 **i. Western blot analysis of *C. elegans***
901 Western blot analysis was performed with 30–100 adult day-one animals, or approximately 400
902 30-36 hr. larvae as indicated. Animals were harvested in 15 µl of 1X PBS (pH 7.4), and 4X
903 Laemmli sample buffer (catalog no. 1610737, Bio-Rad) supplemented with 10% β-
904 mercaptoethanol was added and samples were boiled for 30 min. Whole-worm lysates were
905 resolved on 12% SDS-PAGE gels and transferred onto nitrocellulose membrane (catalog no.
906 1620115, Bio-Rad). Membranes were blocked with Odyssey Blocking Buffer (part no. 927–50000,
907 LI-COR). Immunoblots were imaged using LI-COR Odyssey Infrared Imaging System (LI-COR
908 Biotechnology, Lincoln, NE). Mouse anti-FLAG M2 antibody (catalog no. F1804,
909 RRID:AB_262044,_Sigma Aldrich) was used at 1:500 to detect CEP-1::FLAG. Mouse anti-HA
910 antibody (Thermofisher; 2-2.2.14), was used at 1:1000 to detect ILC-17.1::HA. Mouse anti-α-
911 tubulin primary antibody (AA4.3, RRID:AB_579793), developed by C. Walsh, was obtained from
912 the Developmental Studies Hybridoma Bank (DSHB), created by the National Institute of Child
913 Health and Human Development (NICHD) of the National Institute of Health (NIH), and
914 maintained at the Department of Biology, University of Iowa. The following secondary antibodies
915 were used: Donkey anti-mouse IgG (H and L) Antibody IRDye 800CW Conjugated (Licor) and
916 Alexa Fluor 680 goat anti-rabbit IgG (H+L) (Invitrogen). LI-COR Image Studio software
917 (RRID:SCR_015795) was used to quantify protein levels in different samples, relative to α-tubulin
918 levels. Fold change of protein levels was calculated relative to wildtype (N2)/ controls.
919 **ii. Western blot analysis of epithelial cell lines**

920 A549 epithelial cells were lysed in a modified M2 buffer containing 20mM
921 tris[hydroxymethyl]aminomethane, 150mM NaCl at pH 7.4, 0.5% NP40, 3mM EDTA, 3mM
922 EGTA, 4mM PMSF, and a cOmplete Mini, EDTA-free protease inhibitor tablet according to the
923 manufacturer's instructions (Roche, #11836170001). Epithelial cells were collected by
924 mechanical dislodgment in lysis buffer at individual time points, incubated for 20 minutes on ice,
925 and spun at 14,000 x g for 5 minutes to remove insoluble material. 25ug protein was resolved
926 by NuPAGE™ 4-12% Bis-Tris gel (Invitrogen) and transferred to PVDF for immunoblotting. Anti-
927 p53 (Cell Signaling Technology, #9282) and β-actin (DSHB, 224-236-1) primary antibodies were
928 used with HRP-conjugated secondary antibodies to anti-rabbit IgG (Jackson ImmunoResearch,
929 #111-035-003) and anti-mouse IgG (Invitrogen, #62-6520). Densitometry was analyzed with
930 ImageJ software.
931
932 **RNA extraction and real-time quantitative reverse-transcriptase PCR (RT-PCR)**
933 Worms were bleach-hatched as described above and ~400-800 eggs/plate (2 plates/strain) were
934 seeded on fresh OP50 plates and were allowed to grow (i) for 30-34 hrs. at 25°C or (ii) for 36 hrs.
935 at 20°C and then harvested for RNA extraction. RNA was extracted as described earlier [126].
936 Briefly, plates were washed with sterile water and centrifuged. Water was carefully removed and
937 300 µl of Trizol (catalog no. 400753, Life Technologies) was added and snap-frozen immediately
938 in liquid nitrogen. Samples were thawed on ice and then lysed using a Precellys 24 homogenizer
939 (Bertin Corp.). RNA was then purified as detailed with appropriate volumes of reagents modified
940 to 300 µl of Trizol. The RNA pellet was dissolved in 17 µl of RNase-free water. The purified RNA
941 was then treated with deoxyribonuclease using the TURBO DNA-free kit (catalog no. AM1907,
942 Life Technologies) as per the manufacturer's protocol. cDNA was generated by using the iScript
943 cDNA Synthesis Kit (catalog no. 170–8891, Bio-Rad). qRT-PCR was performed using PowerUp
944 SYBR Green Master Mix (catalog no. A25742, Thermo Fisher Scientific) in QuantStudio 3 Real-
945 Time PCR System (Thermo Fisher Scientific) at a 10 µl sample volume, in a 96-well plate (catalog

946 no. 4346907, Thermo Fisher Scientific). The relative amounts of mRNA were determined using
947 the $\Delta\Delta C_t$ method for quantitation. We selected *pmp-3* as an appropriate internal control for gene
948 expression analysis in *C. elegans*.
949
950 All relative changes of mRNA were normalized to either that of the wild-type control or the control
951 for each genotype (specified in figure legends). Each experiment was repeated a minimum of
952 three times. For qPCR reactions, the amplification of a single product with no primer dimers was
953 confirmed by melt-curve analysis performed at the end of the reaction. Primers were designed
954 using Primer3 software and generated by Integrated DNA Technologies. The primers used for
955 the qRT-PCR analysis are listed below:

Gene	**Forward primer (5'-3')**	**Reverse primer (5'-3')**
pfk-1.2	TTGCATCGAATCTGTGAAGC	TCGCTGCAGTCAAAGCTAGA
cyc-2.2	CGGTGGAGCTATTCCAGAAG	GCAACTTGTCCGGATTGTCT
egl-1	TCCAAGCTAGCAGCAATGTG	GCGAAAAAGTCCAGAAGACG
ced-13	GCAACTCAAACACCGTTGAA	CAATGCTGGCATACGTCTTG
phg-1	CAGAGGAGCTTGTACCGACA	TCGTCTCTAGCAGTGCATGT
sod-3	CACTGCTTCAAAGCTTGTTCA	ATGGGAGATCTGGGAGAGTG
mtl-1	TGGATGTAAGGGAGACTGCAA	CATTTTAATGAGCCGCAGCA
lys-7	GCCGTCAAACTTGGCATCTT	GGGTTGTATGCACGAACGAA
pmp-3	TAGAGTCAAGGGTCGCAGTG	ATCGGCACCAAGGAAACTGG
cep-1(a+b isoform)	GCTCACTCTGTCGACTGCTGAGT	AACCCAAGTGTATCTGGGAACTTT
cep-1(a isoform)	GTTGTGCTCGACTCCCAAAAG	GGCACGCTTCTCAATTACAAGTT

956

957 **Chromatin immunoprecipitation (ChIP)**

958 Chromatin immunoprecipitation (ChIP) was performed as described earlier (Das et al., 2020).
959 Day-one adult worms were bleach-hatched as described above and ~1600 eggs were seeded
960 (~800 eggs/plate and 2 plates/genotype) on fresh OP5O plates. Plates were kept at 25°C for 30-
961 34 hrs. and larvae were washed with 1X PBS (pH 7.4) and cross-linked with freshly prepared 2%
962 formaldehyde (catalog no. 252549, Sigma Aldrich) at room temperature for 10 min followed by
963 addition of 250 mM Tris (pH 7.4) at room temperature for 10 min. Samples were then washed
964 three times in ice-cold 1X PBS supplemented with protease inhibitor cocktail and snap-frozen in
965 liquid nitrogen. The worm pellet was resuspended in FA buffer [50 mM HEPES (pH 7.4), 150 mM
966 NaCl, 50 mM EDTA, 1% Triton-X-100, 0.5% SDS and 0.1% sodium deoxycholate], supplemented
967 with 1 mM DTT and protease inhibitor cocktail. The suspended worm pellet was lysed using a
968 Precellys 24 homogenizer (Bertin Corp.), and then sonicated in a Bioruptor Pico Sonication
969 System (catalog no. B0106001, Diagenode) (15 cycles of 30 s on/off).

970 Endogenous CEP-1 was immunoprecipitated with anti-FLAG M2 magnetic bead (catalog no. M-
971 8823, Sigma-Aldrich). Beads were first pre-cleared with salmon sperm DNA (catalog no. 15632–
972 011, Invitrogen). Worm lysate was incubated at 4°C overnight with the pre-cleared FLAG beads.
973 Beads were washed with low salt, high salt and LiCl wash buffers and then eluted in buffer
974 containing EDTA, SDS and sodium bicarbonate. The elute was then de-crosslinked overnight in
975 presence of Proteinase K. The DNA was purified by ChIP DNA purification kit (catalog no. D5205,
976 Zymo Research). qPCR analysis of DNA was performed as described above using primer sets
977 specific for different target genes. For all ChIP experiments, 10% of total lysate was used as 'input'
978 and chromatin immunoprecipitated by different antibodies were expressed as % input values. The
979 primers used for ChIP experiments, and the expected amplicon sizes are as follows:

Gene	Position	Forward primer (5'-3')	Reverse primer (5'-3')	Amplicon size

egl-1	TSS +4 to +123)	CTCACCTTTGCCTCAAC CTC	CGAGGAGAAGTCCTG AGACG	120 bp
ced-13	Promoter (-428 to -310)	CTATTCTTGGCCGTGCT CAT	AGGCAATCTAGCATG CACCT	119 bp
phg-1	Promoter -428 to -294)	GCCAAACCTTCCAGA TTTACA	TTCCTAGATAAGGGT TAGATGATGAGA	135 bp
phg-1	Intron 1 (+223 to +326)	AAGCTGAGCTCCGAA AACAA	TTTCCCGCTAAACGA GACAT	104 bp
cki-1	Promoter (-698 to -722)	TTT TCC ATA CTT CAC TAG TCA AAA CCT	GAC AGT GAG AAG CTT TCG TAT TGA	103 bp
cki-1	Promoter (-542 to -428)	TTC CTC ATA ATC ACG GAG CA	GGA ACC GAA GTG GTC AGA TG	114 bp
cki-1	Promoter (-323 to -217)	TCT CCG ACT GCT GAC CT	CGA GAA GGG GTG GAG TCA TA	106 bp

980

981 **Treatment of mouse epithelial cell lines with human IL-17 and Nutlin3A**

982 A549 epithelial cells were seeded in a 6-well plate overnight and stimulated with 50-100ng/mL
983 recombinant human-IL-17 (Peprotech, SKU 200-17) or 10uM Nutlin3A (Tocris, 675576-98-4),
984 and supernatants and cell lysates were harvested 18 hours later.
985

986 **QUANTIFICATION AND STATISTICAL ANALYSIS**

987 Each 'experiment' refers to a set of independent biological samples that undergo treatment
988 together. No statistical methods were used to predetermine sample size, and experiments were
989 not randomized, but some were blinded. For the assays where we scored dauers, for each
990 experiment, independent biological samples of the different strains were allowed to lay eggs and
991 the eggs were subjected to 'treatment' or 'control' conditions. The results of an experiment
992 generated counts categorized as either (a) dauers, or (b) non-dauers. The counts of dauers/non-
993 dauers for the different types of experiments were used to generate a contingency table, and a
994 chi-squared test was performed to test the independence (whether the results are related or not)
995 of the experiment. This Chi-square statistic, degrees of freedom (df) and p value for each
996 experiment is reported. Yates' continuity correction was used to prevent overestimation of
997 statistical significance for small data. For qPCR or other experiments, the data were analyzed by
998 using Student's t-test and/or one-way ANOVA with Tukey's correction (GraphPad Prism software)
999 as described in respective figure legends. P values are indicated as follows: *p<0.05; **p< 0.01;
1000 ***p<0.001, ns, not significant.
1001

1002 **DATA AVAILABILITY**

1003 The following data sets were generated
1004 Genes deferentially expressed in the following *C. elegans* larvae bleach-hatched and allowed to
1005 grow for 30-36 hr. at 25°C: wild type (N2), *ilc-17.1*(syb5296) X and praEx022 (*unc-54*p::*ilc-17.1*
1006 cDNA::3XFLAG::*tbb-2* 3'UTR; p*dat-1*::GFP::*unc-54* 3'UTR).
1007

1008 Genes deferentially expressed in the following *C. elegans* larvae bleach-hatched and allowed to
1009 grow for 15 hr. and 32 hr. at 25°C: wild type (N2), *ilc-17.1*(syb5296) X, *cep-1* (gk138) I, *ilc-*
1010 *17.1*(syb5296) X; *cep-1* (gk138) I, and VEP036 (unc-119 (ed4); gtIs1 [CEP-1::GFP + unc-119
1011 (+)].
1012
1013 The data discussed in this publication have been deposited in NCBI's Gene Expression
1014 Omnibus (Edgar et al., 2002) and are accessible through GEO Series accession number
1015 GSE218596, , https://www.ncbi.nlm.nih.gov/geo/query/acc.cgi?acc=GSE218596 and
1016 GSE229132, https://www.ncbi.nlm.nih.gov/geo/query/acc.cgi?acc=GSE229132
1017

Figure 1

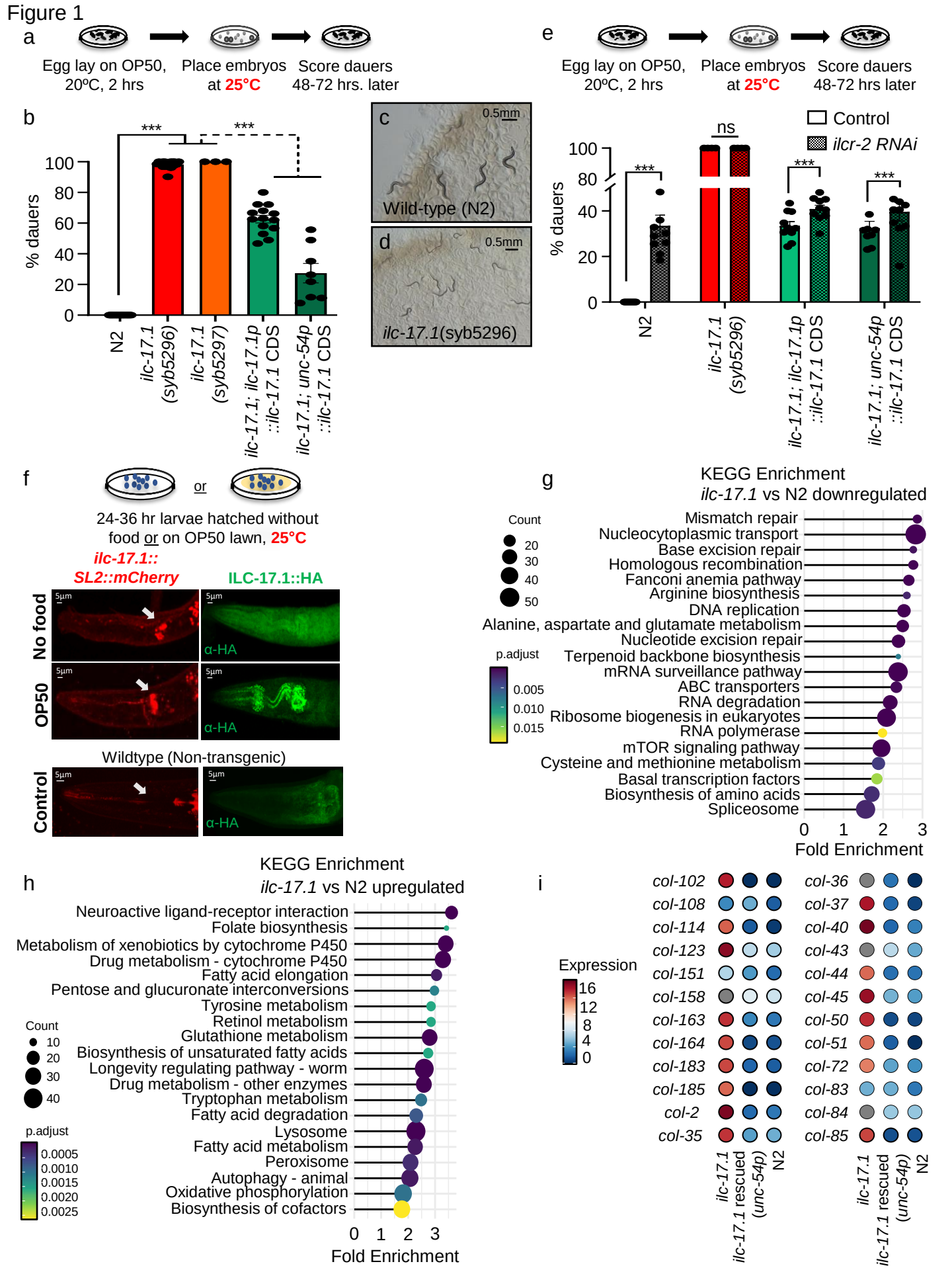
a
Egg lay on OP50, 20ºC, 2 hrs
Place embryos at 25°C
Score dauers 48-72 hrs. later
b
% dauers
***
***
N2
ilc-17.1 (syb5296)
ilc-17.1 (syb5297)
ilc-17.1; ilc-17.1p ::ilc-17.1 CDS
ilc-17.1; unc-54p ::ilc-17.1 CDS
c
0.5mm
Wild-type (N2)
d
0.5mm
ilc-17.1(syb5296)
e
Egg lay on OP50, 20ºC, 2 hrs
Place embryos at 25°C
Score dauers 48-72 hrs later
Control
ilcr-2 RNAi
ns
% dauers
N2
ilc-17.1 (syb5296)
ilc-17.1; ilc-17.1p ::ilc-17.1 CDS
ilc-17.1; unc-54p ::ilc-17.1 CDS
f
or
24-36 hr larvae hatched without food or on OP50 lawn, 25°C
ilc-17.1:: SL2::mCherry
ILC-17.1::HA
No food
OP50
Control
Wildtype (Non-transgenic)
5µm
α-HA
g
KEGG Enrichment
ilc-17.1 vs N2 downregulated
Count
p.adjust
Mismatch repair
Nucleocytoplasmic transport
Base excision repair
Homologous recombination
Fanconi anemia pathway
Arginine biosynthesis
DNA replication
Alanine, aspartate and glutamate metabolism
Nucleotide excision repair
Terpenoid backbone biosynthesis
mRNA surveillance pathway
ABC transporters
RNA degradation
Ribosome biogenesis in eukaryotes
RNA polymerase
mTOR signaling pathway
Cysteine and methionine metabolism
Basal transcription factors
Biosynthesis of amino acids
Spliceosome
Fold Enrichment
h
KEGG Enrichment
ilc-17.1 vs N2 upregulated
Count
p.adjust
Neuroactive ligand-receptor interaction
Folate biosynthesis
Metabolism of xenobiotics by cytochrome P450
Drug metabolism - cytochrome P450
Fatty acid elongation
Pentose and glucuronate interconversions
Tyrosine metabolism
Retinol metabolism
Glutathione metabolism
Biosynthesis of unsaturated fatty acids
Longevity regulating pathway - worm
Drug metabolism - other enzymes
Tryptophan metabolism
Fatty acid degradation
Lysosome
Fatty acid metabolism
Peroxisome
Autophagy - animal
Oxidative phosphorylation
Biosynthesis of cofactors
Fold Enrichment
i
Expression
col-102
col-108
col-114
col-123
col-151
col-158
col-163
col-164
col-183
col-185
col-2
col-35
col-36
col-37
col-40
col-43
col-44
col-45
col-50
col-51
col-72
col-83
col-84
col-85
ilc-17.1
ilc-17.1 rescued (unc-54p)
N2

1018 **Figure 1: ILC-17.1 is released by larval amphid neurons in response to food availability and**
1019 **reduced ILC-17.1 signaling causes dauer arrest.**
1020 **a.** Schematic of experiment to assess dauer arrest. For each experiment, independent samples
1021 of 10 day-one adults of each strain laid eggs for two hours at 20°C on 60 mm NGM plates with
1022 OP50 lawns. Adults were removed, and embryos were transferred to 25°C. Approximately 48 hr.
1023 later, larval phenotype was scored and categorized as either dauers, or larvae that continued
1024 development into stage 4 larvae (L4) and/or young adults. If unsure, SDS-resistance was used to
1025 confirm dauer arrest. Extent of crowding on plates was comparable. [Representative average
1026 numbers of embryos/plates from experiments in **b** are 64, 68, 56, 46 and 65 for wildtype (N2), *ilc-*
1027 *17.1*(syb5296) X, *ilc-17.1*(syb5297) X, *ilc-17.1*(syb5296) rescued with *ilc-17.1p::ilc-17.1*, and *ilc-*
1028 *17.1*(syb5296) rescued with *unc-54p::ilc-17.1* respectively]. Pearson's Chi-squared test with
1029 Yates' continuity correction was used to determine significance throughout the manuscript, unless
1030 otherwise stated. Chi-squared values were calculated for whole experiments, and pair-wise
1031 comparisons. All legends show Chi-squared, df and p values for the whole experiment; p values
1032 for pair-wise comparisons are depicted on graphs using ***$p < 0.001$, **$p < 0.01$, *$p < 0.05$ and ns,
1033 not significant.
1034
1035 **b.** Percentage larvae that arrest as dauers. ***$p<0.001$. (*n*=3-12 experiments; Chi-squared =
1036 2359.6, df = 4, p-value < 2.2e-16.)
1037
1038 **c**, **d**. Representative micrographs 48 hours post-hatching at 25°C. **Top:** Wildtype (N2) grew to
1039 L4s. **Bottom:** *ilc-17.1*(syb5296) larvae arrested as dauers. Scale bar, 0.5mm.
1040
1041 **e. Top**: Schematic of experiment. **Bottom**: Percentage of wildtype (N2) and *ilc-17.1* larvae that
1042 arrest as dauers on control (L4440) and *ilcr-2* RNAi. ***$p < 0.001$, ns, not significant (n=3-10
1043 experiments. Chi-squared = 1815.1, df = 7, p-value < 2.2e-16.)

1044

1045 **f. Top:** Schematic of experiment to localize *ilc-17.1* mRNA and ILC-17.1 protein in the presence
1046 and absence of food (OP50). Embryos were hatched at 20°C and imaged after 24-36 hours (L1
1047 stage larvae). **Left panels:** Representative micrographs of z-section showing mCherry co-
1048 expressed with *ilc-17.1* mRNA in amphid neurons. **Right panels**: projection of z-sections showing
1049 immunostaining with anti-HA antibody to visualize CRISPR tagged endogenous ILC-17.1::HA
1050 protein. Pharyngeal region of larvae **(top panel)** hatched in the absence of food, and **(middle**
1051 **panel)** in the presence of food (OP50). B**ottom panels:** Controls (N2) that do not express HA or
1052 mCherry used to assess specificity of the fluorescence signal. (n>3 experiments, 4-5 larvae each).
1053 Scale bar, 5μm.

1054

1055 **g.** KEGG enrichments associated with differentially downregulated genes (p.adjust <0.05) in *ilc-*
1056 *17.1* mutant larvae (RNA-seq on 32-36 hr. larvae).

1057

1058 **h**. KEGG enrichments associated with differentially upregulated genes (p.adjust <0.05) in *ilc-17.1*
1059 mutant larvae (RNA-seq on 32-36 hr. larvae).

1060

1061 **i**. Heatmap depicting expression levels (log_2 normalized counts) of the major dauer-specific
1062 collagens in wildtype (N2), *ilc-17.1* deletion mutants and *ilc-17.1* deletion mutants rescued with
1063 *unc-54p::ilc-17.1.*

1064

1065 Bars show mean ± S.E.M. Individual data points in the bar graphs in **b** and **e** represent the %
1066 dauers/experiment, and the bar graph depicts mean of these percentages.

1067

Figure 2

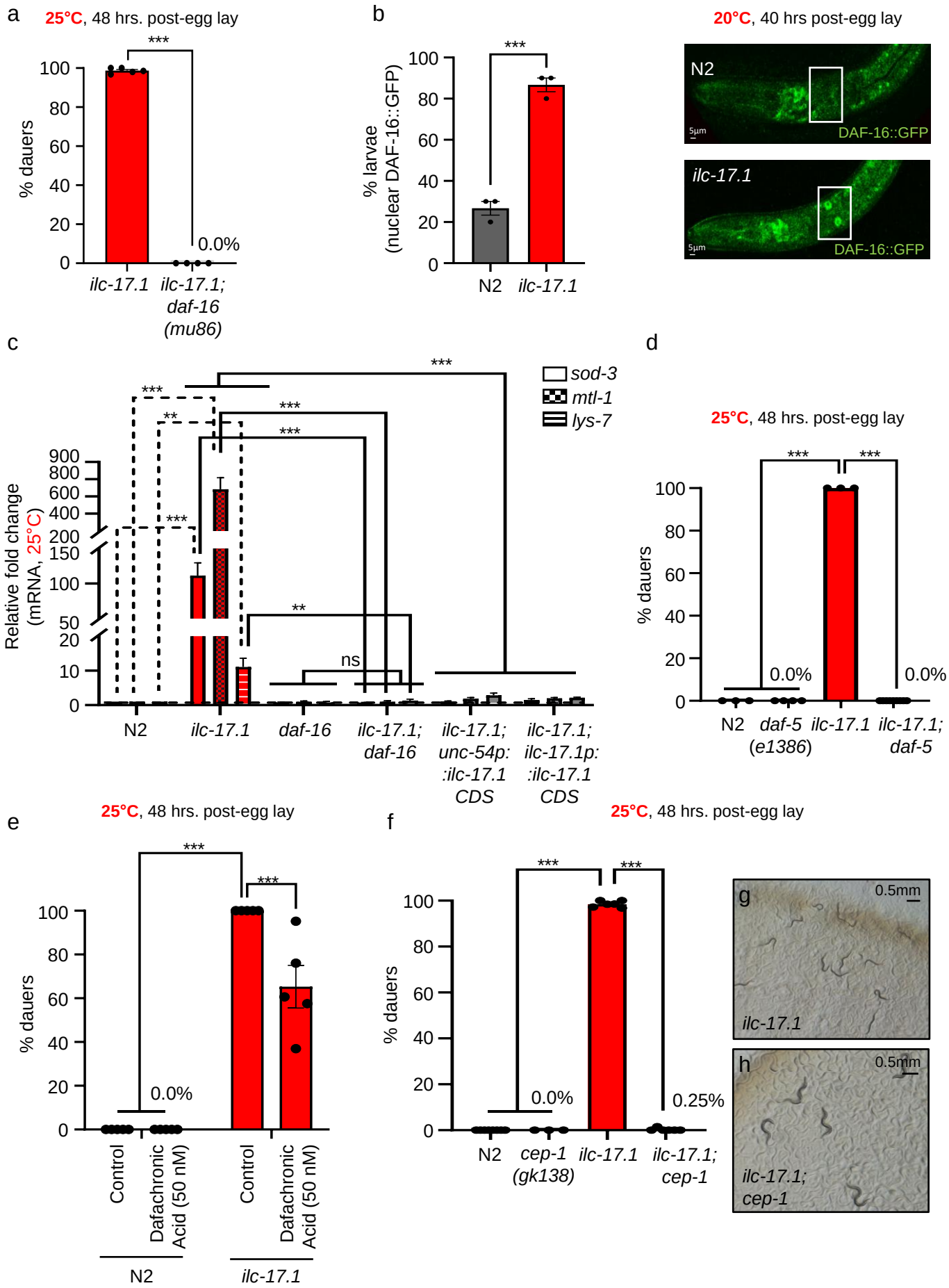
a
25°C, 48 hrs. post-egg lay
% dauers
0.0%
ilc-17.1
ilc-17.1; daf-16 (mu86)
b
20°C, 40 hrs post-egg lay
% larvae (nuclear DAF-16::GFP)
N2
ilc-17.1
DAF-16::GFP
5µm
c
sod-3
mtl-1
lys-7
Relative fold change (mRNA, 25°C)
N2
daf-16
ilc-17.1; daf-16
ilc-17.1; unc-54p::ilc-17.1 CDS
ilc-17.1; ilc-17.1p::ilc-17.1 CDS
ns
d
25°C, 48 hrs. post-egg lay
daf-5 (e1386)
ilc-17.1; daf-5
e
Control
Dafachronic Acid (50 nM)
f
cep-1 (gk138)
ilc-17.1; cep-1
0.25%
g
h
0.5mm

1068 **Figure 2: Reduced ILC-17.1 signaling acts through DAF-16/FOXO, DAF-3/SMAD-DAF-**
1069 **5/Ski complex and CEP-1/p53 to control dauer arrest.**
1070 **a.** Percent dauers in *ilc-17.1* deletion mutants and *ilc-17.1;daf-16* double mutant larvae.
1071 ***p < 0.001, (*n*=4-8 experiments, Chi-squared = 497.65, df = 1, p-value < 2.2e-16).
1072
1073 **b. Left**: Percent larvae showing DAF-16::GFP nuclear localization in intestinal cells. Larvae were
1074 grown at 20°C for 36 hrs**.** *n*=3 experiments with 10-15 larvae each. Each data point represents
1075 average no. of larvae with nuclear DAF-16::GFP/experiment. ***p < 0.001, (unpaired t-test). Note:
1076 experiments were conducted at 20°C, since DAF-16::GFP localized constitutively in intestinal
1077 nuclei even in wildtype larvae at 25°C. **Right:** representative micrographs showing intestinal DAF-
1078 16::GFP (boxed) in wildtype and *ilc-17.1* deletion mutant larvae. Scale bar, 5μm
1079
1080 **c.** Average *sod-3, mtl-1, and lys-7* mRNA levels in larvae 32-36 hr. post-hatching at 25°C. mRNA
1081 levels were determined relative to *pmp-3* and normalized to wildtype (N2) values. *n*=4-10
1082 experiments. ***p < 0.001, **p < 0.01, ns=not significant, (unpaired t-test).
1083
1084 **d.** Percent dauers in *ilc-17.1* mutants and *ilc-17.1;daf-5* double mutants. ***p < 0.001, (*n*=3-5
1085 experiments, Chi-squared = 787.3, df = 3, p-value < 2.2e-16).
1086
1087 **e.** Percent dauers in *ilc-17.1* mutants on control (H_2O) and exogenous 50nM Δ7-dafachronic acid.
1088 ***p < 0.001, (*n*=3-5 experiments, Chi-squared = 784.32, df = 3, p-value < 2.2e-16).
1089
1090 **f-h. f,** percent dauers in *ilc-17.1* mutants and *ilc-17.1;cep-1* double mutants. ***p < 0.001, (*n*=3-5
1091 experiments, Chi-squared = 1029.2, df = 3, p-value < 2.2e-16). Representative micrographs of **g,**
1092 *ilc-17.1* deleted larvae arrested as dauers, and **h,** *ilc-17.1;cep-1* double mutants that grew to L4s,
1093 48 hr. post-hatching at 25°C. Scale bar, 0.5mm

1094

1095 Bars show the mean ± S.E.M. Individual data points in bar graphs in **a, d, e, f** represent the

1096 average % dauers/experiment, Pearson's Chi-squaredd test with Yates' continuity correction.

1097

Figure 3

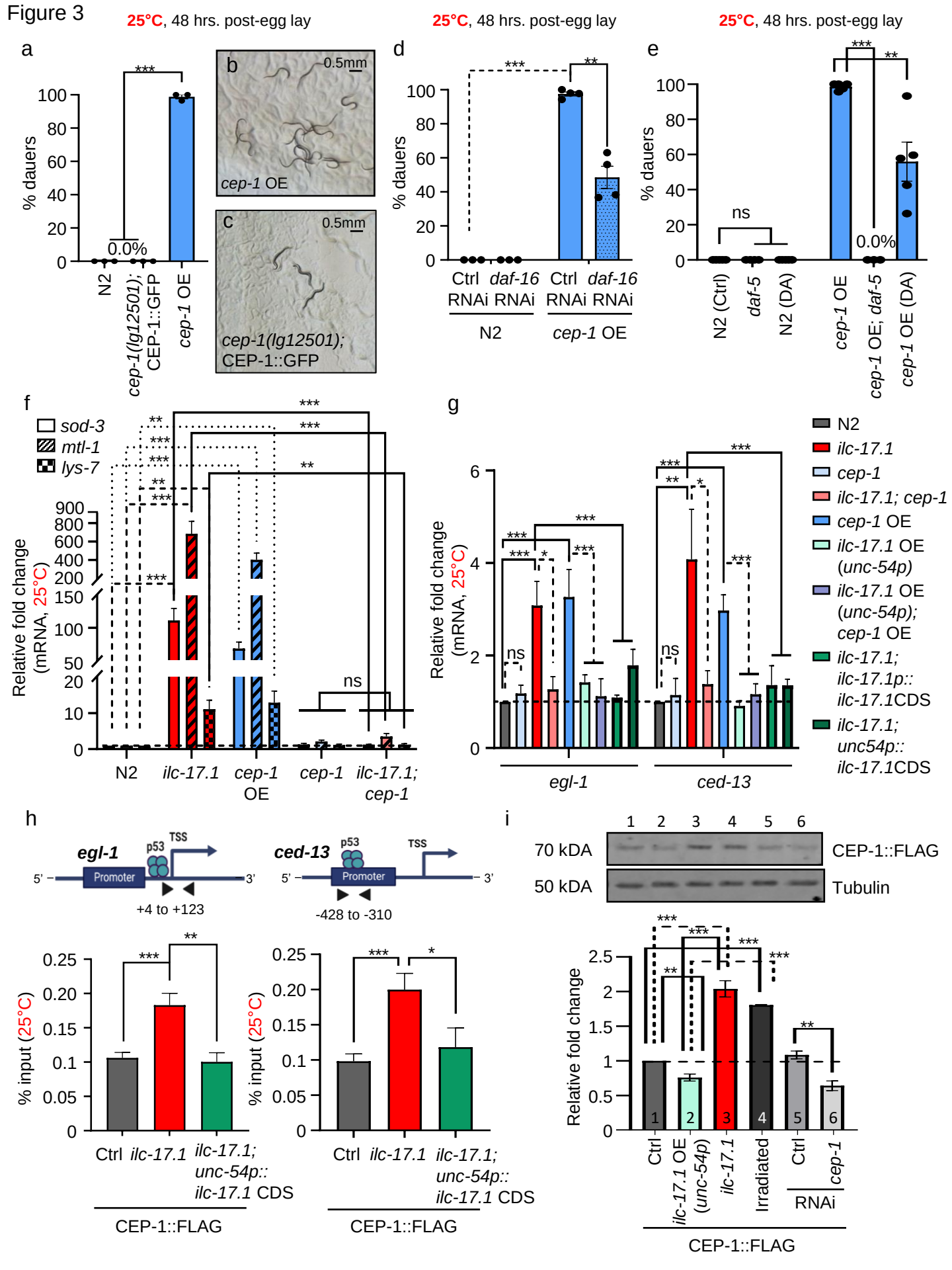
25°C, 48 hrs. post-egg lay
a
% dauers
0.0%
N2
cep-1(lg12501); CEP-1::GFP
cep-1 OE
b
0.5mm
cep-1 OE
c
0.5mm
cep-1(lg12501); CEP-1::GFP
d
Ctrl RNAi
daf-16 RNAi
N2
cep-1 OE
e
ns
N2 (Ctrl)
daf-5
N2 (DA)
cep-1 OE; daf-5
cep-1 OE (DA)
f
sod-3
mtl-1
lys-7
Relative fold change (mRNA, 25°C)
ilc-17.1
cep-1 OE
cep-1
ilc-17.1; cep-1
g
N2
ilc-17.1
cep-1
ilc-17.1; cep-1
cep-1 OE
ilc-17.1 OE (unc-54p)
ilc-17.1 OE (unc-54p); cep-1 OE
ilc-17.1; ilc-17.1p:: ilc-17.1CDS
ilc-17.1; unc54p:: ilc-17.1CDS
egl-1
ced-13
h
egl-1
p53
TSS
Promoter
5'
3'
+4 to +123
ced-13
-428 to -310
% input (25°C)
Ctrl
ilc-17.1
ilc-17.1; unc-54p:: ilc-17.1 CDS
CEP-1::FLAG
i
70 kDA
50 kDA
CEP-1::FLAG
Tubulin
Relative fold change
Ctrl
ilc-17.1 OE (unc-54p)
ilc-17.1
Irradiated
Ctrl
cep-1
RNAi
CEP-1::FLAG

1098 **Figure 3: CEP-1/p53 acts downstream of reduced ILC-17.1 signaling and activates DAF-**
1099 **16/FOXO, DAF-3/SMAD-DAF-5/Ski complex to control dauer entry.**

1100 **a-c. a,** Percent dauers in wildtype (N2), *cep-1 (lg12501)*;CEP-1::GFP animals that do not
1101 overexpress CEP-1/p53, and CEP-1/p53 overexpressing larvae. ***p < 0.001, (n=3-4
1102 experiments, Chi-squared = 569.35, df = 2, p-value < 2.2e-16). For *cep-1* mRNA expression levels
1103 see **Supplementary Fig. S6a**. Representative micrographs 48 hrs. post-hatching at 25°C,
1104 showing in **b,** CEP-1/p53 overexpressing larvae arrested as dauers and **c,** *cep-1 (lg12501)*; CEP-
1105 1::GFP as L4s. Scale bar, 0.5mm.

1106

1107 **d.** Percent dauers in wildtype (N2), and CEP-1/p53 overexpressing larvae on control (Ctrl; L4440)
1108 and *daf-16* RNAi. ***p < 0.001, **p <0.01 (n=3-4 experiments, Chi-squared = 494.22, df = 3, p-
1109 value < 2.2e-16).

1110

1111 **e.** Percent dauers in wildtype (N2), *daf-5* (e1386), CEP-1/p53 overexpressing larvae, CEP-1/p53
1112 overexpressing larvae crossed to *daf-5* (e1386), and N2 and CEP-1/p53 overexpressing larvae
1113 treated with 50nM Δ7-dafachronic acid (DA). ***p < 0.001, **p<0.01, ns, not significant, (n=3-4
1114 experiments, Chi-squared = 982.66, df = 5, p-value < 2.2e-16).

1115

1116 **f**. Average *sod-3, mtl-1, and lys-7* mRNA levels in larvae 32-36 hr. post-hatching at 25°C. mRNA
1117 levels were determined relative to *pmp-3* and normalized to wildtype (N2) values. n=4-10
1118 experiments. ***p < 0.001, **p < 0.01, ns=not significant, (unpaired t-test).

1119

1120 **g**. Average *egl-1* and *ced-13* mRNA levels in 32-36 hr. larvae grown at 25°C. mRNA levels were
1121 determined relative to *pmp-3* and normalized to wildtype (N2) values. n=6-7 experiments.
1122 ***p < 0.001, **p < 0.01, *p < 0.05, ns=not significant, (unpaired t-test).

1123

1124 **h.** CEP-1 occupancy (expressed as percent input) in 32-36 hr. larvae grown at 25°C, measured
1125 at the promoter proximal regions of *egl-1* and *ced-13* (**Top,** schematic). CEP-1 occupancy was
1126 assayed in animals where endogenous *cep-1* was FLAG tagged at its C-terminus using
1127 CRISPR/Cas9, and immunoprecipitated with anti-FLAG antibody. Strains used: CEP-1::FLAG
1128 expressing animals in control wildtype background (Ctrl), in *ilc-17.1* background, and in *ilc-17.1*
1129 rescued from dauer arrest by *unc-54p::ilc-17.1* (*ilc-17.1;unc-54p::ilc-17.1* CDS). n=4 experiments.
1130 ***$p < 0.001$, **$p < 0.01$, *$p < 0.05$. (unpaired t-test).
1131
1132 **i. Top**: Representative Western blot showing CEP-1::FLAG and tubulin when crossed into *unc-*
1133 *54p::ilc-17.1,* and *ilc-17.1* deletion backgrounds. *cep-1* RNAi serves to show specificity. Samples
1134 constitute 32-36 hr. larvae grown at 25°C, except for positive control, irradiated sample (4; adults).
1135 **Bottom**: CEP-1 levels were quantified relative to tubulin and normalized to values from control
1136 animals (Ctrl; CEP-1::FLAG in wildtype background). n=4 experiments. Numbers in data bars
1137 correspond to representative bands on western. ***$p < 0.001$, **$p < 0.01$ (unpaired t-test).
1138
1139 Bars show the mean ± S.E.M. Individual points in bar graphs in **a, d, e** represent the %
1140 dauers/experiment, Pearson's Chi-squaredd test with Yates' continuity correction.
1141
1142

Figure 4

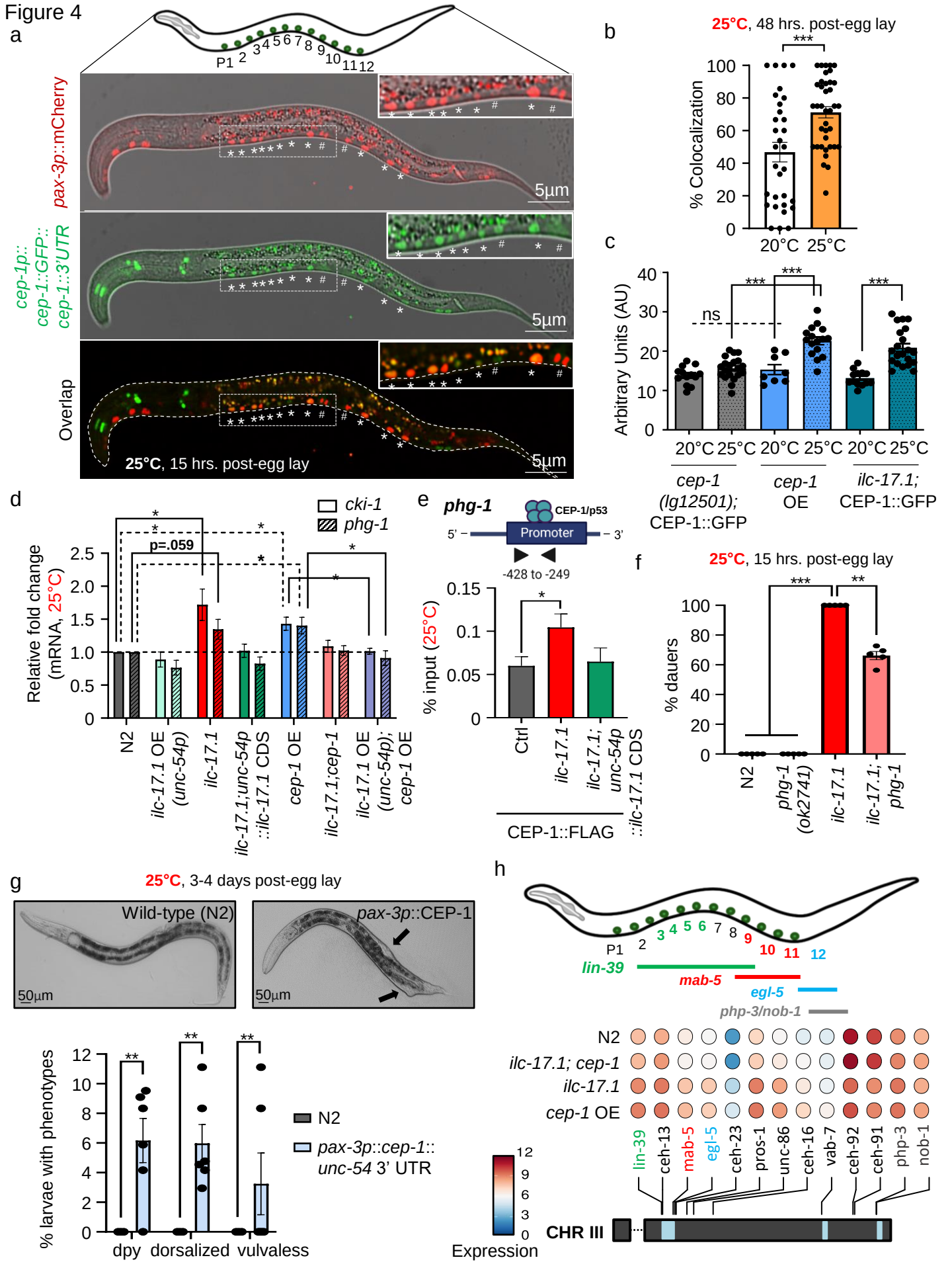
a
P1 2 3 4 5 6 7 8 9 10 11 12
pax-3p::mCherry
cep-1p::
cep-1::GFP::
cep-1::3'UTR
Overlap
5µm
25°C, 15 hrs. post-egg lay
b
25°C, 48 hrs. post-egg lay
% Colocalization
20°C 25°C
c
Arbitrary Units (AU)
ns
20°C 25°C 20°C 25°C 20°C 25°C
cep-1 (lg12501); CEP-1::GFP
cep-1 OE
ilc-17.1; CEP-1::GFP
d
cki-1
phg-1
Relative fold change (mRNA, 25°C)
p=.059
N2
ilc-17.1 OE (unc-54p)
ilc-17.1
ilc-17.1;unc-54p ::ilc-17.1 CDS
cep-1 OE
ilc-17.1;cep-1
ilc-17.1 OE (unc-54p); cep-1 OE
e
phg-1
CEP-1/p53
5' –
Promoter
– 3'
-428 to -249
% input (25°C)
Ctrl
ilc-17.1
ilc-17.1; unc-54p ::ilc-17.1 CDS
CEP-1::FLAG
f
25°C, 15 hrs. post-egg lay
% dauers
N2
phg-1 (ok2741)
ilc-17.1
ilc-17.1; phg-1
g
25°C, 3-4 days post-egg lay
Wild-type (N2)
pax-3p::CEP-1
50µm
% larvae with phenotypes
dpy
dorsalized
vulvaless
N2
pax-3p::cep-1:: unc-54 3' UTR
h
P1 2 3 4 5 6 7 8 9 10 11 12
lin-39
mab-5
egl-5
php-3/nob-1
N2
ilc-17.1; cep-1
ilc-17.1
cep-1 OE
lin-39 ceh-13 mab-5 egl-5 ceh-23 pros-1 unc-86 ceh-16 vab-7 ceh-92 ceh-91 php-3 nob-1
CHR III
Expression

1143 **Figure 4. CEP-1/p53 accumulates in multipotent progenitor cells (P cells) during dauer**
1144 **entry, upregulates cell cycle inhibitors, and modulates cell fate.**
1145 **a.** Representative micrographs of 15 hr. L1 larvae at 25°C, showing *pax-3p::*mCherry marking
1146 ventral postembryonic blast cells (P cells; **top panel**; see schematic above), CEP-1::GFP
1147 expression (**middle panel**), and overlap (**bottom panel**) to show co-localization. Co-localized
1148 cells are marked with *. CEP-1::GFP expressing cells that do not co-localize with *pax-3p*::mCherry
1149 marked with #. Insets: zoom-in on the P blast cells. Scale bar=5um.
1150
1151 **b.** Percent co-localization between *pax-3p::*mCherry-expressing cells and CEP-1::GFP
1152 expressing cells at 20°C and 25°C. n=3 experiments, 10-15 larvae/experiment.***$p < 0.001$,
1153 (unpaired t-test). Each data point represents the percent of *pax-3p;mCherry*-expressing cells that
1154 colocalize with CEP-1::GFP in one animal.
1155
1156 **c.** Fluorescent intensity (arbitrary units; AU) measured in P cells of L1 larvae, 15 hr. post-hatching
1157 at 20°C and 25°C. Strains used: *cep-1* (Ig12501); CEP-1::GFP animals that do not overexpress
1158 CEP-1/p53, CEP-1/p53 overexpressing larvae, and *ilc-17.1* deletion mutants expressing CEP-
1159 1::GFP. n=3 experiments, 5-6 larvae/experiment. ***$p < 0.001$, ns, not significant (unpaired t-test).
1160 Each data point represents the average fluorescence intensity value across five P cells in one
1161 animal (see **Material and Methods**).
1162
1163 **d**. Average *cki-1* and *phg-1* mRNA levels in 32-36 hr. larvae grown at 25°C. mRNA levels were
1164 determined relative to *pmp-3* and normalized to wildtype (N2) values. n=4-6 experiments.
1165 *$p < 0.05$. (unpaired t-test).
1166
1167 **e**. CEP-1 occupancy (expressed as percent input) in 32-36 hr. larvae grown at 25°C, measured
1168 at the promoter proximal region of *phg-1* (**Top,** schematic). CEP-1 occupancy was assayed in

1169 animals where endogenous *cep-1* was FLAG tagged at its C-terminus using CRISPR/Cas9, and
1170 immunoprecipitated with anti-FLAG antibody. Stains used: CEP-1::FLAG expressing animals in
1171 control wildtype background (Ctrl), in *ilc-17.1* background, and in *ilc-17.1* rescued from dauer with
1172 *ilc-17.1; unc-54p::ilc-17.1* CDS. n=4 experiments. *$p < 0.05$. (unpaired t-test).
1173
1174 **f**. Percent dauers in *ilc-17.1* larvae and *ilc-17.1;phg-1* double mutants. **$p < 0.05$, ***$p<0.001$ (n=6
1175 experiments, Chi-squared = 826.95, df = 3, p-value< 2.2e-16). Individual points in the bar graph
1176 represent the % dauers/experiment, Pearson's Chi-squared test with Yates' continuity correction.
1177
1178 **g**. **Top:** Representative micrographs of wildtype (N2) animals and animals overexpressing CEP-
1179 1 driven by the *pax*-3 promoter or 25°C. Scale bar, 50µm. **Bottom:** Percent larvae that displayed
1180 body morphology defects. **$p<0.01$, (unpaired t-test)
1181
1182 **h**. **Top:** Schematic showing homeobox gene expression patterns during post-embryonic
1183 development. **Bottom:** Heatmap depicting expression levels (log_2 normalized counts) of the
1184 homeobox genes on Chromosome III, 32 hrs post-hatching at 25°C, in *ilc-17.1* deletion mutants
1185 and CEP-1 overexpressing larvae that enter dauer, compared to *ilc-17.1; cep-1* double mutants
1186 and wildtype (N2) larvae that continue development. (Also see **Supplementary Table 12**).
1187
1188 Bars show the mean ± S.E.M.
1189
1190

Figure 5

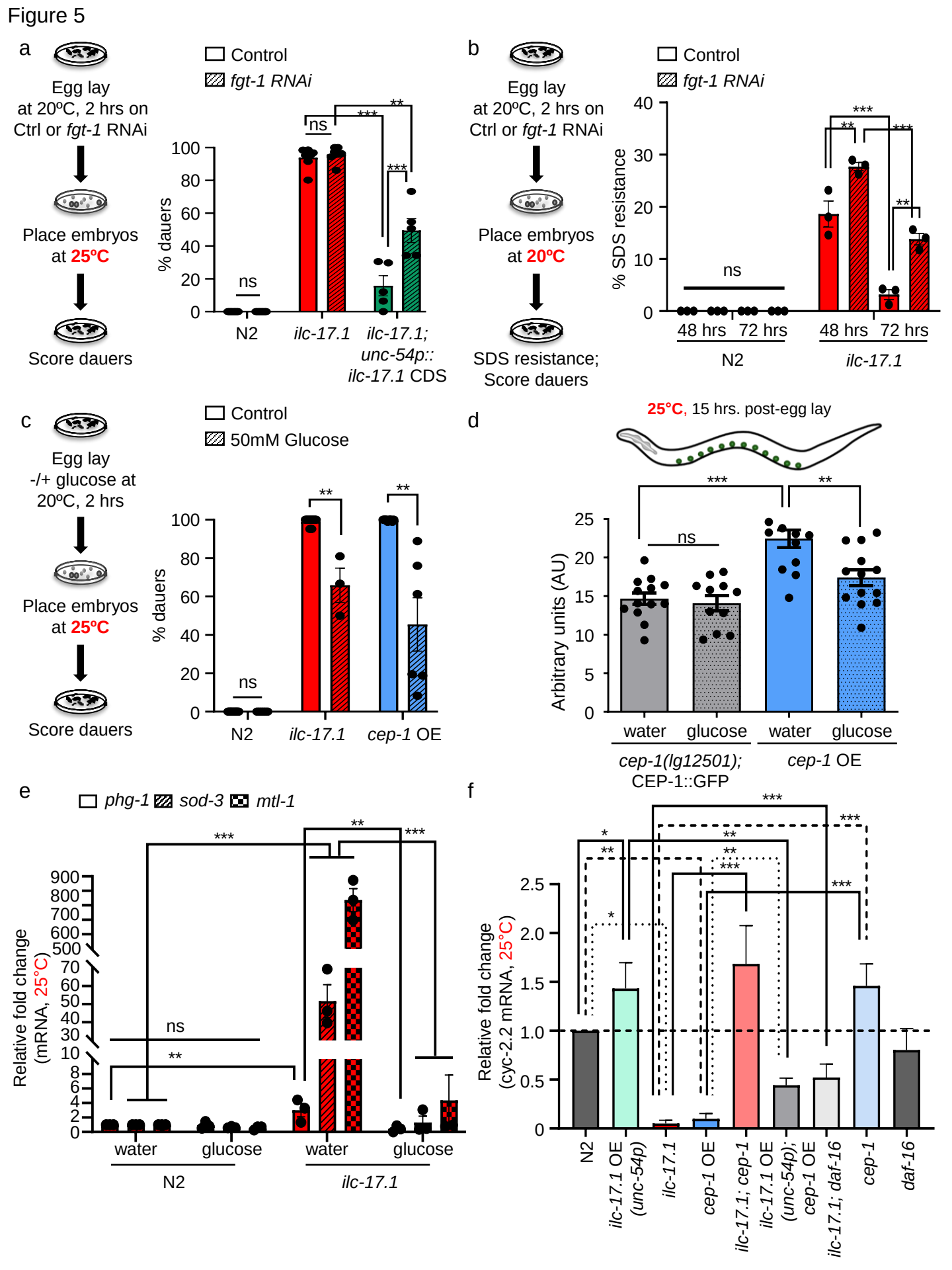
a
Egg lay
at 20ºC, 2 hrs on
Ctrl or fgt-1 RNAi
Place embryos
at 25ºC
Score dauers
Control
fgt-1 RNAi
% dauers
ns
***
**
N2
ilc-17.1
ilc-17.1;
unc-54p::
ilc-17.1 CDS
b
Egg lay
at 20ºC, 2 hrs on
Ctrl or fgt-1 RNAi
Place embryos
at 20ºC
SDS resistance;
Score dauers
% SDS resistance
48 hrs
72 hrs
N2
ilc-17.1
c
Egg lay
-/+ glucose at
20ºC, 2 hrs
Place embryos
at 25ºC
Score dauers
Control
50mM Glucose
cep-1 OE
d
25°C, 15 hrs. post-egg lay
Arbitrary units (AU)
water
glucose
cep-1(lg12501);
CEP-1::GFP
cep-1 OE
e
phg-1
sod-3
mtl-1
Relative fold change
(mRNA, 25°C)
f
Relative fold change
(cyc-2.2 mRNA, 25°C)
N2
ilc-17.1 OE
(unc-54p)
ilc-17.1
cep-1 OE
ilc-17.1; cep-1
ilc-17.1 OE
(unc-54p);
cep-1 OE
ilc-17.1; daf-16
cep-1
daf-16

1191 **Figure 5. Impaired glucose utilization in ILC-17.1 deficient larvae activates CEP-1/p53**
1192 **and decreases the expression of Cytochrome C.**

1193 **a. Left**: Schematic of experimental design. **Right**: Percent dauers at 25°C amongst wildtype (N2),
1194 *ilc-17.* deletion mutants, and *ilc-17.1* deletion mutants rescued by expressing *unc-54p::ilc-17.1* on
1195 Control (L4440) and *fgt-1* RNAi. ***p < 0.001, **p < 0.01, ns, not significant. (n= 5 experiments,
1196 Chi-squared = 1817.1, df = 5, p-value < 2.2e-16).

1197

1198 **b. Left**: Schematic of experimental design. **Right**: Percent SDS (1%)-resistant dauers that
1199 accumulate amongst wildtype (N2) and *ilc-17.1* deletion mutants growing on Control (L4440) and
1200 *fgt-1* RNAi under optimal growth conditions of 20°C. ***p < 0.001, **p < 0.01, ns, not significant.
1201 (n= 3 experiments, Chi-squared = 206.82, df = 7, p-value < 2.2e-16).

1202

1203 **c. Left**: Schematic of experimental design. **Right**: Percent dauers amongst wildtype (N2) larvae,
1204 *ilc-17.1* deletion mutants and CEP-1/p53 overexpressing animals on Control (H_2O) and 50mM
1205 glucose at 25°C. **p < 0.01, ns, not significant. (n= 3-6 experiments, Chi-squared = 2882.3, df =
1206 5, p-value < 2.2e-16).

1207

1208 **d**. Fluorescent intensity (arbitrary units; AU) measured in P cells in L1 larvae on Control (H_2O)
1209 and 50mM glucose, 15 hrs. post-hatching at 25°C. Strains: *cep-1* (lg12501); CEP-1::GFP and
1210 CEP-1/p53 overexpressing larvae. n=2-3 experiments, 3-5 larvae/experiment. ***p < 0.001,
1211 **p < 0.01, ns, not significant (unpaired t-test). Each data point indicates the average fluorescence
1212 intensity value across five P cells in one animal.

1213

1214 **e.** Average *phg-1, sod-3 and mtl-1* mRNA levels in 32-36 hr. larvae that arrest as dauers (on H_2O,
1215 control) and larvae that bypass dauer (50mM glucose) at 25°C. mRNA levels were determined

1216 relative to *pmp-3* and normalized to wildtype (N2) values. n=3 experiments. ***$p < 0.001$, **

1217 $p < 0.01$, ns, not significant (unpaired t-test).

1218

1219 **f**. Average *cyc-2.2* mRNA levels in 32-36 hr. larvae grown at 25°C. mRNA levels were determined

1220 relative to *pmp-3* and normalized to the wildtype (N2) values. n=4-6 experiments. ***$p < 0.001$,

1221 **$p < 0.01$, *$p < 0.05$. (unpaired t-test).

1222

1223 Bars show the mean ± S.E.M. Individual points in the bar graphs in **a, b, c** represent the %

1224 dauers/experiment, Pearson's Chi-squared test with Yates' continuity correction.

1225

Figure 6

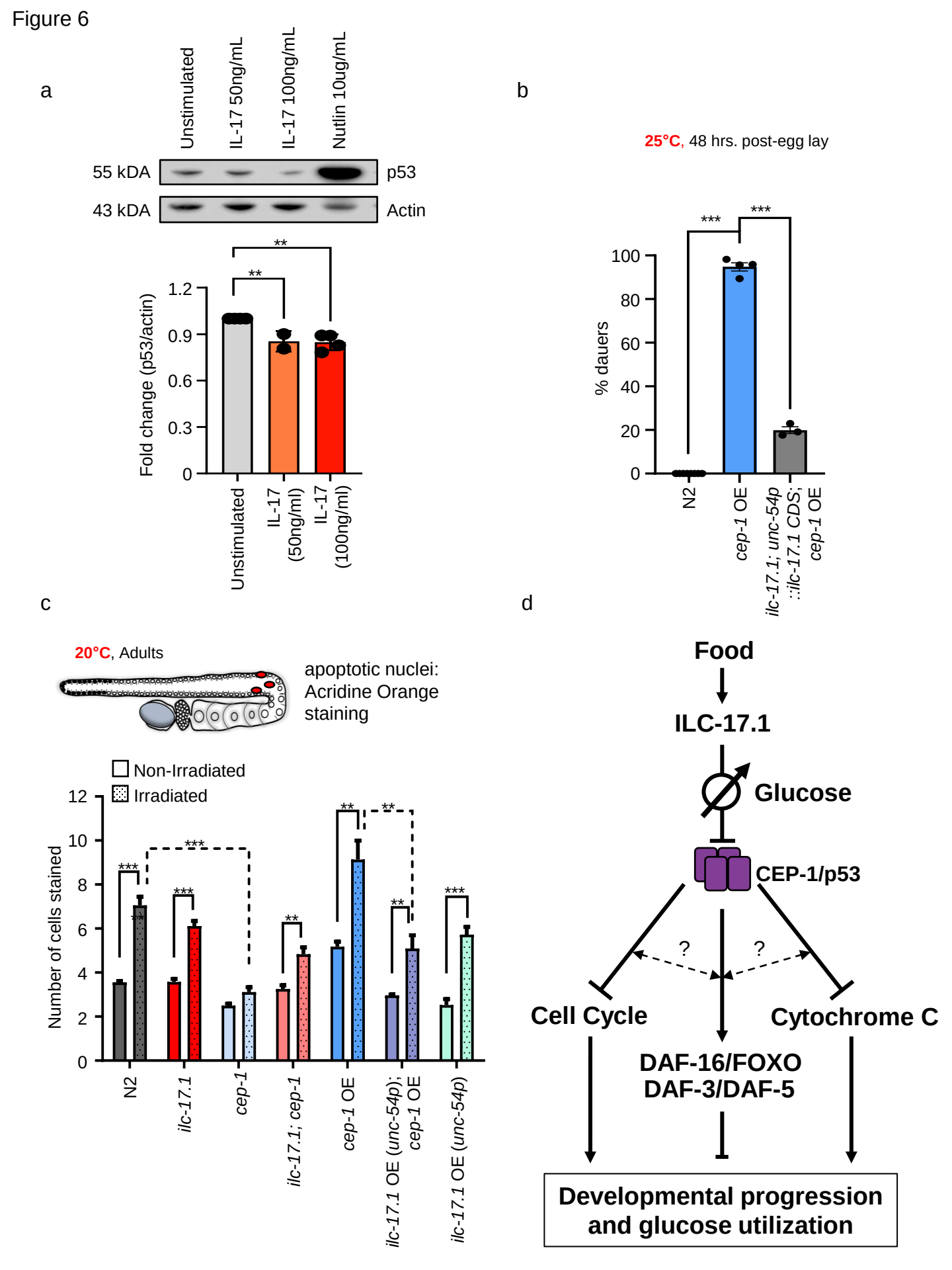
a
Unstimulated
IL-17 50ng/mL
IL-17 100ng/mL
Nutlin 10ug/mL
55 kDA
p53
43 kDA
Actin
Fold change (p53/actin)
1.2
0.9
0.6
0.3
0
**
**
Unstimulated
IL-17 (50ng/ml)
IL-17 (100ng/ml)
b
25°C, 48 hrs. post-egg lay
% dauers
100
80
60
40
20
0
***
***
N2
cep-1 OE
ilc-17.1; unc-54p ::ilc-17.1 CDS; cep-1 OE
c
20°C, Adults
apoptotic nuclei: Acridine Orange staining
Non-Irradiated
Irradiated
Number of cells stained
12
10
8
6
4
2
0
N2
ilc-17.1
cep-1
ilc-17.1; cep-1
cep-1 OE
ilc-17.1 OE (unc-54p); cep-1 OE
ilc-17.1 OE (unc-54p)
d
Food
ILC-17.1
Glucose
CEP-1/p53
?
?
Cell Cycle
Cytochrome C
DAF-16/FOXO
DAF-3/DAF-5
Developmental progression and glucose utilization

1226 **Figure 6: ILC-17.1 suppresses CEP-1/p53 in *C. elegans* and mammalian epithelial cells.**

1227 **a. Top:** Representative Western blot showing p53 levels in A459 epithelial cells stimulated for
1228 18hrs. with increasing doses of rIL-17. β-actin was used as a loading control and Nutlin was used
1229 as a positive control. **Bottom:** Quantification of p53 levels normalized to actin levels. n= 4
1230 independent experiments. **p<0.01. (One-Way ANOVA with uncorrected Fisher's LSD; df=2).

1231

1232 **b.** Percent dauers upon overexpressing ILC-17.1 (expression under the *unc-54* promoter) in *cep-*
1233 *1* overexpressing larvae at 25°C. ***p < 0.001. (n=4 experiments, Chi-squared = 1245.4, df = 2,
1234 p-value < 2.2e-16).

1235

1236 **c. Top:** Schematic of germline apoptosis (apoptotic cells in red) scored with Acridine Orange.
1237 **Bottom:** Average numbers of apoptotic cells in day-two adult animals under control, non-
1238 irradiated conditions, and upon irradiation with 75 Gy (day-one adults were irradiated). n= 3
1239 experiments, and 12 gonad arms/experiment. ***p < 0.001, **p < 0.01 (analysis of variance
1240 (ANOVA) with Tukey's correction, df=13). Note: p values between N2 vs *ilc-17.1* OE (*unc-54p*),
1241 non-irradiated and irradiated are p=0.0192 and p=0.0623, if compared by themselves (unpaired
1242 t-test), but do not rise to significance when corrected for the multiple comparisons.

1243

1244 **d**. Working model: ILC-17.1 secretion from larval amphid neurons that occurs in response to food
1245 availability links cell fate decisions with glucose metabolism and DAF-16, DAF-3/DAF-5 activation
1246 through CEP-1/p53.

1247

1248 Data in all graphs show mean ± S.E.M.

Figure S1

a

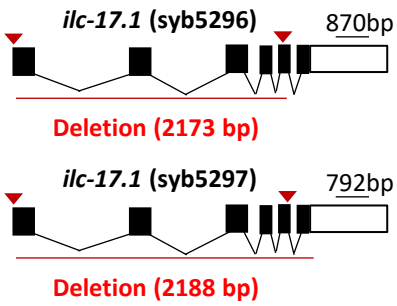

b

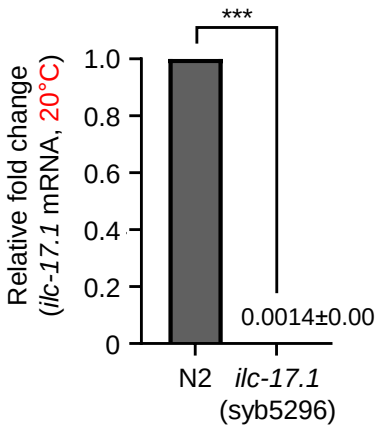

c

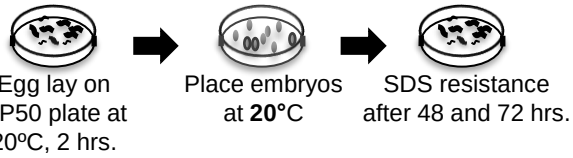

d

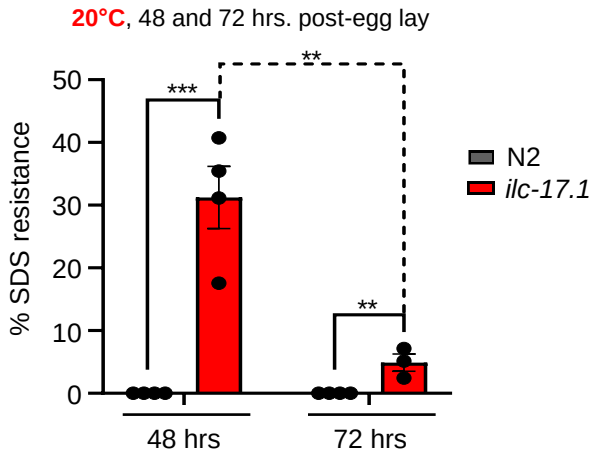

e

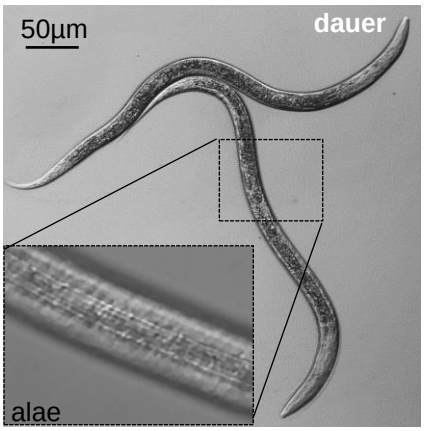

f

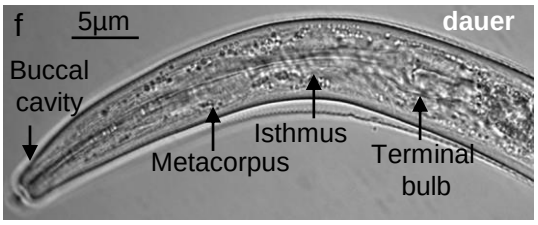

h

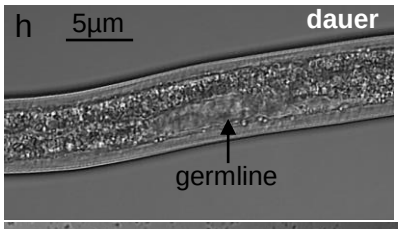

g

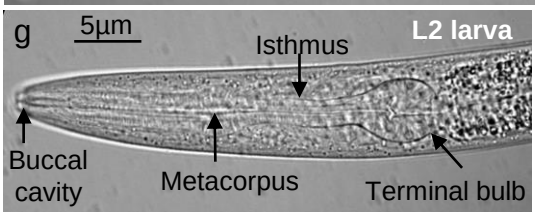

i

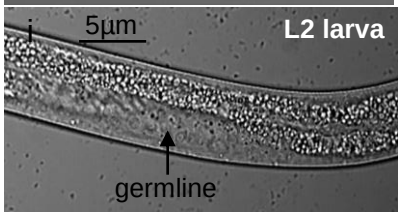

j

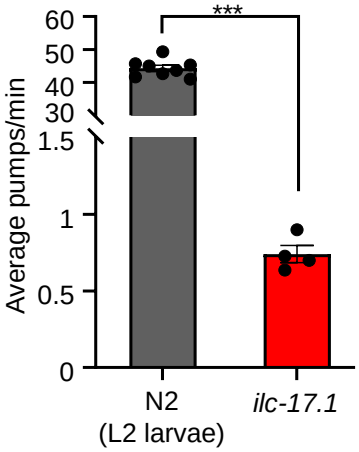

k

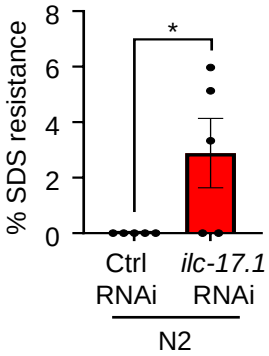

1249 **Supplementary Figure S1: ILC-17.1 modulates *C. elegans* developmental diapause.**

1250 **a.** Schematic of *ilc-17.1* gene depicting the syb5296 and syb5297 deletions made by
1251 CRISPR/Cas9 editing using two distinct guide RNAs. *ilc-17.1* (syb5296) X deletion mutants were
1252 used in all future experiments.

1253

1254 **b.** Average mRNA expression in *ilc-17.1* deletion mutants relative to wildtype (N2). n=4-8
1255 experiments. ***$p < 0.001$ (unpaired t-test,).

1256

1257 **c.** Schematic of experiment leveraging the resistance of dauers to 1% SDS used to identify
1258 dauers developing under optimal growth conditions at 20°C.

1259

1260 **d.** Percent *ilc-17.1* larvae that transiently enter the dauer state as seen by SDS-resistance 48 hrs
1261 and 72 hrs. post-hatching under optimal conditions at 20°C. ***$p < 0.001$, **$p < 0.01$ (n=4
1262 experiments, Chi-squared = 166.53, df = 3, p-value < 2.2e-16).

1263

1264 **e-i.** Representative micrographs showing DIC images of **e**, whole *ilc-17.1* deletion mutant dauer
1265 larvae (inset shows alae), **f,** pharyngeal region and **h,** arrested germline 72 hr. post-hatching at
1266 25°C. Wildtype (N2) larval stage 2 (L2) animals used as comparisons: **g**, pharyngeal region and
1267 **i**, germline. Scale bar, a=50µm, f-i, 5 µm.

1268

1269 **j**. Average pharyngeal pumping rates/minute in *ilc-17.1* deletion mutants relative to wildtype (N2)
1270 larval stage 2 (L2) animals. n=4-8 experiments. ***$p < 0.001$, (unpaired t-test).

1271

1272 **k. Top:** Schematic of experiment. **Bottom:** Percent wildtype (N2) larvae that arrest as dauers as
1273 determined by SDS-resistance, 48 hrs post-hatching on control (Ctrl; L4440) and *ilc-17.1* RNAi at
1274 25°C. *$p < 0.05$. (*n*=5 experiments, Chi-squared = 5.1712, df = 1, p-value = 0.02296).

1275 Bars show the mean ± S.E.M**.** Individual points in the bar graphs in **d, k** represent the %

1276 dauers/experiment, Pearson's Chi-squared test with Yates' continuity correction.

1277

Figure S2

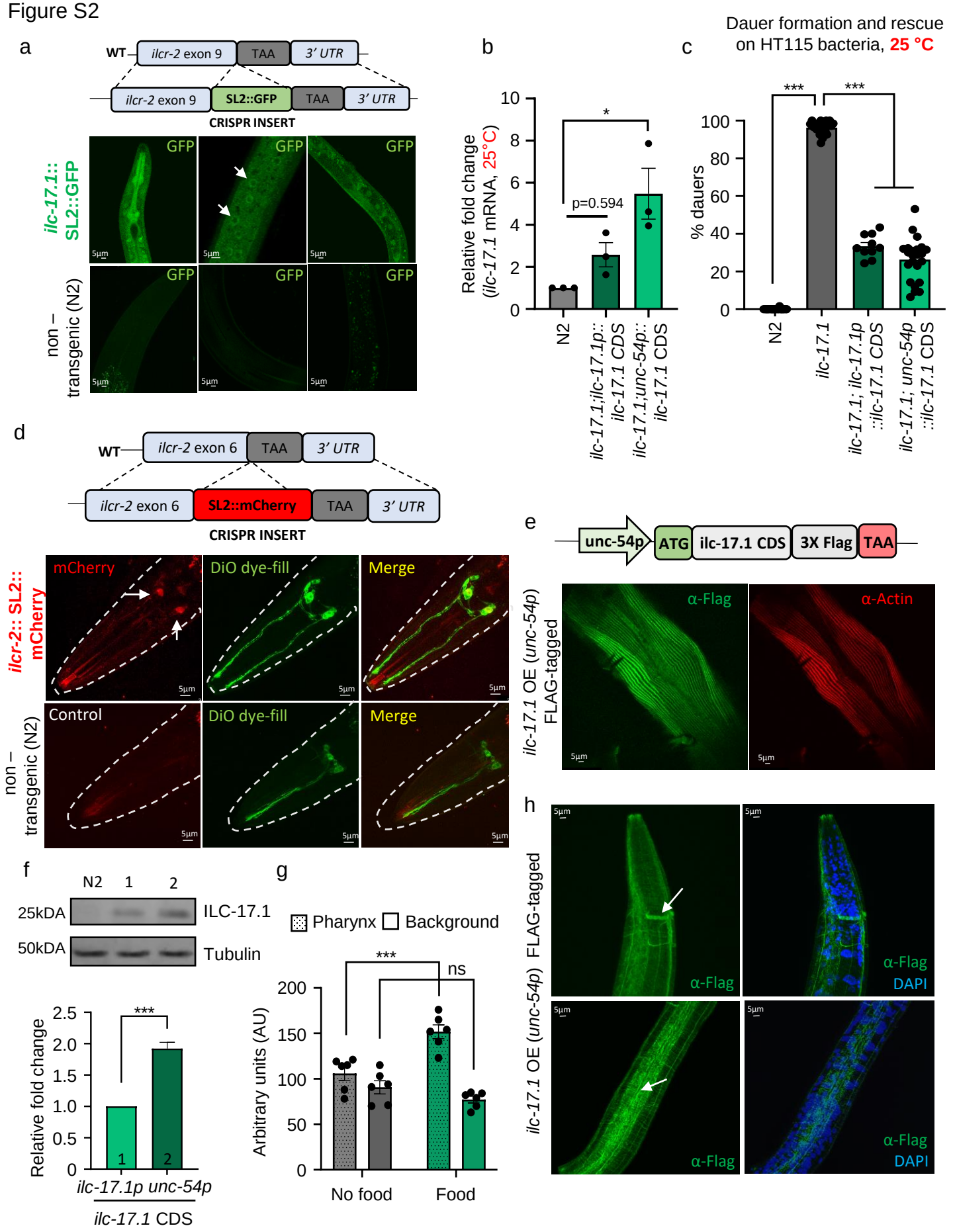
a
WT
ilcr-2 exon 9
TAA
3' UTR
ilcr-2 exon 9
SL2::GFP
TAA
3' UTR
CRISPR INSERT
ilc-17.1:: SL2::GFP
non – transgenic (N2)
GFP
5µm
b
Relative fold change (ilc-17.1 mRNA, 25°C)
p=0.594
*
N2
ilc-17.1;ilc-17.1p:: ilc-17.1 CDS
ilc-17.1;unc-54p:: ilc-17.1 CDS
c
Dauer formation and rescue on HT115 bacteria, 25 °C
% dauers
***
N2
ilc-17.1
ilc-17.1; ilc-17.1p ::ilc-17.1 CDS
ilc-17.1; unc-54p ::ilc-17.1 CDS
d
WT
ilcr-2 exon 6
TAA
3' UTR
ilcr-2 exon 6
SL2::mCherry
TAA
3' UTR
CRISPR INSERT
ilcr-2:: SL2:: mCherry
mCherry
DiO dye-fill
Merge
Control
e
unc-54p
ATG
ilc-17.1 CDS
3X Flag
TAA
ilc-17.1 OE (unc-54p) FLAG-tagged
α-Flag
α-Actin
f
N2
1
2
25kDA
ILC-17.1
50kDA
Tubulin
Relative fold change
***
ilc-17.1p unc-54p
ilc-17.1 CDS
g
Pharynx
Background
Arbitrary units (AU)
***
ns
No food
Food
h
ilc-17.1 OE (unc-54p) FLAG-tagged
α-Flag
DAPI

1278 **Supplementary Figure S2: Characterization of ILC-17.1 signaling pathway components in**
1279 ***C. elegans*.**
1280 **a. Top:** Schematic of CRISPR insertion of SL2::GFP into *ilcr-2* locus to identify sites of *ilcr-2*
1281 expression. **Bottom, Upper panels:** Representative micrographs showing GFP expression in
1282 cells of the pharynx (**left**), epidermis (**middle**; arrows) and gonad (**right**). **Bottom, lower panels:**
1283 Control, wildtype (N2) non-transgenic animals not expressing GFP confirm specificity of GFP
1284 expression. Scale bar=5μm.
1285
1286 **b.** Average expression in *ilc-17.1* mRNA in 32-26 hr. larvae of wildtype (N2), *ilc-17.1* deletion
1287 mutants rescued with *ilc-17.1p::ilc-17.1* and *unc-54p::ilc-17.1*. Values normalized to *pmp-3* and
1288 shown relative to wildtype (N2) values. *$p<0.05$ (unpaired t-test).
1289
1290 **c.** Percentage of wildtype (N2) and *ilc-17.1* larvae that arrest as dauers on control HT115
1291 (L4440) bacteria. ***$p < 0.001$ (n=10-20 experiments, Chi-squared = 3206, df = 3, p-value <
1292 2.2e-16). Representative average numbers of embryos/plates of wildtype (N2), *ilc-17.1*, *ilc-17.1*
1293 rescued with *ilc-17.1p::ilc-17.1*, and *ilc-17.1* rescued with *unc-54p::ilc-17.1* on HT115 (L4440)
1294 bacteria are 59, 66, 66, 46 respectively. Individual points in the bar graphs represent the %
1295 dauers/experiment, Pearson's Chi-squareddtest with Yates' continuity correction.
1296
1297 **d. Top:** Schematic of CRISPR insertion of SL2::mCherry into *ilc-17.1* locus. **Bottom, upper**
1298 **panel**: Representative z-section micrographs showing mCherry expression in amphid neurons
1299 of *C. elegans* expressing mCherry as a bicistronic SL2 cassette along with the endogenous *ilc-*
1300 *17.1* gene to report on sites of *ilc-17.1* mRNA expression. Amphid neurons were identified by
1301 DiO dye filling (green); mCherry overlapped with a subset of DiO filled neurons. **Bottom, lower**
1302 **panel**: Control, wildtype (N2) animals not expressing mCherry confirm specificity of mCherry
1303 expression. Scale bar=5μm.

1304

1305 **e. Top:** Schematic of *ilc-17.1::*flag driven by the *unc-54* promoter [*ilc-17.1* OE *(unc-54p)*] that
1306 was used to rescue *ilc-17.1* deletion mutants to assess ILC-17.1 protein localization. **Bottom:**
1307 Representative micrographs showing a z-section of these animals immunostained with α-FLAG
1308 antibody, and α-actin (to show expression in body wall muscle cells). Scale bar=5μm

1309

1310 **f. Top:** Representative Western blots showing (**upper panel**) expression of ILC-17.1::FLAG
1311 rescue constructs under the *ilc-17.1* promoter (1) and under the *unc-54* promoter (2) in *ilc-17.1*
1312 deletion mutants. Wildtype (N2) were used to show specificity of α-FLAG antibody. (**lower**
1313 **panel**), tubulin. **Bottom:** Quantification of ILC-17.1::FLAG levels in *ilc-17.1* deletion mutant
1314 animals relative to tubulin, and normalized to FLAG levels in (1). n=3 experiments. ***$p < 0.001$
1315 (unpaired t-test).

1316

1317 **g.** Quantification of fluorescent intensity in pharynx versus background (arbitrary units; AU), in
1318 larvae harboring CRISPR tagged endogenous ILC-17.1::HA**,** immunostained with anti-HA
1319 (**Figure 1f)**. n=3 experiments. 5-6 larvae/experiment. ***$p < 0.001$, (unpaired t-test).

1320

1321 Representative micrographs showing z-sections through animals overexpressing ILC-17.1::FLAG
1322 in their body wall muscle cells as in **e**. Note: ILC-17.1::FLAG is detected at the amphid
1323 commissures near the pharynx (**top panel**; arrow) and in the epidermis (**bottom panel**; arrows)
1324 in addition to the body wall muscle cells (**e**), Scale bar=5μm

1325

1326 Bars show the mean ± S.E.M.

1327

1328

Figure S3

a

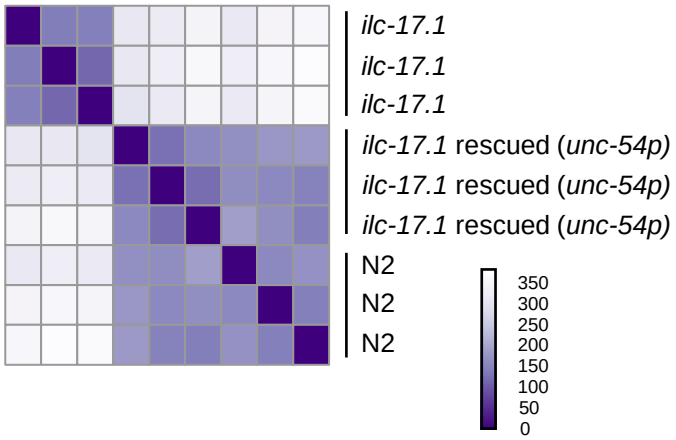

b

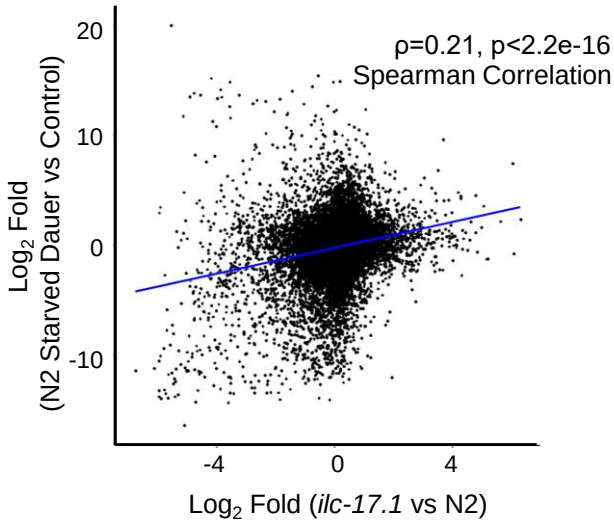

c

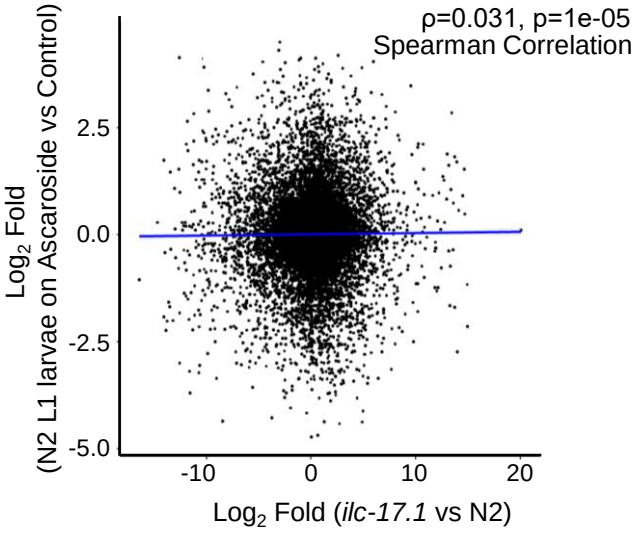

1329 **Supplementary Figure S3: RNA-seq analysis of ILC-17.1 deficient larvae.**

1330 **a.** Pair-wise distance matrix of RNA-seq samples shows the expected clustering of total RNA of
1331 the biological triplicates of each strain [Strains used: wildtype (N2), *ilc-17.1*, and *ilc-17.1* rescued
1332 with *unc-54p::ilc-17.1* CDS]

1333

1334 **b.** Spearman correlation between all genes in a microarray analysis of dauer larvae that were
1335 induced by starvation and *ilc-17.1* deleted larvae *en route* to dauer arrest grown for 32-36 hrs. at
1336 25°C.

1337

1338 **c**. Spearman correlation between all genes in L1 larvae exposed to ascarosides and *ilc-17.1*
1339 deleted larvae *en route* to dauer arrest grown for 32-36 hrs. at 25°C.

1340

Figure S4

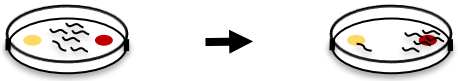

a

Day-one adults placed at center of plate and control (H_2O), OP50, or odor placed at opposite end. Chemotaxis index, after 1 hour

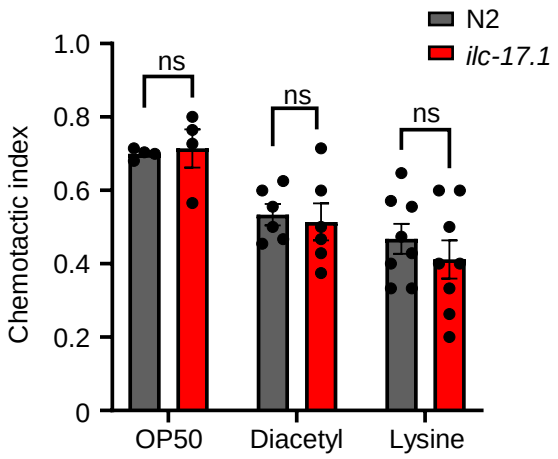

b

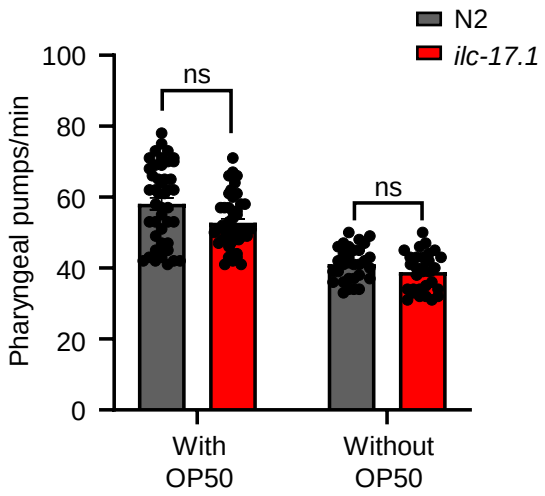

c

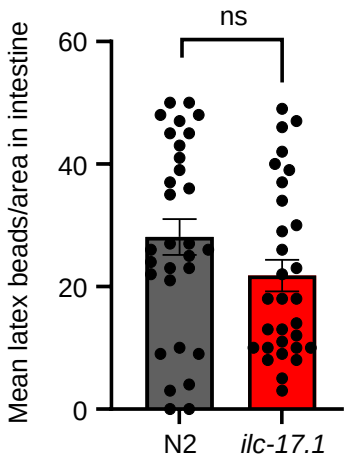

d

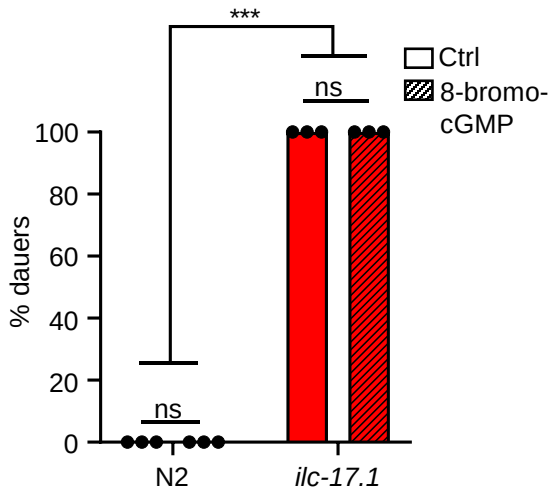

e

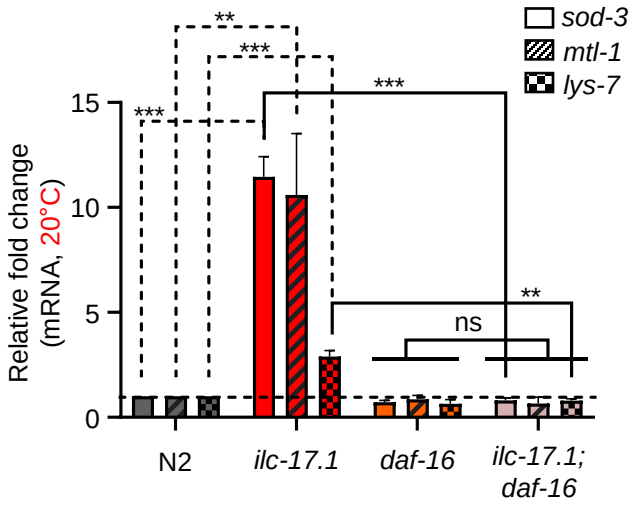

1341 **Supplementary Figure S4: ILC-17.1 loss does not affect the animal's chemotaxis or**
1342 **pumping and is associated with changes in *daf-16* target gene expression.**
1343 **a. Top:** Schematic of experimental design. **Bottom:** Average chemotaxis index towards OP50,
1344 0.01% v/v diacetyl, and 1M lysine for *ilc-17.1* deletion mutants and wildtype (N2) day-one adults
1345 at 20°C. n= 5-8 experiments. ns, not significant (unpaired t-test). Data points: average
1346 chemotaxis/experiment.
1347
1348 **b.** Number of pharyngeal pumps/min in *ilc-17.1* deletion mutants and wildtype (N2) day-one adults
1349 at 20°C, on OP50 lawns, and on plates without food. n=3 experiments, with at least 5
1350 animals/experiment scored. Data points: pumping rates of individual animals. ns, not significant
1351 (unpaired t-test).
1352
1353 **c.** Average numbers of fluorescent latex beads in similar areas of distal gut lumen of 40-hour *ilc-*
1354 *17.1* deletion mutants and wildtype (N2) larvae at 20°C. n=3 experiments, with at least 10
1355 animals/experiment. Data points: the numbers of beads in individual animals. ns, not significant
1356 (unpaired t-test).
1357
1358 **d.** Percent dauers amongst wildtype (N2) and *ilc-17.1* deletion mutants raised on Control (H_2O)
1359 and 5mM 8-bromo-cGMP at 25°C. ***$p < 0.001$, Pearson's Chi-squared test with Yates
1360 correction, (n=3 experiments. Chi squared = 798, df = 3, p-value <2e-16.). Individual points in
1361 the bar graphs represent the % dauers/experiment,
1362
1363 **e.** Average *sod-3, mtl-1, and lys-7* mRNA levels in 40 hr. old larvae grown at 20°C. mRNA levels
1364 were determined relative to *pmp-3* and normalized to wildtype (N2) values. n=3 experiments.
1365 ***$p < 0.001$, **$p < 0.01$, ns, not significant (unpaired t-test).
1366

1367 Data in all graphs show mean ± S.E.M.

1368

Figure S5

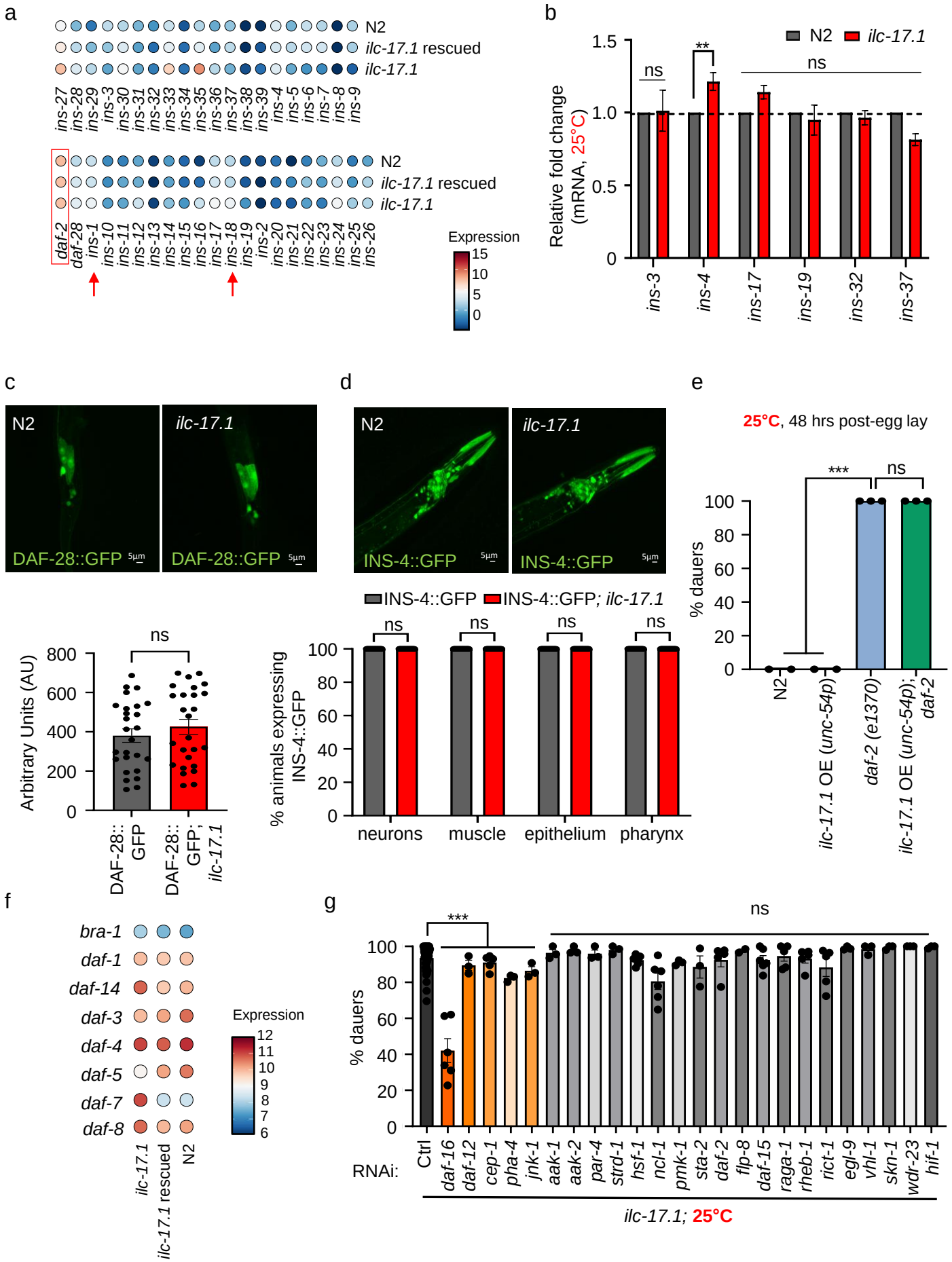
a
N2
ilc-17.1 rescued
ilc-17.1
ins-27 ins-28 ins-29 ins-3 ins-30 ins-31 ins-32 ins-33 ins-34 ins-35 ins-36 ins-37 ins-38 ins-39 ins-4 ins-5 ins-6 ins-7 ins-8 ins-9
daf-2 daf-28 ins-1 ins-10 ins-11 ins-12 ins-13 ins-14 ins-15 ins-16 ins-17 ins-18 ins-19 ins-2 ins-20 ins-21 ins-22 ins-23 ins-24 ins-25 ins-26
Expression
15
10
5
0
b
N2
ilc-17.1
Relative fold change (mRNA, 25°C)
1.5
1.0
0.5
0
ns
**
ns
ins-3
ins-4
ins-17
ins-19
ins-32
ins-37
c
N2
ilc-17.1
DAF-28::GFP
5µm
Arbitrary Units (AU)
800
600
400
200
0
ns
DAF-28::GFP
DAF-28::GFP; ilc-17.1
d
N2
ilc-17.1
INS-4::GFP
INS-4::GFP; ilc-17.1
% animals expressing INS-4::GFP
100
80
60
40
20
0
ns
neurons
muscle
epithelium
pharynx
e
25°C, 48 hrs post-egg lay
% dauers
***
ns
N2
ilc-17.1 OE (unc-54p)
daf-2 (e1370)
ilc-17.1 OE (unc-54p); daf-2
f
bra-1
daf-1
daf-14
daf-3
daf-4
daf-5
daf-7
daf-8
ilc-17.1
ilc-17.1 rescued
N2
Expression
12
11
10
9
8
7
6
g
% dauers
***
ns
RNAi:
Ctrl
daf-16
daf-12
cep-1
pha-4
jnk-1
aak-1
aak-2
par-4
strd-1
hsf-1
ncl-1
pmk-1
sta-2
daf-2
flp-8
daf-15
raga-1
rheb-1
rict-1
egl-9
vhl-1
skn-1
wdr-23
hif-1
ilc-17.1; 25°C

1369 **Supplementary Figure S5: ILC-17.1 deficiency does not alter the expression levels of**
1370 **Insulin signaling- or TGFβ signaling- pathway components.**
1371 **a.** Heatmap depicting expression levels (log_2 normalized counts) of *daf-2* (boxed) and insulin
1372 ligands in the *ilc-17.1* deletion mutants, *ilc-17.1* deletion mutants rescued by *unc-54p::ilc-17.1* and
1373 wildtype (N2). Arrows highlight lack of changes in *ins-1* and *ins-18* mRNA. RNA-seq data from
1374 larvae grown for 32-36 hrs. at 25°C.
1375
1376 **b.** Average mRNA levels (insulins) in 32-36 hr. larvae grown at 25°C. mRNA levels were
1377 determined relative to *pmp-3* and normalized to wildtype (N2) values. n=3 experiments.
1378 **$p < 0.001$, ns, not significant (unpaired t-test).
1379
1380 **c. Top**: Representative micrographs showing DAF-28::GFP expression in the last intestinal cell
1381 of 32-36hr. larvae at 25°C of *ilc-17.1* deletion mutants and wildtype (N2). Images are projections
1382 of confocal z-sections. Scale bar: 5μm. **Bottom:** Quantification of fluorescent intensity (arbitrary
1383 units, AU) of DAF-28::GFP. n=3 experiments. Data points: the fluorescence intensity of DAF-
1384 28::GFP in individual animals. ns, not significant (unpaired t-test).
1385
1386 **d. Top**: Representative micrographs showing INS-4::GFP expression in the pharynx and
1387 neurons of 32-36 hr. larvae at 25°C in *ilc-17.1* deletion mutants and wildtype (N2). Images are
1388 projections of confocal z-sections. Scale bar: 5μm. **Bottom:** Bars represent percent larvae that
1389 express GFP in the different tissues where INS-4 is known to be expressed. n=3 experiments of
1390 5-10 larvae of each strain. ns, not significant (unpaired t-test).
1391
1392 **e.** Overexpressing ILC-17.1 under *unc-54p::ilc-17.1* CDS [*ilc-17.1* OE (*unc-54p)*] in *daf-2*
1393 (e1370) III strains does not rescue their dauer arrest. ***$p < 0.001$, ns, not significant (n=3
1394 experiments, Chi-squared = 521, df = 3, p-value < 2.2e-16).

1395

1396 **f.** Heatmap depicting expression levels (log_2 normalized counts) of TGFβ signaling pathway
1397 components in the *ilc-17.1* deletion mutants, *ilc-17.1* deletion mutants rescued by *unc-54p::ilc-*
1398 *17.1*, and wildtype (N2).

1399

1400 **g.** Percent dauers in *ilc-17.1* deletion mutant larvae following RNAi-mediated downregulation of
1401 several genes known to interact with DAF-16 and DAF3/DAF-5. *daf-16* RNAi was used as a
1402 positive control. ***$p < 0.001$, ns, not significant. (*n=3*-5 experiments, Chi-squared = 156.66, df =
1403 3, p-value < 2.2e-16).

1404

1405 Data in all graphs show mean ± S.E.M. Individual points in the bar graphs in **e**, **g**, represent the
1406 % dauers/experiment, Pearson's Chi-squared test with Yates' continuity correction.

1407

Figure S6

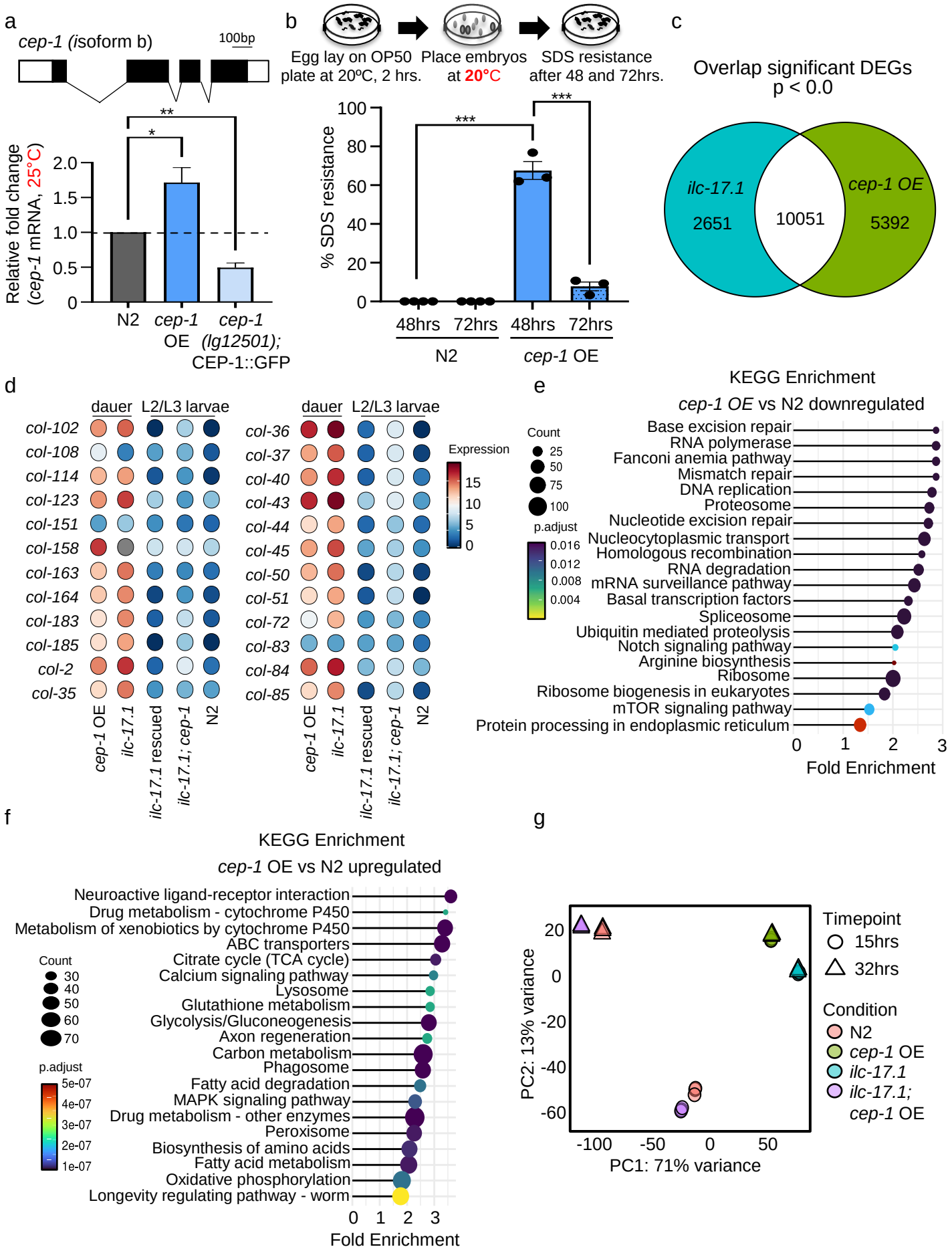
a
cep-1 (isoform b)
100bp
Relative fold change (cep-1 mRNA, 25°C)
2.0
1.5
1.0
0.5
0
**
*
N2
cep-1 OE
cep-1 (lg12501); CEP-1::GFP
b
Egg lay on OP50 plate at 20ºC, 2 hrs.
Place embryos at 20°C
SDS resistance after 48 and 72hrs.
% SDS resistance
100
80
60
40
20
0
***
***
48hrs
72hrs
48hrs
72hrs
N2
cep-1 OE
c
Overlap significant DEGs
p < 0.0
ilc-17.1
2651
10051
cep-1 OE
5392
d
dauer
L2/L3 larvae
col-102
col-108
col-114
col-123
col-151
col-158
col-163
col-164
col-183
col-185
col-2
col-35
col-36
col-37
col-40
col-43
col-44
col-45
col-50
col-51
col-72
col-83
col-84
col-85
cep-1 OE
ilc-17.1
ilc-17.1 rescued
ilc-17.1; cep-1
N2
Expression
15
10
5
0
e
KEGG Enrichment
cep-1 OE vs N2 downregulated
Count
25
50
75
100
p.adjust
0.016
0.012
0.008
0.004
Base excision repair
RNA polymerase
Fanconi anemia pathway
Mismatch repair
DNA replication
Proteosome
Nucleotide excision repair
Nucleocytoplasmic transport
Homologous recombination
RNA degradation
mRNA surveillance pathway
Basal transcription factors
Spliceosome
Ubiquitin mediated proteolysis
Notch signaling pathway
Arginine biosynthesis
Ribosome
Ribosome biogenesis in eukaryotes
mTOR signaling pathway
Protein processing in endoplasmic reticulum
0
1
2
3
Fold Enrichment
f
KEGG Enrichment
cep-1 OE vs N2 upregulated
Count
30
40
50
60
70
p.adjust
5e-07
4e-07
3e-07
2e-07
1e-07
Neuroactive ligand-receptor interaction
Drug metabolism - cytochrome P450
Metabolism of xenobiotics by cytochrome P450
ABC transporters
Citrate cycle (TCA cycle)
Calcium signaling pathway
Lysosome
Glutathione metabolism
Glycolysis/Gluconeogenesis
Axon regeneration
Carbon metabolism
Phagosome
Fatty acid degradation
MAPK signaling pathway
Drug metabolism - other enzymes
Peroxisome
Biosynthesis of amino acids
Fatty acid metabolism
Oxidative phosphorylation
Longevity regulating pathway - worm
0
1
2
3
Fold Enrichment
g
PC2: 13% variance
20
0
-20
-40
-60
-100
-50
0
50
PC1: 71% variance
Timepoint
15hrs
32hrs
Condition
N2
cep-1 OE
ilc-17.1
ilc-17.1; cep-1 OE

1408 **Supplementary Figure S6: CEP-1/p53 overexpression induces dauer arrest.**

1409 **a. Top:** Schematic of *cep-1* mRNA, isoform b. **Bottom:** Average *cep-1* isoform b mRNA levels in
1410 32-36 hr. larvae grown at 25°C. mRNA levels were determined relative to *pmp-3* and normalized
1411 to wildtype (N2) values. *n*=3 experiments. **p < 0.001, *p < 0.05 (unpaired t-test).

1412

1413 **b. Top:** Schematic of SDS treatment to assess dauer formation at 20°C. **Bottom:** Percent of
1414 wildtype (N2) and *cep-1* overexpressing larvae (*cep-1* OE) that enter a dauer state during
1415 development, 48 hrs. and 72 hrs. post-hatching at 20°C. ***p < 0.001, (n=3 experiments, Chi-
1416 squared = 414.65, df = 3, p-value < 2.2e-16). Individual points in the bar graphs represent the %
1417 dauers/experiment, Pearson's Chi-squared test with Yates' continuity correction.

1418

1419 **c**. Venn diagram depicting overlap between significantly differentially expressed genes (p<0.05)
1420 in *ilc-17.1* deletion mutants and CEP-1/p53 overexpressing larvae, 32-36 hr. post-hatching at
1421 25°C *en route* to dauer entry. p=0.0; hypergeometric test (Also see **Supplementary Tables 9,**
1422 **10**)

1423

1424 **d**. Heatmap comparing expression levels (log_2 normalized counts) of the major dauer-specific
1425 collagens in the *ilc-17.1* deletion mutants, CEP-1/p53 overexpressing larvae, *ilc-17.1; cep-1*
1426 double mutants, *ilc-17.1* deletion mutants rescued by *unc-54p::ilc-17.1,* and wildtype (N2).

1427

1428 **e.** KEGG enrichments associated with differentially downregulated genes (p.adjust <0.05) in CEP-
1429 1/p53 overexpressing larvae [RNA-seq: 32-36 hr. larvae grown at 25°C; **Supplementary Tables**
1430 **9**].

1431

1432 **f**. KEGG enrichments associated with differentially upregulated genes (padjust <0.05) in CEP-
1433 1/p53 overexpressing larvae [RNA-seq: 32-36 hr. larvae grown at 25°C; **Supplementary Tables**
1434 **9**].
1435
1436 **g.** Principle Component Analysis **(PCA)** of the observed variance in the triplicate RNA-seq
1437 samples collected during development, 15 hrs. and 32 hrs. post-hatching at 25°C, of *ilc-17.1*
1438 deletion mutants, CEP-1/p53 overexpressing larvae, *ilc-17.1; cep-1* double mutants and
1439 wildtype (N2) larvae (**Supplementary Tables 9).**.
1440
1441 Data in all graphs show mean ± S.E.M.

Figure S7

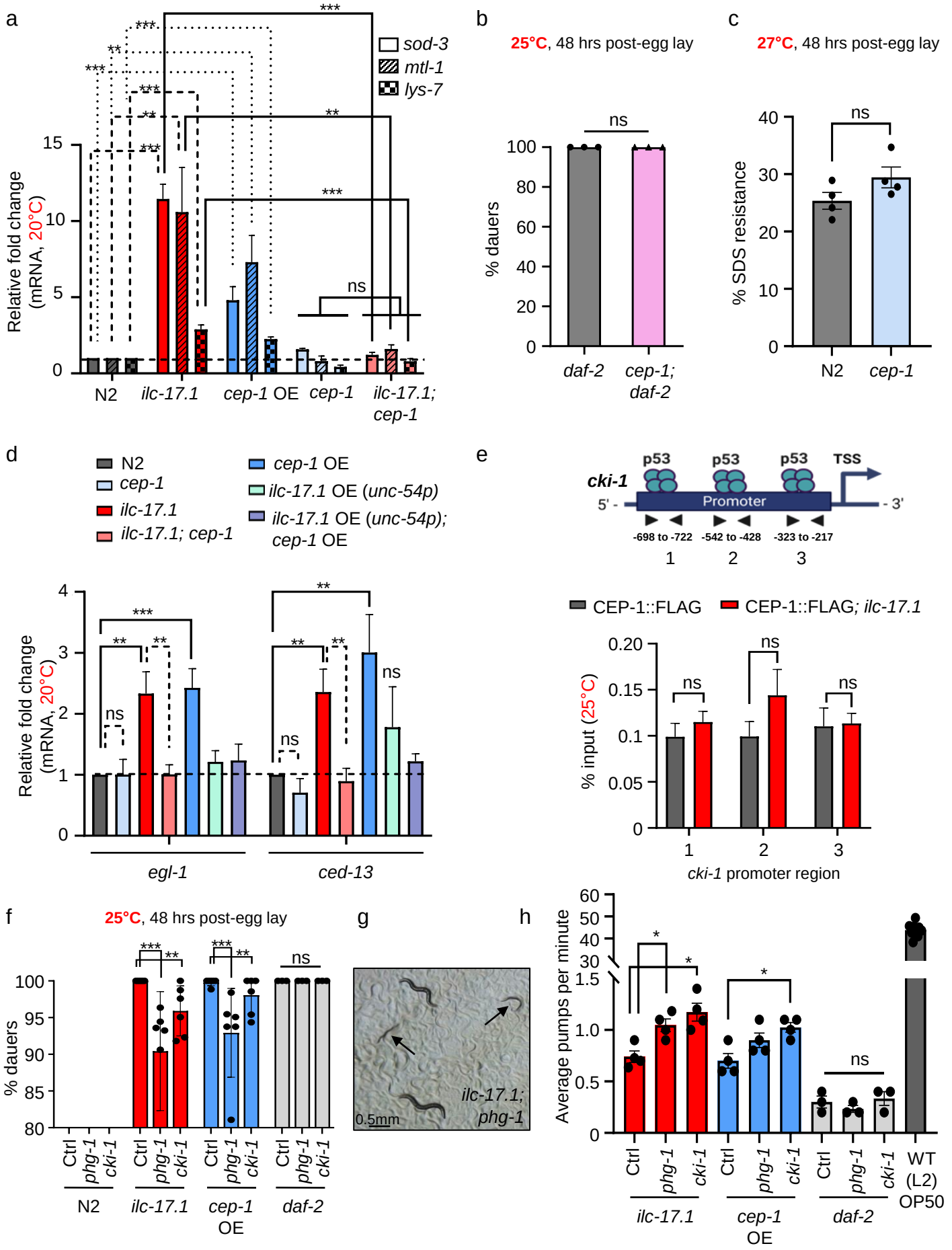
a
sod-3
mtl-1
lys-7
Relative fold change (mRNA, 20°C)
N2
ilc-17.1
cep-1 OE
cep-1
ilc-17.1; cep-1
ns
b
25°C, 48 hrs post-egg lay
% dauers
daf-2
cep-1; daf-2
c
27°C, 48 hrs post-egg lay
% SDS resistance
N2
cep-1
d
N2
cep-1
ilc-17.1
ilc-17.1; cep-1
cep-1 OE
ilc-17.1 OE (unc-54p)
ilc-17.1 OE (unc-54p); cep-1 OE
Relative fold change (mRNA, 20°C)
egl-1
ced-13
e
cki-1
p53
TSS
Promoter
5' -
- 3'
-698 to -722
-542 to -428
-323 to -217
1
2
3
CEP-1::FLAG
CEP-1::FLAG; ilc-17.1
% input (25°C)
cki-1 promoter region
f
25°C, 48 hrs post-egg lay
% dauers
Ctrl
phg-1
cki-1
N2
ilc-17.1
cep-1 OE
daf-2
g
ilc-17.1; phg-1
0.5mm
h
Average pumps per minute
WT (L2) OP50

1442 **Supplementary Figure S7: CEP-1/p53 overexpression upregulates DAF-16/FOXO targets**
1443 **and cell cycle inhibitors to induce dauer arrest.**
1444 Average *sod-3, mtl-1, and lys-7* mRNA levels in 40 hr. larvae grown at 20°C. mRNA levels were
1445 determined relative to *pmp-3* and normalized to wildtype (N2) values. Strains used are on X-axis.
1446 n=6-10 experiments. ***$p < 0.001$, **$p < 0.01$, ns, not significant. (unpaired t-test).
1447
1448 **b.** Percent dauers in *daf-2* and *cep-1;daf-2* double mutants. Note: no rescue. n=3 experiments.
1449 ns, not significant. (Chi-squared = Not appropriate, df = 1, p-value = no significant)
1450
1451 **c.** Percent high temperature (27.5°C; HID phenotype) dauers in wildtype (N2) and *cep-1* deletion
1452 mutants. ns, not significant. (n=4 experiments, Chi-squared = 0.67295, df = 1, p-value = 0.412).
1453
1454 **d.** Average *egl-1* and *ced-13* mRNA levels in 40 hr. larvae grown at 20°C. mRNA levels were
1455 determined relative to *pmp-3* and normalized to wildtype (N2) values. n=6-7 experiments.
1456 ***$p < 0.001$, **$p < 0.01$, ns, not significant (unpaired t-test).
1457
1458 **e.** CEP-1 occupancy (expressed as percent input) in 32-36 hr. larvae grown at 25°C, measured
1459 at three promoter proximal regions of *cki-1* (Schematic on **top**). Strains used: CEP-1::FLAG
1460 expressing animals in wildtype background (Ctrl), in *ilc-17.1* deletion background. n=4
1461 experiments. ns, not significant. (unpaired t-test).
1462
1463 **f.** Percent dauers in *ilc-17.1* larvae, CEP-1/p53 overexpressing larvae and *daf-2* larvae upon RNAi
1464 induced downregulation of *cki-1* and *phg-1.* ***$p < 0.001$, **$p < 0.01$, ns, not significant (n=6
1465 experiments, Chi-squared = 7443.7, df = 14, p-value < 2.2e-16).
1466

1467 **g**. Representative micrograph of *ilc-17.1; phg-1* double mutants showing the dauer rescue of
1468 some individuals but not others (dauers marked with arrow).
1469
1470 **h.** Average pumps/minute in *ilc-17.1, cep-1 and daf-2* dauers when subjected to control (L4440;
1471 Ctrl), *cki-1* and *phg-1* RNAi. n= 4 experiments, and 10 dauers were scored per experiment.
1472 *$p < 0.05$, ns, not significant (unpaired t-test). Pumping rates in wildtype (N2), L2 larvae are shown
1473 for comparison.
1474
1475 Data in all graphs show mean ± S.E.M. Individual points in the bar graphs in **b**, **c**, **f**, represent
1476 the % dauers/experiment, Pearson's Chi-squared test with Yates' continuity correction.
1477

Figure S8

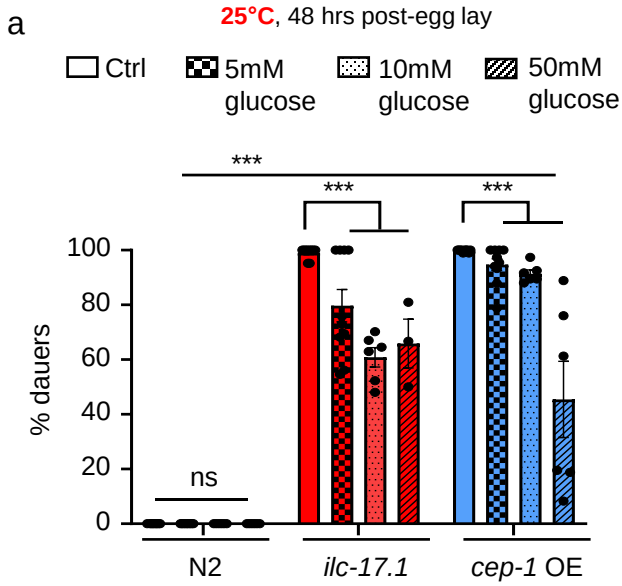
a
25°C, 48 hrs post-egg lay
Ctrl
5mM glucose
10mM glucose
50mM glucose
***
***
***
ns
% dauers
100
80
60
40
20
0
N2
ilc-17.1
cep-1 OE

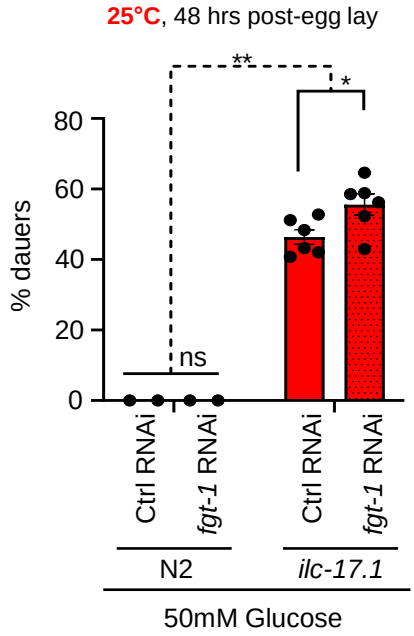
25°C, 48 hrs post-egg lay
b
**
*
ns
% dauers
80
60
40
20
0
Ctrl RNAi
fgt-1 RNAi
Ctrl RNAi
fgt-1 RNAi
N2
ilc-17.1
50mM Glucose

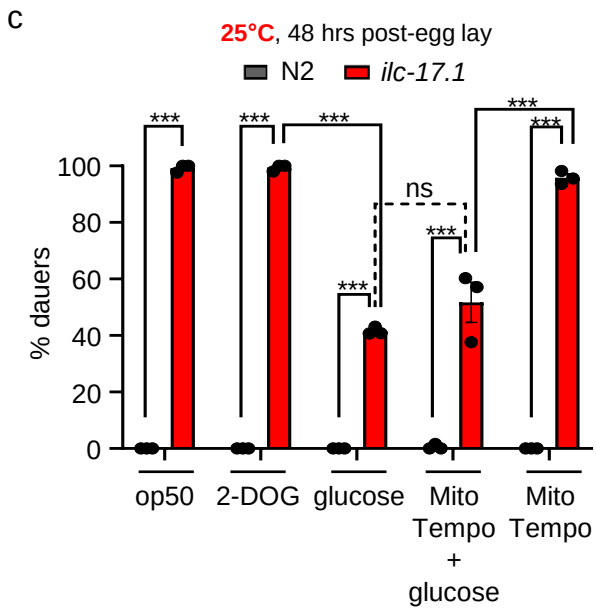
c
25°C, 48 hrs post-egg lay
N2
ilc-17.1
***
***
***
***
***
***
ns
% dauers
100
80
60
40
20
0
op50
2-DOG
glucose
Mito Tempo + glucose
Mito Tempo

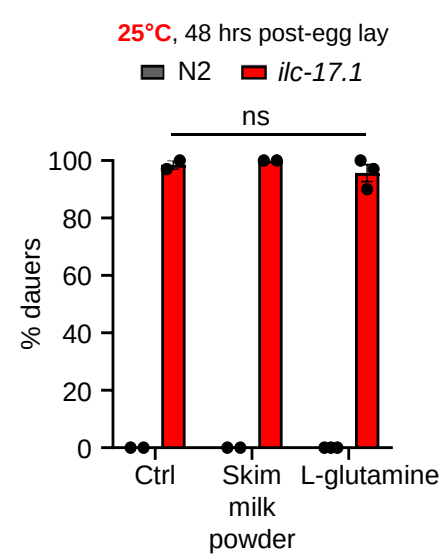
d
25°C, 48 hrs post-egg lay
N2
ilc-17.1
ns
% dauers
100
80
60
40
20
0
Ctrl
Skim milk powder
L-glutamine

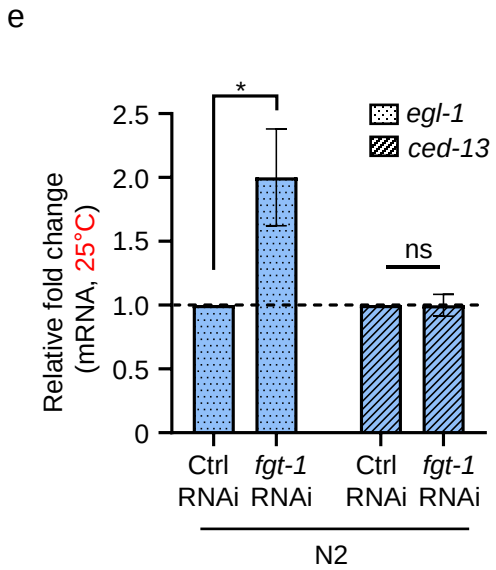
e
*
egl-1
ced-13
ns
Relative fold change (mRNA, 25°C)
2.5
2.0
1.5
1.0
0.5
0
Ctrl RNAi
fgt-1 RNAi
Ctrl RNAi
fgt-1 RNAi
N2

1478 **Supplementary Figure S8: CEP-1/p53 activity can be repressed by glucose**
1479 **supplementation.**

1480 **a.** Percent dauers amongst *ilc-17.1* deletion mutants, CEP-1/p53 overexpressing larvae and
1481 wildtype (N2) larvae on 5 mM, 10mM and 50 mM glucose at 25°C. ***p < 0.001, **p < 0.01, ns, not
1482 significant. (*n*= 5-9 experiments, Chi-squared = 5263.6, df = 11, p-value < 2.2e-16)

1483

1484 **b.** Percent dauers amongst *ilc-17.1* deletion mutants and wildtype (N2) larvae on 50mM glucose
1485 on Control (Ctrl; L4440) and *fgt-1* RNAi. **p < 0.01, *p < 0.05, ns, not significant. (*n*=6 experiments,
1486 Chi-squared = 299.36, df = 3, p-value < 2.2e-16).

1487

1488 **c.** Percent dauers amongst *ilc-17.1* deletion mutants and wildtype (N2) larvae upon exposure to
1489 50mM DOG, 50mM glucose, and 0.1mM MitoTEMPO at 25°C (see X-axis for different conditions).
1490 ***p < 0.001, ns, not significant, (n=3- experiments, Chi-squared = 1251.7, df = 9, p-value < 2.2e-
1491 16).

1492

1493 **d.** Percent dauers amongst *ilc-17.1* deletion mutants and wildtype (N2) larvae on 20mM Skim
1494 Milk powder and 0.26 mM L-Glutamine at 25°C. ns, not significant, (n=3 experiments, Chi-squared
1495 = 648.89, df = 5, p-value < 2.2e-16).

1496

1497 **e.** Average mRNA levels of *egl-1* and *ced-13* in wildtype (N2) larvae subjected to Control (Ctrl;
1498 L4440) and *fgt-1* RNAi. mRNA levels were determined relative to *pmp-3* and normalized to
1499 wildtype (N2) values. *n=3* experiments, *p < 0.05, ns, not significant (unpaired t-test).

1500

1501 Data in all graphs show mean ± S.E.M. Individual points in the bar graphs in **a-d** represent the %
1502 dauers/experiment, Pearson's Chi-squared test with Yates' continuity correction.

1503

Figure S9

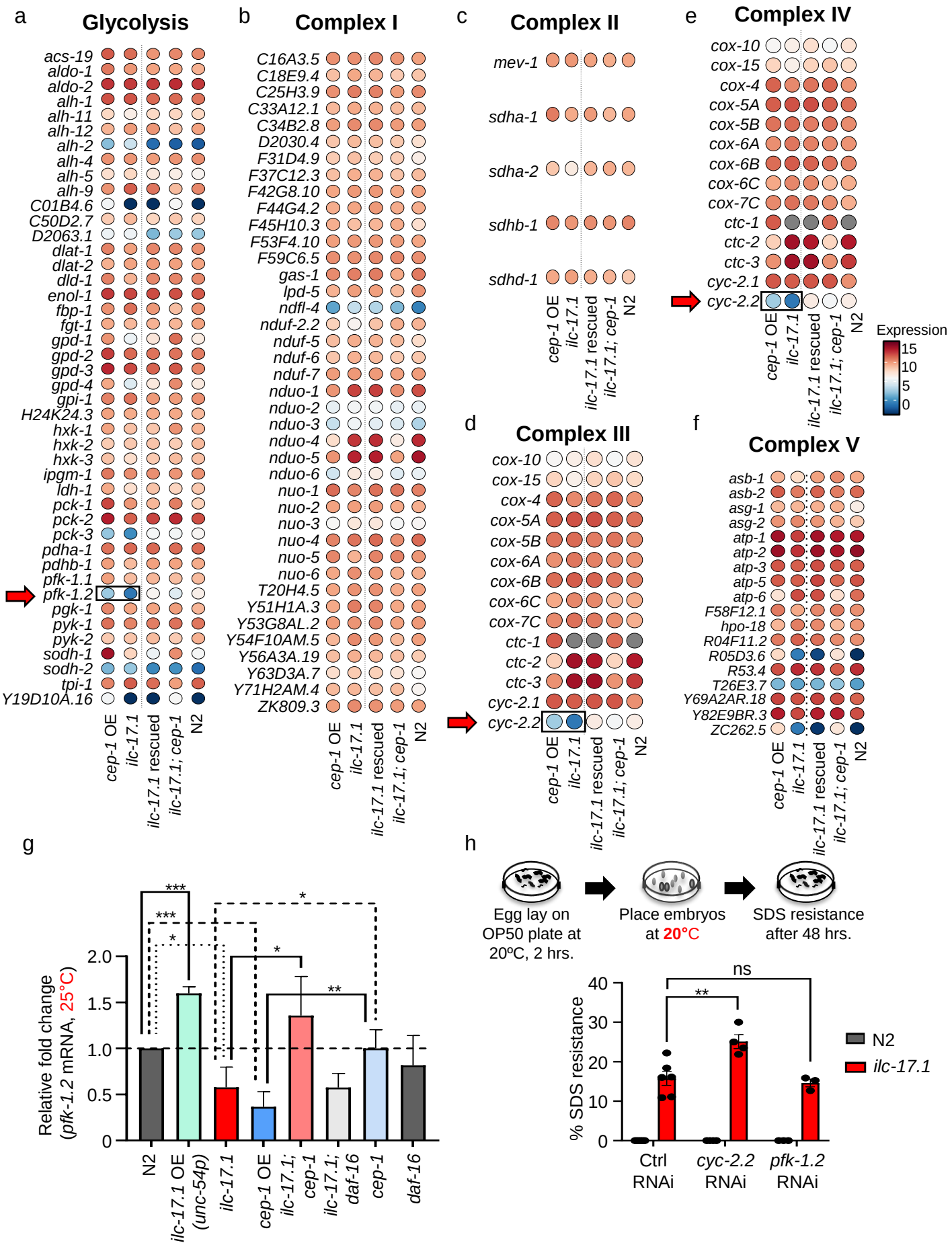
a
Glycolysis
acs-19
aldo-1
aldo-2
alh-1
alh-11
alh-12
alh-2
alh-4
alh-5
alh-9
C01B4.6
C50D2.7
D2063.1
dlat-1
dlat-2
dld-1
enol-1
fbp-1
fgt-1
gpd-1
gpd-2
gpd-3
gpd-4
gpi-1
H24K24.3
hxk-1
hxk-2
hxk-3
ipgm-1
ldh-1
pck-1
pck-2
pck-3
pdha-1
pdhb-1
pfk-1.1
pfk-1.2
pgk-1
pyk-1
pyk-2
sodh-1
sodh-2
tpi-1
Y19D10A.16
cep-1 OE
ilc-17.1
ilc-17.1 rescued
ilc-17.1; cep-1
N2
b
Complex I
C16A3.5
C18E9.4
C25H3.9
C33A12.1
C34B2.8
D2030.4
F31D4.9
F37C12.3
F42G8.10
F44G4.2
F45H10.3
F53F4.10
F59C6.5
gas-1
lpd-5
ndfl-4
nduf-2.2
nduf-5
nduf-6
nduf-7
nduo-1
nduo-2
nduo-3
nduo-4
nduo-5
nduo-6
nuo-1
nuo-2
nuo-3
nuo-4
nuo-5
nuo-6
T20H4.5
Y51H1A.3
Y53G8AL.2
Y54F10AM.5
Y56A3A.19
Y63D3A.7
Y71H2AM.4
ZK809.3
c
Complex II
mev-1
sdha-1
sdha-2
sdhb-1
sdhd-1
e
Complex IV
cox-10
cox-15
cox-4
cox-5A
cox-5B
cox-6A
cox-6B
cox-6C
cox-7C
ctc-1
ctc-2
ctc-3
cyc-2.1
cyc-2.2
Expression
15
10
5
0
d
Complex III
f
Complex V
asb-1
asb-2
asg-1
asg-2
atp-1
atp-2
atp-3
atp-5
atp-6
F58F12.1
hpo-18
R04F11.2
R05D3.6
R53.4
T26E3.7
Y69A2AR.18
Y82E9BR.3
ZC262.5
g
Relative fold change
(pfk-1.2 mRNA, 25°C)
2.0
1.5
1.0
0.5
0
***
***
*
*
*
**
N2
ilc-17.1 OE
(unc-54p)
ilc-17.1
cep-1 OE
ilc-17.1;
cep-1
ilc-17.1;
daf-16
cep-1
daf-16
h
Egg lay on
OP50 plate at
20ºC, 2 hrs.
Place embryos
at 20°C
SDS resistance
after 48 hrs.
% SDS resistance
40
30
20
10
0
ns
**
N2
ilc-17.1
Ctrl
RNAi
cyc-2.2
RNAi
pfk-1.2
RNAi

1504 **Supplementary Figure S9: ILC-17.1 deficiency and CEP-1/p53 overexpression modulate**
1505 **key glucose metabolic enzymes.**
1506 **a-f**. Heatmap depicting expression levels (log_2 normalized counts) of glycolysis and mitochondrial
1507 OXPHOS genes in the *ilc-17.1* deletion mutants, CEP-1/p53 overexpressing animals, *ilc-17.1;*
1508 *cep-1* double mutants, *ilc-17.1* rescued with *unc-54p::ilc-17.1*, and wildtype (N2). Arrows:
1509 highlight decreases in *pfk-1.2* and *cyc-2.2* mRNA levels in *ilc-17.1* deleted and CEP-1/p53
1510 overexpressing larvae (Boxed). RNA-seq data was collected as previously described.
1511
1512 **g**. Average *pfk-1.2* mRNA levels in 32-36 hr. old larvae grown at 25°C. mRNA levels were
1513 determined relative to *pmp-3* and normalized to wildtype (N2) values. Strain names on X-axis.
1514 n=4-6 experiments. ***$p < 0.001$, **$p < 0.01$, *$p < 0.05$. (unpaired t-test).
1515
1516 **h. Top:** Schematic of SDS treatment to assess dauer formation at 20°C. **Bottom:** Percent of
1517 wildtype (N2) and *ilc-17.1* deletion mutant larvae that enter a dauer state at 20°C, 48 hr. post-
1518 hatching, when subjected to control (Ctrl; L4440), *cyc-2.2* and *pfk-1.2* RNAi. **$p < 0.01$, ns, not
1519 significant (*n*=3-4 experiments, Chi-squared = 213.38, df = 5, p-value < 2.2e-16) . Individual
1520 points in the bar graphs represent the % dauers/experiment, Pearson's Chi-squared test with
1521 Yates' continuity correction.
1522
1523 Data in all graphs show mean ± S.E.M.

Figure S10

a

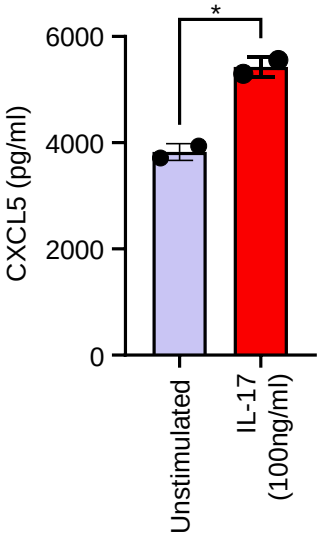

1524 **Supplementary Figure S10: rIL-17 induces the expected cytokine response in human**
1525 **epithelial cells.**
1526 **a.** Soluble CXCL5 levels in the supernatant of A459 epithelial cells stimulated for 18hrs. with rIL-
1527 17 measured by ELISA. Data is a summary of 2 independent experiments, performed in
1528 triplicates. *$p<0.05$, (unpaired t-test). Data show mean ± S.E.M.
1529
1530
1531
1532
1533
1534
1535

1536 References

1537

1538 1. Golden, J.W. & Riddle, D.L. The Caenorhabditis elegans dauer larva: developmental
1539 effects of pheromone, food, and temperature. *Dev Biol* **102**, 368-78 (1984).
1540 2. Swanson, M.M. & Riddle, D.L. Critical periods in the development of the Caenorhabditis
1541 elegans dauer larva. *Dev Biol* **84**, 27-40 (1981).
1542 3. Hu, P.J. Dauer. *WormBook*, 1-19 (2007).
1543 4. Karp, X. Working with dauer larvae. *WormBook* **2018**, 1-19 (2018).
1544 5. Fielenbach, N. & Antebi, A. C. elegans dauer formation and the molecular basis of
1545 plasticity. *Genes Dev* **22**, 2149-65 (2008).
1546 6. Burnell, A.M., Houthoofd, K., O'Hanlon, K. & Vanfleteren, J.R. Alternate metabolism during
1547 the dauer stage of the nematode Caenorhabditis elegans. *Exp Gerontol* **40**, 850-6 (2005).
1548 7. Rashid, S., Wong, C. & Roy, R. Developmental plasticity and the response to nutrient
1549 stress in Caenorhabditis elegans. *Dev Biol* **475**, 265-276 (2021).
1550 8. Cohen, S.M., Wrobel, C.J.J., Prakash, S.J., Schroeder, F.C. & Sternberg, P.W. Formation
1551 and function of dauer ascarosides in the nematodes Caenorhabditis briggsae and
1552 Caenorhabditis elegans. *G3 (Bethesda)* **12**(2022).
1553 9. Braendle, C., Milloz, J. & Felix, M.A. Mechanisms and evolution of environmental
1554 responses in Caenorhabditis elegans. *Curr Top Dev Biol* **80**, 171-207 (2008).
1555 10. Diaz, S.A. & Viney, M. The evolution of plasticity of dauer larva developmental arrest in
1556 the nematode Caenorhabditis elegans. *Ecol Evol* **5**, 1343-53 (2015).
1557 11. Ewald, C.Y., Landis, J.N., Porter Abate, J., Murphy, C.T. & Blackwell, T.K. Dauer-
1558 independent insulin/IGF-1-signalling implicates collagen remodelling in longevity. *Nature*
1559 **519**, 97-101 (2015).
1560 12. Harvey, S.C., Shorto, A. & Viney, M.E. Quantitative genetic analysis of life-history traits of
1561 Caenorhabditis elegans in stressful environments. *BMC Evol Biol* **8**, 15 (2008).

1562 13. Zhu, J. & Thompson, C.B. Metabolic regulation of cell growth and proliferation. *Nat Rev*
1563 *Mol Cell Biol* **20**, 436-450 (2019).
1564 14. Altan-Bonnet, G. & Mukherjee, R. Cytokine-mediated communication: a quantitative
1565 appraisal of immune complexity. *Nat Rev Immunol* **19**, 205-217 (2019).
1566 15. Mills, K.H.G. IL-17 and IL-17-producing cells in protection versus pathology. *Nat Rev*
1567 *Immunol* (2022).
1568 16. Li, X., Bechara, R., Zhao, J., McGeachy, M.J. & Gaffen, S.L. IL-17 receptor-based
1569 signaling and implications for disease. *Nat Immunol* **20**, 1594-1602 (2019).
1570 17. Hall, P.A. & Lane, D.P. Tumor suppressors: a developing role for p53? *Curr Biol* **7**, R144-
1571 7 (1997).
1572 18. Jain, A.K. & Barton, M.C. p53: emerging roles in stem cells, development and beyond.
1573 *Development* **145**(2018).
1574 19. Levine, A.J. p53: 800 million years of evolution and 40 years of discovery. *Nat Rev Cancer*
1575 **20**, 471-480 (2020).
1576 20. Rutkowski, R., Hofmann, K. & Gartner, A. Phylogeny and function of the invertebrate p53
1577 superfamily. *Cold Spring Harb Perspect Biol* **2**, a001131 (2010).
1578 21. Lu, W.J., Amatruda, J.F. & Abrams, J.M. p53 ancestry: gazing through an evolutionary
1579 lens. *Nat Rev Cancer* **9**, 758-62 (2009).
1580 22. Bowen, M.E., Mulligan, A.S., Sorayya, A. & Attardi, L.D. Puma- and Caspase9-mediated
1581 apoptosis is dispensable for p53-driven neural crest-based developmental defects. *Cell*
1582 *Death Differ* **28**, 2083-2094 (2021).
1583 23. Van Nostrand, J.L. *et al.* Inappropriate p53 activation during development induces features
1584 of CHARGE syndrome. *Nature* **514**, 228-32 (2014).
1585 24. Chen, C. *et al.* IL-17 is a neuromodulator of Caenorhabditis elegans sensory responses.
1586 *Nature* **542**, 43-48 (2017).

1587 25. Flynn, S.M. *et al.* MALT-1 mediates IL-17 neural signaling to regulate C. elegans behavior,
1588 immunity and longevity. *Nat Commun* **11**, 2099 (2020).
1589 26. Lillis, M., Zaccardi, N.J. & Heiman, M.G. Axon-dendrite and apical-basolateral sorting in a
1590 single neuron. *Genetics* **221**(2022).
1591 27. Golden, J.W. & Riddle, D.L. A pheromone-induced developmental switch in
1592 Caenorhabditis elegans: Temperature-sensitive mutants reveal a wild-type temperature-
1593 dependent process. *Proc Natl Acad Sci U S A* **81**, 819-23 (1984).
1594 28. Thomas, J.H., Birnby, D.A. & Vowels, J.J. Evidence for parallel processing of sensory
1595 information controlling dauer formation in Caenorhabditis elegans. *Genetics* **134**, 1105-17
1596 (1993).
1597 29. Vowels, J.J. & Thomas, J.H. Genetic analysis of chemosensory control of dauer formation
1598 in Caenorhabditis elegans. *Genetics* **130**, 105-23 (1992).
1599 30. Ailion, M. & Thomas, J.H. Isolation and characterization of high-temperature-induced
1600 Dauer formation mutants in Caenorhabditis elegans. *Genetics* **165**, 127-44 (2003).
1601 31. Holt, S.J. Staying alive in adversity: transcriptome dynamics in the stress-resistant dauer
1602 larva. *Funct Integr Genomics* **6**, 285-99 (2006).
1603 32. Cohen, S.M., Sun, J.J., Schroeder, F.C. & Sternberg, P.W. Transcriptional Response to a
1604 Dauer-Inducing Ascaroside Cocktail in Late L1 in C. elegans. *MicroPubl Biol* **2021**(2021).
1605 33. Wang, J. & Kim, S.K. Global analysis of dauer gene expression in Caenorhabditis elegans.
1606 *Development* **130**, 1621-34 (2003).
1607 34. Wirick, M.J. *et al.* daf-16/FOXO blocks adult cell fate in Caenorhabditis elegans dauer
1608 larvae via lin-41/TRIM71. *PLoS Genet* **17**, e1009881 (2021).
1609 35. Kyani-Rogers, T. *et al.* Developmental history modulates adult olfactory behavioral
1610 preferences via regulation of chemoreceptor expression in Caenorhabditiselegans.
1611 *Genetics* **222**(2022).

1612 36. Ow, M.C., Borziak, K., Nichitean, A.M., Dorus, S. & Hall, S.E. Early experiences mediate
1613 distinct adult gene expression and reproductive programs in Caenorhabditis elegans.
1614 *PLoS Genet* **14**, e1007219 (2018).
1615 37. Bargmann, C.I. Chemosensation in C. elegans. *WormBook*, 1-29 (2006).
1616 38. Motola, D.L. *et al.* Identification of ligands for DAF-12 that govern dauer formation and
1617 reproduction in C. elegans. *Cell* **124**, 1209-23 (2006).
1618 39. Vowels, J.J. & Thomas, J.H. Multiple chemosensory defects in daf-11 and daf-21 mutants
1619 of Caenorhabditis elegans. *Genetics* **138**, 303-16 (1994).
1620 40. Lin, K., Dorman, J.B., Rodan, A. & Kenyon, C. daf-16: An HNF-3/forkhead family member
1621 that can function to double the life-span of Caenorhabditis elegans. *Science* **278**, 1319-22
1622 (1997).
1623 41. Libina, N., Berman, J.R. & Kenyon, C. Tissue-specific activities of C. elegans DAF-16 in
1624 the regulation of lifespan. *Cell* **115**, 489-502 (2003).
1625 42. Lee, S.S., Kennedy, S., Tolonen, A.C. & Ruvkun, G. DAF-16 target genes that control C.
1626 elegans life-span and metabolism. *Science* **300**, 644-7 (2003).
1627 43. Kenyon, C. & Murphy, C.T. Enrichment of regulatory motifs upstream of predicted DAF-
1628 16 targets. *Nat Genet* **38**, 397-8; author reply 398 (2006).
1629 44. da Graca, L.S. *et al.* DAF-5 is a Ski oncoprotein homolog that functions in a neuronal TGF
1630 beta pathway to regulate C. elegans dauer development. *Development* **131**, 435-46
1631 (2004).
1632 45. Pierce, S.B. *et al.* Regulation of DAF-2 receptor signaling by human insulin and ins-1, a
1633 member of the unusually large and diverse C. elegans insulin gene family. *Genes Dev* **15**,
1634 672-86 (2001).
1635 46. Ritter, A.D. *et al.* Complex expression dynamics and robustness in C. elegans insulin
1636 networks. *Genome Res* **23**, 954-65 (2013).

1637 47. Gems, D. *et al.* Two pleiotropic classes of daf-2 mutation affect larval arrest, adult
1638 behavior, reproduction and longevity in Caenorhabditis elegans. *Genetics* **150**, 129-55
1639 (1998).
1640 48. Zecic, A. & Braeckman, B.P. DAF-16/FoxO in Caenorhabditis elegans and Its Role in
1641 Metabolic Remodeling. *Cells* **9**(2020).
1642 49. Oh, S.W. *et al.* JNK regulates lifespan in Caenorhabditis elegans by modulating nuclear
1643 translocation of forkhead transcription factor/DAF-16. *Proc Natl Acad Sci U S A* **102**, 4494-
1644 9 (2005).
1645 50. Greer, E.L. *et al.* An AMPK-FOXO pathway mediates longevity induced by a novel method
1646 of dietary restriction in C. elegans. *Curr Biol* **17**, 1646-56 (2007).
1647 51. Leiser, S.F., Begun, A. & Kaeberlein, M. HIF-1 modulates longevity and healthspan in a
1648 temperature-dependent manner. *Aging Cell* **10**, 318-26 (2011).
1649 52. Perrin, A.J. *et al.* Noncanonical control of C. elegans germline apoptosis by the
1650 insulin/IGF-1 and Ras/MAPK signaling pathways. *Cell Death Differ* **20**, 97-107 (2013).
1651 53. Gurkar, A.U. *et al.* Dysregulation of DAF-16/FOXO3A-mediated stress responses
1652 accelerates oxidative DNA damage induced aging. *Redox Biol* **18**, 191-199 (2018).
1653 54. Baruah, A. *et al.* CEP-1, the Caenorhabditis elegans p53 homolog, mediates opposing
1654 longevity outcomes in mitochondrial electron transport chain mutants. *PLoS Genet* **10**,
1655 e1004097 (2014).
1656 55. Ewald, C.Y., Castillo-Quan, J.I. & Blackwell, T.K. Untangling Longevity, Dauer, and
1657 Healthspan in Caenorhabditis elegans Insulin/IGF-1-Signalling. *Gerontology* **64**, 96-104
1658 (2018).
1659 56. Derry, W.B., Putzke, A.P. & Rothman, J.H. Caenorhabditis elegans p53: role in apoptosis,
1660 meiosis, and stress resistance. *Science* **294**, 591-5 (2001).

1661 57. Schumacher, B., Hofmann, K., Boulton, S. & Gartner, A. The C. elegans homolog of the
1662 p53 tumor suppressor is required for DNA damage-induced apoptosis. *Curr Biol* **11**, 1722-
1663 7 (2001).
1664 58. Schumacher, B. *et al.* Translational repression of C. elegans p53 by GLD-1 regulates DNA
1665 damage-induced apoptosis. *Cell* **120**, 357-68 (2005).
1666 59. Levi-Ferber, M. *et al.* It's all in your mind: determining germ cell fate by neuronal IRE-1 in
1667 C. elegans. *PLoS Genet* **10**, e1004747 (2014).
1668 60. Hicks, T. *et al.* R-loop-induced irreparable DNA damage evades checkpoint detection in
1669 the C. elegans germline. *Nucleic Acids Res* **50**, 8041-8059 (2022).
1670 61. Arum, O. & Johnson, T.E. Reduced expression of the Caenorhabditis elegans p53
1671 ortholog cep-1 results in increased longevity. *J Gerontol A Biol Sci Med Sci* **62**, 951-9
1672 (2007).
1673 62. Lee, C.C. *et al.* Mutation of a Nopp140 gene dao-5 alters rDNA transcription and increases
1674 germ cell apoptosis in C. elegans. *Cell Death Dis* **5**, e1158 (2014).
1675 63. Gartner, A., Boag, P.R. & Blackwell, T.K. Germline survival and apoptosis. *WormBook*, 1-
1676 20 (2008).
1677 64. Greiss, S., Schumacher, B., Grandien, K., Rothblatt, J. & Gartner, A. Transcriptional
1678 profiling in C. elegans suggests DNA damage dependent apoptosis as an ancient function
1679 of the p53 family. *BMC Genomics* **9**, 334 (2008).
1680 65. Schumacher, B. *et al.* C. elegans ced-13 can promote apoptosis and is induced in
1681 response to DNA damage. *Cell Death Differ* **12**, 153-61 (2005).
1682 66. Schertel, C. & Conradt, B. C. elegans orthologs of components of the RB tumor
1683 suppressor complex have distinct pro-apoptotic functions. *Development* **134**, 3691-701
1684 (2007).

1685 67. Sendoel, A., Kohler, I., Fellmann, C., Lowe, S.W. & Hengartner, M.O. HIF-1 antagonizes
1686 p53-mediated apoptosis through a secreted neuronal tyrosinase. *Nature* **465**, 577-83
1687 (2010).
1688 68. Sulston, J.E. & Horvitz, H.R. Post-embryonic cell lineages of the nematode,
1689 Caenorhabditis elegans. *Dev Biol* **56**, 110-56 (1977).
1690 69. Sternberg, P.W. Vulval development. *WormBook*, 1-28 (2005).
1691 70. Horvitz, H.R. & Sternberg, P.W. Nematode postembryonic cell lineages. *J Nematol* **14**,
1692 240-8 (1982).
1693 71. Chisholm, A.D. & Hardin, J. Epidermal morphogenesis. *WormBook*, 1-22 (2005).
1694 72. Herman, M.A. Hermaphrodite cell-fate specification. *WormBook*, 1-16 (2006).
1695 73. Costa, M., Weir, M., Coulson, A., Sulston, J. & Kenyon, C. Posterior pattern formation in
1696 C. elegans involves position-specific expression of a gene containing a homeobox. *Cell*
1697 **55**, 747-56 (1988).
1698 74. Euling, S. & Ambros, V. Reversal of cell fate determination in Caenorhabditis elegans
1699 vulval development. *Development* **122**, 2507-15 (1996).
1700 75. Braendle, C. & Felix, M.A. Plasticity and errors of a robust developmental system in
1701 different environments. *Dev Cell* **15**, 714-24 (2008).
1702 76. Karp, X. & Greenwald, I. Control of cell-fate plasticity and maintenance of multipotency by
1703 DAF-16/FoxO in quiescent Caenorhabditis elegans. *Proc Natl Acad Sci U S A* **110**, 2181-
1704 6 (2013).
1705 77. Tenen, C.C. & Greenwald, I. Cell Non-autonomous Function of daf-18/PTEN in the
1706 Somatic Gonad Coordinates Somatic Gonad and Germline Development in C. elegans
1707 Dauer Larvae. *Curr Biol* **29**, 1064-1072 e8 (2019).
1708 78. Hong, Y., Roy, R. & Ambros, V. Developmental regulation of a cyclin-dependent kinase
1709 inhibitor controls postembryonic cell cycle progression in Caenorhabditis elegans.
1710 *Development* **125**, 3585-97 (1998).

1711 79. Karp, X. & Ambros, V. Dauer larva quiescence alters the circuitry of microRNA pathways
1712 regulating cell fate progression in C. elegans. *Development* **139**, 2177-86 (2012).
1713 80. O'Keeffe, C. & Greenwald, I. EGFR signal transduction is downregulated in C. elegans
1714 vulval precursor cells during dauer diapause. *Development* **149**(2022).
1715 81. Colella, E., Li, S. & Roy, R. Developmental and Cell Cycle Quiescence Is Mediated by the
1716 Nuclear Hormone Receptor Coregulator DIN-1S in the Caenorhabditis elegans Dauer
1717 Larva. *Genetics* **203**, 1763-76 (2016).
1718 82. Narbonne, P. & Roy, R. Inhibition of germline proliferation during C. elegans dauer
1719 development requires PTEN, LKB1 and AMPK signalling. *Development* **133**, 611-9
1720 (2006).
1721 83. Wong, C., Kadekar, P., Jurczak, E. & Roy, R. Germline stem cell integrity and quiescence
1722 are controlled by an AMPK-dependent neuronal trafficking pathway. *PLoS Genet* **19**,
1723 e1010716 (2023).
1724 84. Vousden, K.H. & Ryan, K.M. p53 and metabolism. *Nat Rev Cancer* **9**, 691-700 (2009).
1725 85. van den Heuvel, S. Cell-cycle regulation. *WormBook*, 1-16 (2005).
1726 86. Derry, W.B. *et al.* Regulation of developmental rate and germ cell proliferation in
1727 Caenorhabditis elegans by the p53 gene network. *Cell Death Differ* **14**, 662-70 (2007).
1728 87. Cameron, S., Clark, S.G., McDermott, J.B., Aamodt, E. & Horvitz, H.R. PAG-3, a Zn-finger
1729 transcription factor, determines neuroblast fate in C. elegans. *Development* **129**, 1763-74
1730 (2002).
1731 88. Thompson, K.W. *et al.* The Paired-box protein PAX-3 regulates the choice between lateral
1732 and ventral epidermal cell fates in C. elegans. *Dev Biol* **412**, 191-207 (2016).
1733 89. Salser, S.J. & Kenyon, C. Patterning C. elegans: homeotic cluster genes, cell fates and
1734 cell migrations. *Trends Genet* **10**, 159-64 (1994).
1735 90. Sternberg, P.W. Genetic control of cell type and pattern formation in Caenorhabditis
1736 elegans. *Adv Genet* **27**, 63-116 (1990).

1737 91. Burglin, T.R. & Ruvkun, G. The Caenorhabditis elegans homeobox gene cluster. *Curr*
1738 *Opin Genet Dev* **3**, 615-20 (1993).
1739 92. Jones, R.G. *et al.* AMP-activated protein kinase induces a p53-dependent metabolic
1740 checkpoint. *Mol Cell* **18**, 283-93 (2005).
1741 93. Feng, Y., Williams, B.G., Koumanov, F., Wolstenholme, A.J. & Holman, G.D. FGT-1 is the
1742 major glucose transporter in C. elegans and is central to aging pathways. *Biochem J* **456**,
1743 219-29 (2013).
1744 94. Schulz, T.J. *et al.* Glucose restriction extends Caenorhabditis elegans life span by
1745 inducing mitochondrial respiration and increasing oxidative stress. *Cell Metab* **6**, 280-93
1746 (2007).
1747 95. Wu, Z. *et al.* Dietary Restriction Extends Lifespan through Metabolic Regulation of Innate
1748 Immunity. *Cell Metab* **29**, 1192-1205 e8 (2019).
1749 96. Walker, M.D. *et al.* WormPaths: Caenorhabditis elegans metabolic pathway annotation
1750 and visualization. *Genetics* **219**(2021).
1751 97. Li, Q. *et al.* IL-17 induces radiation resistance of B lymphoma cells by suppressing p53
1752 expression and thereby inhibiting irradiation-triggered apoptosis. *Cell Mol Immunol* **12**,
1753 366-72 (2015).
1754 98. Chen, K. *et al.* IL-17 Receptor Signaling in the Lung Epithelium Is Required for Mucosal
1755 Chemokine Gradients and Pulmonary Host Defense against K. pneumoniae. *Cell Host*
1756 *Microbe* **20**, 596-605 (2016).
1757 99. Liu, Y. *et al.* p53 regulates hematopoietic stem cell quiescence. *Cell Stem Cell* **4**, 37-48
1758 (2009).
1759 100. Cheung, T.H. & Rando, T.A. Molecular regulation of stem cell quiescence. *Nat Rev Mol*
1760 *Cell Biol* **14**, 329-40 (2013).
1761 101. Das, S., Min, S. & Prahlad, V. Gene bookmarking by the heat shock transcription factor
1762 programs the insulin-like signaling pathway. *Mol Cell* **81**, 4843-4860 e8 (2021).

1763 102. Das, S. *et al.* Serotonin signaling by maternal neurons upon stress ensures progeny
1764 survival. *Elife* **9**(2020).
1765 103. Tatum, M.C. *et al.* Neuronal serotonin release triggers the heat shock response in C.
1766 elegans in the absence of temperature increase. *Curr Biol* **25**, 163-174 (2015).
1767 104. Ooi, F.K. & Prahlad, V. Olfactory experience primes the heat shock transcription factor
1768 HSF-1 to enhance the expression of molecular chaperones in C. elegans. *Sci Signal*
1769 **10**(2017).
1770 105. Venkatesh, H. & Monje, M. Neuronal Activity in Ontogeny and Oncology. *Trends Cancer*
1771 **3**, 89-112 (2017).
1772 106. Curry, R.N. & Glasgow, S.M. The Role of Neurodevelopmental Pathways in Brain Tumors.
1773 *Front Cell Dev Biol* **9**, 659055 (2021).
1774 107. Gibson, D.G. *et al.* Enzymatic assembly of DNA molecules up to several hundred
1775 kilobases. *Nat Methods* **6**, 343-5 (2009).
1776 108. Nonet, M.L. *et al.* Caenorhabditis elegans rab-3 mutant synapses exhibit impaired function
1777 and are partially depleted of vesicles. *J Neurosci* **17**, 8061-73 (1997).
1778 109. Nika, L., Gibson, T., Konkus, R. & Karp, X. Fluorescent Beads Are a Versatile Tool for
1779 Staging Caenorhabditis elegans in Different Life Histories. *G3 (Bethesda)* **6**, 1923-33
1780 (2016).
1781 110. Krueger, F. TrimGalore. (2021).
1782 111. Kopylova, E., Noe, L. & Touzet, H. SortMeRNA: fast and accurate filtering of ribosomal
1783 RNAs in metatranscriptomic data. *Bioinformatics* **28**, 3211-7 (2012).
1784 112. Yates, A.D. *et al.* Ensembl Genomes 2022: an expanding genome resource for non-
1785 vertebrates. *Nucleic Acids Res* **50**, D996-D1003 (2022).
1786 113. Dobin, A. *et al.* STAR: ultrafast universal RNA-seq aligner. *Bioinformatics* **29**, 15-21
1787 (2013).

1788 114. Liao, Y., Smyth, G.K. & Shi, W. The R package Rsubread is easier, faster, cheaper and
1789 better for alignment and quantification of RNA sequencing reads. *Nucleic Acids Research*
1790 **47**, e47-e47 (2019).
1791 115. Love, M.I., Huber, W. & Anders, S. Moderated estimation of fold change and dispersion
1792 for RNA-seq data with DESeq2. *Genome Biol* **15**, 550 (2014).
1793 116. Davis, P. *et al.* WormBase in 2022-data, processes, and tools for analyzing
1794 Caenorhabditis elegans. *Genetics* **220**(2022).
1795 117. Cohen, S.M., Sun, J.J., Schroeder, F.C. & Sternberg, P.W. Transcriptional Response to a
1796 Dauer-Inducing Ascaroside Cocktail in Late L1 in C. elegans. (microPublication Biology,
1797 2021).
1798 118. Hu, M., Crossman, D., Prasain, J.K., Miller, M.A. & Serra, R.A. Transcriptomic Profiling of
1799 DAF-7/TGFβ Pathway Mutants in C. elegans. *Genes* **11**, 288 (2020).
1800 119. Shen, L. & Sinai, M. GeneOverlap: Test and visualize gene overlaps. (2019).
1801 120. Chen, H. VennDiagram: Generate High-Resolution Venn and Euler Plots. (2018).
1802 121. Wu, T. *et al.* clusterProfiler 4.0: A universal enrichment tool for interpreting omics data.
1803 *Innovation (N Y)* **2**, 100141 (2021).
1804 122. Carlson, M. org.Ce.eg.db: Genome wide annotation for Worm. (2019).
1805 123. Kanehisa, M., Furumichi, M., Sato, Y., Kawashima, M. & Ishiguro-Watanabe, M. KEGG
1806 for taxonomy-based analysis of pathways and genomes. *Nucleic Acids Res* (2022).
1807 124. Gu, Z. Complex heatmap visualization. *iMeta* **1**, e43 (2022).
1808 125. Kolde, R. pheatmap: Pretty Heatmaps. (2019).
1809 126. Chikka, M.R., Anbalagan, C., Dvorak, K., Dombeck, K. & Prahlad, V. The Mitochondria-
1810 Regulated Immune Pathway Activated in the C. elegans Intestine Is Neuroprotective. *Cell*
1811 *Rep* **16**, 2399-414 (2016).
1812
1813

1814 A**cknowledgements**

1815 We thank the V.P. laboratory, Drs. Sarit Smolikove, Josep Comeron, Anna Malkova and Michael
1816 Petrascheck for comments, Dr. Peter Ratcliffe, Oxford, for his generous gift of *CeHIF-1* antibody,
1817 and Dr. Mario de Bono, Institute of Science and Technology Austria (ISTA) for *C. elegans* strains.
1818 Nematode strains were provided by the Caenorhabditis Genetics Center (CGC) (funded by the
1819 NIH Infrastructure Programs P40 OD010440). This work was supported by NIH R01 AG060616
1820 (V.P.).

1821 **Author Contributions**

1822 All authors designed the study, performed experiments, analyzed data, and drafted the

1823 manuscript. P.D.I coordinated the mammalian experiments; V.P. coordinated *C. elegans*

1824 experiments and the project. All authors approved the final version of the manuscript.

1825

1826 **Declaration of Interests**

1827 The authors declare no competing interests

1828